PREDICTION OF SUBGRADE CALIFORNIA BEARING RATIO USING FALLING WEIGHT DEFLECTOMETER FOR PAVEMENT EVALUATION IN KENYA

CATHERINE WAMBUI MUGAI

MASTER OF SCIENCE IN

CIVIL ENGINEERING

(Transportation Engineering)

JOMO KENYATTA UNIVERSITY

OF

AGRICULTURE AND TECHNOLOGY

2026

Prediction of Subgrade California Bearing Ratio using Falling Weight Deflectometer for Pavement Evaluation in Kenya

Catherine Wambui Mugai

A Thesis Submitted in Partial Fulfilment of the Requirements for the Degree of Master of Science in Civil Engineering (Transportation Engineering) of the Jomo Kenyatta University of Agriculture and Technology

2026

DECLARATION

This thesis is my original work and has not been presented for a degree in any other University.

Signature: ………………………… Date: ……………………………..

Catherine Wambui Mugai

This thesis has been submitted for examination with our approval as university supervisors

Signature: …………………………… Date: …………………………..

Dr. Kepha Abongo, PhD

JKUAT, Kenya

Signature: ………………………… Date: ……………………………

Dr. Brian Odero, PhD

JKUAT, Kenya

DEDICATION

To Jewel, my baby, my best friend; thank you for bringing out the best in me.

ACKNOWLEDGEMENT

With many thanks to my supervisors Dr. Kepha Abongo and Dr. Brian Odero for their constant guidance, commitment and encouragement during this research. To my mentor, my consultant, my sister, Dr. Faith, for making me believe in myself. To my daddy, Rev. Edward, for praying for me, encouraging me and always speaking wisdom. To my mum, Hannah, for nurturing in me hope and resilience. To my brother Paul, for giving me balance. To my late sister Monique, aiming for the highest was your undisputed quality, forever to be emulated. To my daughter Jewel, for being the spark to brilliant ideas throughout this research! To the Ministry of Roads and Transport (Kenya) and particularly, Materials Testing and Research Directorate (MTRD), for providing the required study data and FWD analysis software. Above all, to my Heavenly Father, for all the answered prayers and everlasting love.

TABLE OF CONTENTS

LIST OF TABLES

LIST OF FIGURES

LIST OF APPENDICES

LIST OF SYMBOLS

$\mathbf{E_n}$	Subgrade Surface Modulus
$\mathbf{E_s}$	Elastic Modulus
$\mathbf{G_n}$	Deflection at each offset
$\mathbf{M_r}$	Resilient Modulus
$\mathbf{R^2}$	Coefficient of determination
r	Pearson’s correlation coefficient
μ	Poisson’s ratio

ABBREVIATIONS AND ACRONYMS

AASHTO	Association of State Highway and Transportation Officials
ANN	Artificial Neural Networks
ASTM	American Society for Testing and Materials
CBR	California Bearing Ratio
CH	Fat clay
CL	Lean Clay
DCP	Dynamic Cone Penetrometer
DR	Deflection Ratio
FAA	Federal Aviation Administration
FWD	Falling Weight Deflectometer
GIS	Geographic Information System
GM	Silty gravel
GPR	Ground Penetrating Radar
LiDAR	Light Detection and Ranging
LR	Linear Regression
LWD	Light Weight Deflectometer

MDD	Maximum Dry Density
MH	Elastic Silt
ML	Silt with sand
MLR	Multiple Linear Regression
MPa	Mega Pascals
NACOSTI	National Commission for Science, Technology and Innovation
NDG	Nuclear Density Gauge
OMC	Optimum Moisture Content
OWP	Outer Wheel Path
PI	Plasticity Index
PMC	Present Moisture Content
PMS	Pavement Management Systems
RF	Random Forest
RMSE	Root Mean Squared Error
USCS	Unified Soil Classification System

ABSTRACT

Subgrade CBR is a very important parameter which gives an indication of the strength of the pavement's foundation. Kenya's Road Design Manual (Part 3) classifies the subgrade as S1 to S6 depending on their CBR range. The objective of this study was to predict subgrade CBR using FWD for pavement evaluation. A sample of 18 road sections were selected purposively for the study due to availability of data. The data required was FWD data, trench logs, laboratory results for the samples collected from the trenches and construction data. The FWD data was collected at intervals of about 100m using Primax FWD equipment. Trial pits were dug at intervals of about 5 km and the samples collected were tested in the laboratory to establish the soil properties. An average of three FWD readings were obtained at the exact chainage where the trial pits were dug. The materials were first characterized and classified using Unified Classification System (UCS). Lean clay (CL) and Elastic Silt (MH) were found to be the predominant soil classes. The average values of PI, OMC and MDD per road section were found to range from 7 to 23%, 12 to 27% and 1250 to 1821 kg/m^3 respectively. The 4th geophone (D4), which was positioned at 600mm from the centre of the loading plate, was selected for developing the model based on the deflection bowls and surface modulus graphs. 11 models were developed by considering varying independent variables like deflections, contact pressure, air temperature, MDD, OMC, PI and Soil Class the dependent variables were the predicted CBR values. The data for all the road sections was split randomly into two; 80% was used to train the models and 20% to test the models. The models developed were Linear Regression models (LR) and machine learning models which were Random Forest (RF) and Artificial Neural Networks (ANN). Three models had the highest R^2 score of 55 to 61% which means they explained the variability of lab CBR and were the best models. The same models had the lowest RMSE therefore making them the best models for predicting CBR. The CBR values predicted were correlated with the CBR values from the lab and found to have Pearson's correlation coefficient of 0.81 to 0.84. The two machine learning models require specialized software like python to make predictions. The LR model developed was CBR = 5.2215 + (-0.0036 x D4) + (-0.0144 x P_c) + (-0.2522 x T_{air}) + (0.0233 x MDD) + (-0.3732 x OMC). The deflections, contact pressure and air temperature are values obtained from the FWD data. The study recommended that the developed predictive models can be subjected to additional validation by using them to predict CBR from other road sections in future pavement evaluations.

CHAPTER ONE

INTRODUCTION

1.1 Overview

This chapter introduces the importance of subgrade strength, measured by California Bearing Ratio (CBR), for flexible pavement performance and durability. Conventional methods for determining subgrade CBR such as laboratory or plate load tests are time-consuming and costly. The Falling Weight Deflectometer (FWD) is presented as a rapid, non-destructive alternative that measures pavement deflection in real-time. Correlations may be established between FWD deflection data and subgrade CBR, allowing for predictive models. The importance of establishing subgrade strength in terms of CBR is to provide values that are can be interpreted from the specifications provided in the Kenya Road Design Manuals. Such models would streamline pavement rehabilitation design, reduce costs, save time, improve decision making, and lead to more sustainable pavements. This study aims to address the need for rapid, cost-effective, real-time subgrade assessment during pavement evaluation.

1.2 Background of the Study

1.2.1 Global and National Context of Road Infrastructure

Road transport has been found to be the predominant mode of transportation for freight and passenger traffic in most developing countries (Rodrigue, 2020). Globally, there is significant variance in road networks in relation to extent and quality. According to WION News (2024), India has the largest road network in the world, which extends over 6,600,000 km, of which approximately 68% are paved. The United States follows closely with 6,500,000 km with 66% of those roads being paved (U.S. Department of Transportation, 2023). China's road network is nearly 5,500,000 km, with more than 97% being paved (World Bank, 2022). However, many other nations face substantial challenges with unpaved roads. Brazil has 2,000,000 km of roads but only 11% are paved, while Canada has over 1,000,000 km of roads with only 41% paved (CIA World Factbook, 2025).

Recent research that has been carried out globally by utilizing satellite imagery and deep learning frameworks, has established that the proportion of paved roads in a country contributed significantly to country's development trajectory, and correlated significantly with the Human Development Index (HDI) (Magg et al., 2024). The study further indicated that unpaved roads have implications on global economic connectivity. (Magg et al., 2024).

In Kenya, road transport continues to be the primary mode of transportation, which handles more than 90% of both passenger and freight traffic, (Kenya Roads Board, 2023). The Government of Kenya has therefore made substantial investment in road development and maintenance over the past 15 years (Kenya Roads Board, 2024). According to the Kenya Roads Board (KRB), the country’s total road network had increased to 239,105 kilometres by 2023 (Kenya Roads Board, 2024). The condition of the national road network has improved steadily, as evidenced by the reduction in the proportion of the road network in poor condition from 59 percent in 2009 to 29 percent in 2023, while over the same period, the road network in good and fair condition increased from 41 percent to 68 percent (Kenya Roads Board, 2024).

1.2.2 Pavement Types and Subgrade Fundamentals

Pavements are broadly classified into two main categories: rigid pavements and flexible pavements. Rigid pavements are constructed using Portland cement concrete and distribute loads through slab action with high flexural strength. Flexible pavements, which are the focus of this study, are defined as pavements composed of a base made of fairly deformable material such as natural gravel, GCS (granular cemented subbase), or lime/cement improved material with a thin bituminous surfacing (Government of Kenya, 1987). Flexible pavements rely on layered load distribution and derive their strength from the interlocking of aggregates and the stiffness of the bituminous layer.

The subgrade is the foundation upon which all pavement structures are built. Its strength, as measured by parameters like California Bearing Ratio (CBR), directly influences the performance and durability of pavements. According to Rahman et al.

(2011), poor subgrade conditions are among the leading causes of premature pavement failure. As such, understanding the properties of subgrade materials is crucial for ensuring structural adequacy and longevity of transportation infrastructure. Understanding and predicting subgrade strength are essential for designing cost-effective and long-lasting pavements (Huang, 2004).

Subsoil condition is a key factor considered in the design and performance of flexible pavement structures. The foundation is the platform on which the pavement is constructed and comprises either: the top 300 mm of the subgrade below the formation in embankments or cuttings constructed using material complying with the bearing strength requirement of the selected foundation class in two layers of 150 mm thickness compacted to 100 percent Maximum Dry Density (MDD) (AASHTO T99); or, where the subgrade material does not comply with the strength requirements of the selected foundation class, the upper 300 mm of the subgrade completed in 150 mm compacted layers and the capping (Government of Kenya, 2017).

Figure 1-1 presents a schematic illustration of pavement terminologies and the definition of the road foundation. The figure shows the vertical cross-section of a typical flexible pavement, identifying the surfacing, base course, subbase course, subgrade, formation level, and capping layer where applicable.

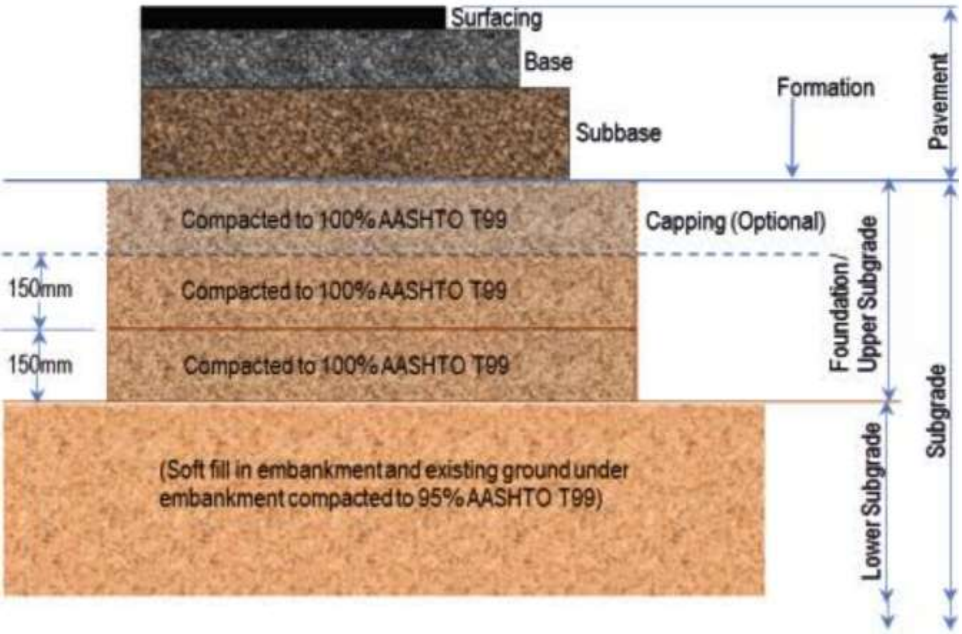

Figure 1.1: Pavement Terminology

(Source: Government of Kenya, 2017)

The pavement structure is considered an elastic multi-layer system in which the materials are characterised by Young's modulus of elasticity and Poisson's ratio. The subgrade is the lowest layer, while the subbase, base, and surfacing are the upper layers (Yoder & Witczak, 1975).

1.2.3 Pavement Evaluation and Non-Destructive Testing

Annually, numerous roads are evaluated to establish their structural condition, surface condition, and mitigation measures for maintenance or reconstruction purposes (Transport Research Laboratory, 2002). These evaluations aim to determine whether the existing pavement can support the traffic loading established during traffic surveys. The structural condition surveys are carried out using both destructive and non-destructive tests to assess both surface condition and structural condition of the pavement (ASTM D4694, 2020). One of the non-destructive testing equipment used is the Falling Weight Deflectometer (FWD).

Figure 1-2 illustrates the characteristic deflection bowl generated by an FWD impact load. The figure shows the peak deflection at the centre of the load plate and the decreasing deflections at increasing distances from the load, forming a bowl-shaped profile. The profile reflects the combined stiffness of the pavement layers and the subgrade.

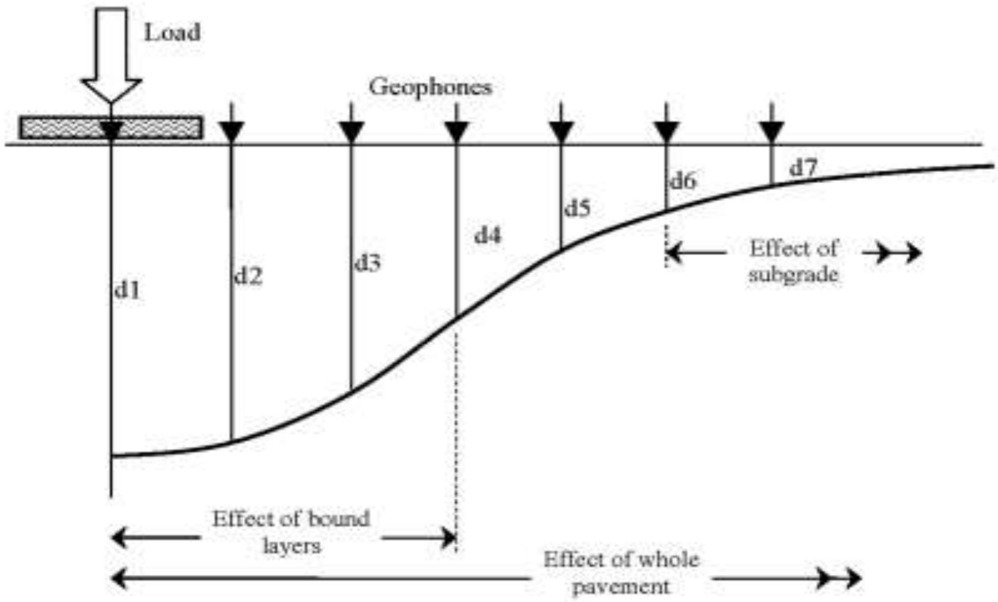

Figure 1.2: Schematic Representation of FWD Deflection Bowl

(Source: ASTM D4694, 2020)

A critical component studied during pavement evaluation are the properties of the subgrade material. Subgrade soil samples are extracted using destructive methods of trenching to obtain samples for laboratory CBR tests or DCP tests inside the test pits (Government of Kenya, 2025b). Conventional methods for determining subgrade strength, such as laboratory tests or field plate load tests, can be time-consuming, labour-intensive, and costly (Das, 2015). Additionally, these methods may not provide timely data for decision-making during pavement evaluation (Scullion & Stokoe, 1997).

FWD is a non-destructive testing method widely used for assessing the structural properties and condition of pavements (AASHTO, 2017). It applies a dynamic load to the pavement surface and measures the deflections that are generated. FWD testing is efficient, rapid, and can be performed in situ, giving real-time data on the response of pavements to loading (Hoffman & Thompson, 1981).

1.3 Statement of the Problem

All layers of the road pavement rest on the subgrade, which forms the pavement foundation. In Kenya, the strength of the subgrade for pavement design and evaluation is represented by CBR values. This value is established destructively by excavating pits and carrying out CBR tests on collected samples. Engineers who attempt to obtain the subgrade value non-destructively during pavement evaluation by using FWD eventually rely on correlations provided in the Road Design Manual. These are correlations between CBR and surface stiffness modulus obtained using plate bearing tests, not FWD. This reliance on design manual correlations, which were not developed specifically for FWD, presents a significant challenge.

The specific challenge is that plate bearing tests and FWD tests apply different loading conditions (static versus dynamic), have different loading plate diameters, and measure different response parameters. Consequently, directly applying plate bearing-based correlations to FWD data introduces unknown errors. Furthermore, there is no dedicated software tool or package specifically designed for predicting subgrade CBR using FWD data within the Kenyan context. While various software applications exist for pavement analysis, design, and management, they do not fully address the unique requirements and challenges associated with subgrade CBR prediction from FWD measurements. Furthermore, no study has been carried out in Kenya comparing directly tested subgrade CBR with FWD deflections and back-calculated elastic modulus of subgrade layers, which would provide a fast and non-destructive method of determining subgrade CBR.

Beyond this methodological gap, the scale of the problem is substantial. Despite investment in Kenya's road infrastructure with a national network of 239,105 kilometres (Kenya Roads Board, 2024) only 25,412 kilometres (approximately 10.6 percent) are paved (Kenya National Bureau of Statistics, 2026). Among paved roads, only 30 percent are reported to be in good condition (Kenya Roads Board, 2024), indicating widespread structural deficiency.

Premature pavement failure imposes a heavy economic burden. Kenya loses approximately KShs. 5.8 billion annually due to pavement damage from axle overloading alone (Ndagea, 2011). Beyond overloading, an estimated 20 to 30 percent of rehabilitated road sections in developing countries fail within a time span of five years of construction or rehabilitation (Transport Research Laboratory, 2002). In Nairobi specifically, a study of urban roads revealed that more than 40 percent of paved roads exhibited significant cracking and deformation within three to seven years of construction, with subgrade-related failures identified as a primary contributing factor (Mwangi & Mwea, 2016). Globally, poor subgrade conditions account for approximately 35 to 45 percent of premature pavement failures (Rahman et al., 2011).

The subgrade serves as the foundation layer upon which the entire pavement structure is built. Inadequate characterization of its strength leads to two problematic outcomes; under-design and over-design. Under-design results in excessive deflections, fatigue cracking, and permanent deformation while over-design wastes construction materials such as aggregates, cement, and bitumen, as well as scarce public funds (Huang, 2004).

Conventional methods for determining subgrade CBR present significant practical challenges. Laboratory CBR testing typically requires 7 to 14 days per sample for sample collection, transportation, sample preparation, soaking, testing and reporting (Das, 2015). This protracted timeline delays decision-making and project scheduling. The cost of digging trial pits, extracting samples, and carrying out laboratory CBR tests ranges from KShs. 15,000 to 25,000 per test location (Kenya Urban Roads Authority, 2023). For a typical 10 km urban road requiring testing at intervals of 500 metres, this translates to testing costs of KShs. 400,000 to 700,000, excluding traffic management and safety measures.

Due to cost and time constraints, testing is typically limited to only 2 to 5 locations per kilometre, with significant portions of the road alignment left uncharacterized (Scullion & Stokoe, 1997). This sparse sampling leads to increased risk of undetected weak zones that may trigger localized failure. Additionally, destructive testing methods also require lane closures and traffic diversions. On high-volume urban roads, a single day of lane closure can result in economic losses in excess of KShs. 500,000 due to increased vehicle operating costs and travel time delays (Kenya National Highways Authority, 2022).

The Falling Weight Deflectometer offers a rapid, non-destructive alternative. However, current practice in Kenya does not utilize FWD deflection data to directly estimate subgrade CBR. FWD is used primarily to assess overall pavement structural condition (Government of Kenya, 2025b). The relationship between FWD-measured deflections and subgrade CBR has not been systematically established for Kenyan subgrade materials, which vary from black cotton soils of the Rift Valley to lateritic and murram soils of other regions.

There is no validated predictive model that exists for estimating subgrade CBR from FWD deflection measurements under Kenyan soil and climatic conditions. Without such a model, pavement engineers cannot fully leverage FWD data for subgrade assessment, leading to continued reliance on costly, time-consuming, and disruptive destructive testing methods.

1.4 Objectives of the Study

1.4.1 Overall Objective

To predict subgrade California Bearing Ratio (CBR) using Falling Weight Deflectometer (FWD) for pavement evaluation.

1.4.2 Specific Objectives

The specific objectives were:

i. To characterize subgrade materials from trench data by determining soil classification, index properties, and laboratory CBR values for at least 55 test locations along selected Kenyan roads for prediction of subgrade CBR using FWD.

ii. To develop predictive models for subgrade CBR from FWD deflection parameters by correlating at least 55 paired datasets for prediction of subgrade CBR using FWD.
iii. To investigate factors influencing the FWD-CBR relationship by analyzing the effects of soil type, density, moisture condition, and temperature on prediction accuracy for prediction of subgrade CBR using FWD.

1.5 Research Questions

The following research questions were formulated to guide the study, aligned with the specific objectives:

i. What are the physical and strength characteristics (soil classification, index properties, and CBR values) of subgrade materials from trench data for at least 55 test locations along selected Kenyan roads?
ii. What predictive models can be developed to estimate subgrade CBR from FWD deflection parameters using at least 55 paired datasets?
iii. How do soil type, moisture condition, pavement layer thickness, and temperature influence the relationship between FWD deflection data and subgrade CBR?

1.6 Justification of the Study

This study was justified by the need to enhance pavement management practices, improve decision-making processes, enhance safety and performance, and address research gaps in pavement engineering. These research gaps pertain to understanding the relationship between FWD deflection measurements and subgrade CBR under Kenyan conditions. By leveraging FWD technology, this study aims to provide practical solutions for predicting subgrade CBR efficiently and accurately in Kenya, leading to more sustainable and resilient transportation infrastructure.

Recent literature supports this justification. Horak (2008) emphasized that deflection-based pavement evaluation offers significant advantages over destructive methods, but noted that local calibration is critical for accurate subgrade characterization. George (2004) demonstrated that FWD data could predict the strength parameter of subgrade with reasonable accuracy when appropriate correlations are developed, yet highlighted that such correlations are unavailable for tropical soils. Kim et al. (2010) successfully used regression and machine learning approaches for FWD back-calculation, but their work was based on temperate climate conditions. These studies collectively indicate that while the approach is viable, locally validated models for Kenya are necessary, which is the gap this study seeks to fill.

1.6.1 Why the Researcher is Conducting This Study

The researcher is conducting this study to address the identified knowledge gap by developing a robust, locally-validated predictive model that estimates subgrade CBR from FWD deflection measurements. The motivation stems from direct observation of shortcomings in current pavement evaluation practice in Kenya which frequently experience delays due to laboratory testing schedules spanning one to two weeks per sample. Budget constraints force engineers to accept sparse subgrade sampling at only one to two locations per five kilometres, which may leave out critical weak zones. Additionally, substantial volumes of FWD data collected during routine pavement evaluations remain underutilized for subgrade characterization, representing a missed opportunity for cost effective infrastructure management.

1.6.2 Beneficiaries of the Study

This study will benefit multiple stakeholders. The Ministry of Roads and Transport will benefit from reduced project timelines and lower testing costs, along with improved ability to prioritize rehabilitation needs. The Kenya National Highways Authority (KeNHA), Kenya Urban Roads Authority (KURA) and Kenya Rural Roads Authority (KeRRA) will benefit from faster structural assessment of roads and denser subgrade characterization with minimal traffic disruption. Consulting engineers will benefit from enhanced analytical capabilities, giving them a competitive advantage. Contractors will experience reduced waiting time for subgrade test results, enabling accelerated project start-up. Road users will enjoy fewer traffic delays, improved pavement quality, and better value for public investment. Academia will gain a validated dataset and predictive model for Kenyan conditions.

1.6.3 Alignment with Sustainable Development Goals (SDGs)

This study contributes to five SDGs. It addresses SDG 9 (Industry, Innovation and Infrastructure) by enabling rapid, cost-effective subgrade assessment for resilient pavements. It contributes to SDG 11 (Sustainable Cities and Communities) by minimizing traffic disruption during evaluations of urban roads. It supports SDG 12 (Responsible Consumption and Production) by reducing over-design that wastes materials and under-design that causes premature failure. It addresses SDG 13 (Climate Action) by enabling climate-resilient pavement design. Finally, it contributes to SDG 8 (Decent Work and Economic Growth) by supporting the productivity of Kenya's transport sector, which handles over 90 percent of freight and passenger traffic (Kenya Roads Board, 2023).

1.7 Scope and Limitations of the Study

1.7.1 Scope

The study focused on characterizing subgrade properties of selected road sections and developing predictive models for subgrade CBR from FWD data. The scope covered 18 selected road sections distributed across Kenya, including roads under KeNHA, KeRRA and KURA jurisdiction. These sections were selected to represent the common subgrade soil types found in Kenya: black cotton soils (expansive clays) from the Rift Valley region, lateritic soils from central and eastern regions, and murram soils from coastal and western regions. The specific roads are listed in Appendix 5.

The study considered only flexible bituminous pavements with unbound granular bases. Subgrade CBR range was limited to 2 to 30 percent (S1 to S5). Only natural, neat subgrade soils were included. The duration of the study was fourteen months, from March 2024 to May 2025.

1.7.2 Limitations

Temperature affects asphalt stiffness and thus deflections. While pavement temperature was recorded, systematic temperature correction for Kenyan conditions was not included. The target sample size could not capture all Kenyan subgrade diversity.

CHAPTER TWO

LITERATURE REVIEW

2.1 Overview

This chapter reviews literature on subgrade characterization, Falling Weight Deflectometer (FWD) technology, predictive modelling techniques, and previous studies on subgrade California Bearing Ratio (CBR) prediction. The review identifies knowledge gaps that inform the present study.

2.2 Subgrade Strength and Its Importance

The subgrade is the foundation upon which pavement structures are built. Its strength directly influences the performance and durability of pavements. According to Rahman et al. (2011), poor subgrade conditions account for approximately 35 to 45 percent of premature pavement failures worldwide. Understanding and predicting subgrade strength are therefore essential for designing cost-effective and long-lasting pavements (Huang, 2004).

All road pavement layers rest on the subgrade, hence the capping, subbase, base, and surfacing layers are designed to protect the subgrade from traffic-induced stresses and environmental variations (Government of Kenya, 2017). Unlike the pavement layers, the subgrade is subjected to moisture variations throughout its service life. During these variations, the subgrade must be protected from damage due to both traffic and environmental stresses, making accurate assessment of subgrade strength critical.

The pavement structure is considered an elastic multi-layer system in which materials are characterised by Young's modulus of elasticity and Poisson's ratio. The subgrade is the lowest layer, while the subbase, base, and surfacing are the upper layers (Yoder & Witczak, 1975).

In Kenya, the first step in pavement design is determination of alignment soil properties and design traffic. The most important characteristic of the subgrade is the elastic modulus, which according to the Road Design Manual (Part 3) is found to be fairly complicated and time-consuming to determine directly. A correlation between CBR range and elastic modulus obtained using plate bearing tests was therefore developed and presented in Part III of the Road Design Manual (Government of Kenya, 1987), as shown in Table 2.1.

Table 2.1: Subgrade Class and Subgrade Moduli Relationship

Soil Class	CBR Range (%)	Median	Modulus (MPa)
S1	2-5	3.5	15
S2	5-10	7.5	50
S3	7-13	10.0	65
S4	10-18	14.0	90
S5	15-30	22.5	125
S6	30-60	45	250

(Source: Government of Kenya, 1987)

The new Road Design Manual Volume 3 for Materials and Pavement Design, specifies subgrade strength in terms of CBR and provides a range of subgrade classes from S1 to S6 with median CBR ranging from 3.5 to 45 (Government of Kenya, 2025a). These classification systems provide the basis for subgrade strength characterization in Kenyan pavement design practice.

2.3 California Bearing Ratio (CBR) Determination Methods

CBR is a measure of the shearing resistance of soils (Odero et al., 2021). It is defined as the ratio, which is expressed as a percentage, of the force per unit area required to penetrate a soil mass using a standard circular plunger of 50 mm diameter at a rate of

1.25 mm per minute to that required for corresponding penetration in a standard crushed stone material. The ratio is usually determined for penetrations of 2.5 mm and 5.0 mm. When the ratio at 5.0 mm is higher than that at 2.5 mm, the ratio at 5.0 mm is used.

CBR remains a critical input parameter in empirical and mechanistic-empirical pavement design methods. Since CBR is a relatively simple and widely used test, it has been retained as a quantitative means of evaluating subgrade bearing strength in many design manuals (Government of Kenya, 1987). However, it is important to note that CBR can be determined using either static methods which are typical for standard laboratory tests, or dynamic methods such as those developed from FWD or other dynamic cone penetration tests. The methods for determining subgrade CBR can be broadly categorized into three: field methods (in-situ), laboratory methods, and advanced methods.

2.3.1 Field Methods (In-Situ)

Field methods allow for direct determination of subgrade strength at the site without requiring extraction and transportation of samples to a laboratory.

Dynamic Cone Penetrometer (DCP): The DCP is a tool used for evaluating the strength of soils on site. It consists of a hardened conical tip, a standard diameter measuring rod, and a standard weight hammer of 8 kg which is dropped from the top of the rod against an anvil to advance the tip into the ground. The penetration of the cone is measured and recorded after each blow to provide a continuous measure of shearing resistance up to 1 m below the ground surface. The results can be correlated to CBR, in-situ density, resilient modulus, and bearing capacity. The advantage of this method is that CBR results can be obtained faster than laboratory tests. Despite being a destructive test, it does not require a large area to be excavated. The disadvantages are that it takes longer to obtain results than non-destructive tests, results sometimes differ greatly from laboratory results, and extraction of the cone can be difficult if the conical tip encounters a stone within the pavement layers.

Plate Load Test (PLT): The plate load test involves applying a static load to a steel plate placed on the subgrade surface and measuring the resulting settlement. The test provides a direct measure of subgrade modulus and bearing capacity, which can be correlated to CBR. However, the test is time-consuming, requires heavy equipment, and is typically limited to a few test locations per project.

2.3.2 Laboratory Methods

Laboratory CBR testing is performed on undisturbed or compacted samples extracted from the field. The test is normally performed on samples compacted at 100 percent maximum dry density (AASHTO T99) after four days of soaking, during which swelling is monitored. CBR is then obtained by considering the maximum dry density and optimum moisture content determined from the Proctor test. The advantages of this method are its simplicity and accuracy. The disadvantages are the duration required to obtain results which is typically 7 to 14 days and the need to excavate trial pits, which leaves points of weakness on the road.

2.3.3 Advanced Methods

Advanced methods for subgrade strength characterization include seismic methods such as spectral analysis of surface waves, ground-penetrating radar, and electrical resistivity imaging. These methods are non-destructive and can provide continuous profiles of subgrade properties, but they require specialized equipment and interpretation expertise. They are often used as complements to FWD testing rather than standalone methods for CBR prediction.

2.4 Falling Weight Deflectometer Technology

A Falling Weight Deflectometer (FWD) is a non-destructive testing device used to evaluate the structural properties of pavements, primarily by measuring pavement deflection under a dynamic load. The FWD is mostly used for pavement evaluation exercises. The FWD used must meet the requirements of ASTM D4694-09, and the test method followed is defined in ASTM D4695-96.

The FWD consists of a loading mechanism, typically a heavy weight dropped onto a loading plate, and various sensors to measure pavement response. It is usually mounted on a vehicle for easy transport and operation. The FWD is positioned over the section of pavement to be tested. The loading plate is lowered until it makes contact with the pavement surface. Then, a heavy weight (the falling weight) is dropped onto the loading plate, which is normally 300 mm in diameter, generating a dynamic load.

As the weight impacts the loading plate, the pavement surface deflects. Sensors measure the deflection response at various points on the pavement surface. These sensors typically include geophones or accelerometers, which detect the movement of the pavement. The deflection measurements are recorded by a data acquisition system which collects and stores data for analysis. The collected data is then analyzed to assess the structural condition of the pavement.

The internal mechanism of the FWD combines mechanical components for load application with electronic components for data collection and processing. Together, these components enable the FWD to assess the structural properties of pavements by measuring their deflection response under dynamic loading conditions. The main advantages of this method are speed and accuracy. The primary disadvantages are the high cost associated with the technology and the necessity of costly pavement design software for data processing and analysis.

The FWD allows for the determination of the resilient modulus of pavement layers through back-calculation. Resilient modulus is the preferred input for mechanistic-empirical pavement design methods, as it represents the elastic response of materials under repeated loading. However, many design methods in Kenya still rely on CBR values. Therefore, establishing a relationship between FWD-derived parameters and CBR is not retrogression but rather a practical bridge between modern non-destructive testing and existing design frameworks that remain in use.

2.5 Back-Calculation and Pavement Design Software

Data obtained from the FWD is processed using pavement design software before analysis. Several software packages are available for FWD data back-calculation. The choice of software for this study was informed by three factors: common usage in pavement engineering practice, availability to the researcher, and demonstrated capability for subgrade modulus extraction. The three software packages discussed below are widely used in both research and practice for FWD data analysis.

AASHTOWare: AASHTOWare is a collection of transportation software products for transportation project design and management. The pavement design software is used for back-calculation of FWD data. The primary output from back-calculation is the subgrade resilient modulus. However, triaxial tests are required to obtain resilient modulus values for comparison and validation.

BAKFAA: BAKFAA software, which is part of the Federal Aviation Administration's collection, is used for back-calculating pavement layer properties from FWD data. The output from the software analysis is an estimation of moduli of the various pavement layers studied. A formula is provided for correlating subgrade modulus to CBR as follows:

$$CBR = (M_R / 1500) \wedge 0.65 \quad \text{......} \textit{Equation 2.1}$$

The accuracy of the CBR value computed using this equation depends on the accuracy of the empirical correlation used to obtain resilient modulus from triaxial tests and the quality of the FWD data.

RoSy: RoSy is a software package that back-calculates elastic modulus from FWD deflections. Other major output values obtained from RoSy software are pavement residual life, overlay requirements, and the critical layer of the pavement.

2.6 Previous Studies on Subgrade California Bearing Ratio Prediction

A study by Chai et al. (2013) compared predictions from three deflection-based models by examining 11 pavement test sites in Brisbane, Australia. The study only considered pavements with a surfacing layer of less than 50 mm and soils classified as A-2-4, A-2-7, and A-7-5 according to the AASHTO soil classification system. The study found that the three models over-predicted CBR when using the D900 sensor, leading the researchers to develop a model using the D450 sensor with the relationship: $CBR_{subgrade} = 2.6523\ (D450) - 1.001$. The gap identified in this study was the need for a model applicable to roads with surfacing exceeding 50 mm and with different subgrade soil properties, such as those found in Kenya. Furthermore, the study recommended the D450 sensor, which is not available on all FWD equipment.

A study by Nazzal and Mohammad (2010) sought to develop regression models to predict resilient modulus of subgrade soils from FWD back-calculated modulus for use in pavement and overlay design. The study examined the ratio between FWD elastic modulus (E_{FWD}) and laboratory measured resilient moduli (E_R). Back-calculation was performed using three different software packages, and the study concluded that the ratio of E_{FWD} to E_R was greatly affected by the method of back-calculation. The gap identified in this study was the lack of correlation between FWD data and laboratory CBR values specifically, as the study focused on resilient modulus rather than CBR.

Kumar et al. (2015) investigated the relationship between subgrade strength in terms of elastic modulus and CBR from DCP tests in India. They found the following regression model to be the most suitable: $\text{Log}\ (E_s \text{ in MPa}) = 2.553 - 0.6438 \times \log\ (DCP_{60^\circ})$. In their conclusion, they noted disparities in relationships for different countries, which they attributed to varying soil types, drainage conditions, layer confinement, depth of testing, and test procedures. The gap identified in this study was the need for a regression model specific to soils found in Kenya.

Powell et al. (1986) developed relationships between plate load test results and CBR for soils with a Poisson's ratio of 0.3 using finite element modelling. However, this study is now outdated and was conducted for conditions significantly different from those in Kenya.

Obafemi (2004) studied cold regions in the North Atlantic and North Central regions of the United States, developing regression models linking subgrade resilient modulus to air and soil temperatures and moisture content. The findings on temperature effects are relevant, but the climatic conditions differ substantially from tropical and sub-tropical Kenya.

2.7 Data Science and Predictive Modelling Techniques

2.7.1 Data Science

The term "data science" represents many areas including data analytics, data mining, text mining, data visualization, and prediction modelling (Hui, 2018). Statistics is important in data science because it helps analysts and data scientists analyze and understand data. Descriptive statistics assists in summarizing data, inferential statistics tests relationships between data sets or samples, and regression analysis explores relationships between multiple variables. Linear regression follows the formula $y = mx + c$, where historical data is used to train the formula to determine m and c, with y as the output variable and x as the input variable.

Modelling generally means the development of a prediction model to predict a variable in data. Prediction models can be developed using regression algorithms, statistical learning algorithms, and machine learning algorithms such as neural networks, support vector machines, naïve Bayes, multiple linear regression, and decision trees (Hui, 2018). Choosing the most suitable technique for estimating subgrade CBR from FWD measurements depends on the specific advantages and disadvantages of each method, as well as how well it fits the intended application (Hasan et al., 2024).

2.7.2 Modelling Techniques

Various methods can be used in developing prediction models. Multiple Linear Regression (MLR), which is a statistical method, is used often to make engineering prediction models based on multiple independent variables. MLR are fairly simple but have the disadvantage of assuming linearity. Artificial Neural Networks (ANNs) are advanced machine learning models which are capable of learning complex, non-linear patterns and can adapt to varied data sets.

Model validation is performed to confirm whether values predicted from a developed model accurately predict outcomes for future subjects that were not used during model development (Harrell, 2015). Three major causes of model validation failure are overfitting, changes in measurement methods or definition of categorical variables, and major changes in subject inclusion criteria.

The two major modes of model validation are internal and external validation. Internal validation involves fitting and validating the model using a single series of subjects, using the combined dataset to estimate the likely performance of the final model on new subjects. External validation is more stringent and involves testing a final model developed in one country or setting on subjects in another country or setting at another time. Testing a finished model on new subjects from the same geographic area but from a different dataset than the subjects used to fit the model is a less stringent form of external validation. The least stringent form of external validation involves using the first m of n observations for model training and using the remaining n-m observations as a test sample, which is similar to data-splitting (Harrell, 2015).

For ordinary multiple regression models, the R^2 index is a good measure of the model's predictive ability, especially when quantifying drop-off in predictive ability when applying the model to other datasets. Two major aspects of predictive accuracy need to be assessed: calibration (or reliability), which is the ability of the model to make unbiased estimates of outcomes, and discrimination, which is the model's ability to separate subjects' outcomes. Validation of the model is recommended even when a data reduction technique is used to ensure accuracy.

2.7.3 Reviewed Predictive Models

Table 2.2 summarizes five predictive models developed by previous researchers for estimating subgrade strength parameters using various testing methods. Regression modelling emerges as the most commonly used technique, with four of the five reviewed studies (Chai et al., 2013; Nazzal & Mohammad, 2010; Obafemi, 2004; Kumar et al., 2015) employing either simple or multiple linear regression approaches. Only Powell et al. (1986) used a finite element model, which required more complex input parameters. Chai et al. (2013) developed a linear regression model for thin bituminous pavements in Brisbane, Australia, correlating FWD deflection at 450 mm (D450) with DCP-derived CBR for specific AASHTO soil classes (A-2-4, A-2-7, and A-7-5). Nazzal and Mohammad (2010) proposed a regression model based on FWD back-calculated modulus and laboratory resilient modulus, reporting that the ratio between FWD elastic modulus and resilient modulus (E_{FWD}/M_R) ranged from 0.51 to 8.10. Obafemi (2004) developed regression models incorporating subgrade resilient modulus, air temperature, soil temperature, and moisture content for cold regions. Kumar et al. (2015) derived a regression model for Indian national highways relating DCP penetration to elastic modulus. Collectively, these studies demonstrate that while regression modelling is the preferred method due to its simplicity, interpretability, and ease of application, most existing models are location-specific, developed for particular soil types or climatic conditions, and none have been validated for Kenyan subgrade materials, which include black cotton clays, lateritic soils, and murram. Furthermore, only Chai et al. (2013) and Kumar et al. (2015) produced directly applicable predictive equations, while others reported correlations or ranges without providing explicit formulas for practical implementation.

Table 2.2: Predictive Models Reviewed

Researcher	Site Location	Sample selection criteria	Modelling Technique	Predictor (Data)	Predictive Model
Chai et al (2013)	Brisbane, Australia	A-2-7, A-7-5 and A-2-4 soils as per AASHTO Soil Classification System	Linear regression	FWD deflection D450 CBR from DCP test	CBR_{sub}= 2.6523 (D450) - 1.001
Nazzal, M.D and Mohammad, L.N. (2010).	Louisiana, US	Soils with similar properties	Regression model	FWD back calculated modulus Laboratory measured resilient modulus	E_{FWD}/M_R (Resilient Moduli) varies from 0.51 and 8.10
Powell et al (1986)	South Pars, Iran	Soils with Poisson ratio of 0.3	Finite element model	PLT and CBR	$E_{CBR} = \frac{1.46\left(1-v^{0.983}\right)\sigma_{\rho} r_{CB}}{u^{1.031}}$
Obafemi, B. (2004)	North Atlantic & North Central Regions, US	Cold regions with similar climatic conditions	Regression analysis	Subgrade resilient modulus, Air and soil temperatures and moisture content	$M_R = M_{R\,(mean)} + A \sin \frac{[2\pi (t}{365}$
Kumar et al (2015)	India	Different sections of National Highway during post monsoon season.	Regression model	DCP and CBR	Log (E_s in MPa) = 2.553– 0.6438x log (DCP_{60}°).

2.8 Factors Influencing the FWD-CBR Relationship

Various factors may influence the relationship between FWD deflection measurements and subgrade CBR values, including pavement structure, material properties, temperature, moisture content, and environmental conditions. Different relationships between FWD data and CBR developed for different countries vary, and this may be due to variations in prevailing soil types, drainage conditions, layer confinement, depth of testing, and procedures followed during testing (Kumar et al., 2015).

Research has shown that temperature affects the resilient modulus of subgrade soil as measured by FWD. Temperature affects both surface tension and matric suction, and hence resilient modulus (Obafemi, 2004). Similarly, moisture content significantly influences subgrade strength, with saturated subgrades exhibiting substantially lower CBR values than dry subgrades.

2.9 Challenges and Opportunities in Subgrade CBR Prediction

2.9.1 Challenges

Predicting subgrade CBR using FWD data offers benefits for pavement engineers in assessing pavement structural condition. However, several challenges and limitations exist: FWD data can vary due to factors such as equipment calibration, operator technique, and environmental conditions. This variability affects the accuracy of predicted CBR values. The natural properties of subgrade materials, including their stiffness, water content, and density, often vary considerably from one location to another. FWD technology is quite costly with significant cost implications both on the equipment and technical personnel involved.

2.9.2 Opportunities

Despite the challenges, many opportunities exist that can be exploited: Combining FWD measurements with data obtained using non-destructive technologies such as ground penetrating radar, seismic methods and geophysical can enhance the accuracy of the models.

2.10 Emerging Trends

Mechanistic-Empirical design methods that blend fundamental mechanical principles with observed data are being adopted in pavement engineering. These approaches simulate how pavements respond to different environmental conditions and loading scenarios, providing a more realistic basis for design. As concerns over climate change intensify, there is increasing attention on developing pavement designs that can withstand the effects of changing weather patterns and extreme events. Ensuring that subgrade performance predictions account for these climate-related factors is becoming a priority. Geographic information systems can be linked with pavement management systems to provide spatial visualisation of pavement data and offer valuable information for decision making.

2.11 Research Gaps

The literature reviewed reveals several gaps that justify the present study.

Limited locally-validated correlation models: Many studies have developed correlation models between FWD parameters and subgrade CBR, but there is a lack of models validated for Kenyan subgrade soils, which include black cotton clays, lateritic gravels, and murram. The existing models from Australia (Chai et al., 2013), the United States (Nazzal & Mohammad, 2010), and India (Kumar et al., 2015) were developed for specific soil types and climatic conditions that differ substantially from those in Kenya. No study has been carried out in Kenya comparing directly tested subgrade CBR with FWD deflections and back-calculated elastic modulus of subgrade layers.

Variability in FWD measurements: The variability in FWD measurements due to equipment calibration, operator technique, and environmental factors affects prediction accuracy. Further research is needed to quantify and mitigate these sources of variability for Kenyan conditions.

Non-uniform loading conditions: The dynamic loading applied by the FWD may not fully represent static loading conditions experienced in service. The effect of this discrepancy on CBR prediction accuracy has not been thoroughly investigated.

Limited validation studies: Many existing studies lack comprehensive validation across different pavement structures, materials, and environmental conditions. This study will include both internal and external validation using independent datasets.

Integration of advanced techniques: While emerging technologies such as machine learning offer opportunities for enhanced prediction, their application to FWD-CBR correlation for Kenyan soils has not been explored.

Absence of local standardization: There are no standardized protocols for subgrade CBR prediction using FWD data specific to Kenya, hindering comparability across studies and projects.

This study directly addresses the first gap (limited locally-validated correlation models) by developing predictive models for subgrade CBR from FWD deflection measurements using data from 18 road sections across Kenya, with at least 55 paired datasets for calibration and 20 for validation. The study will also contribute to addressing the second and fourth gaps by documenting variability sources and including rigorous validation.

2.12 Conceptual Framework

The conceptual framework in Figure 2-1 illustrates the relationships between independent variables, dependent variables, and intervening variables in this study, organized according to the input-process-output paradigm.

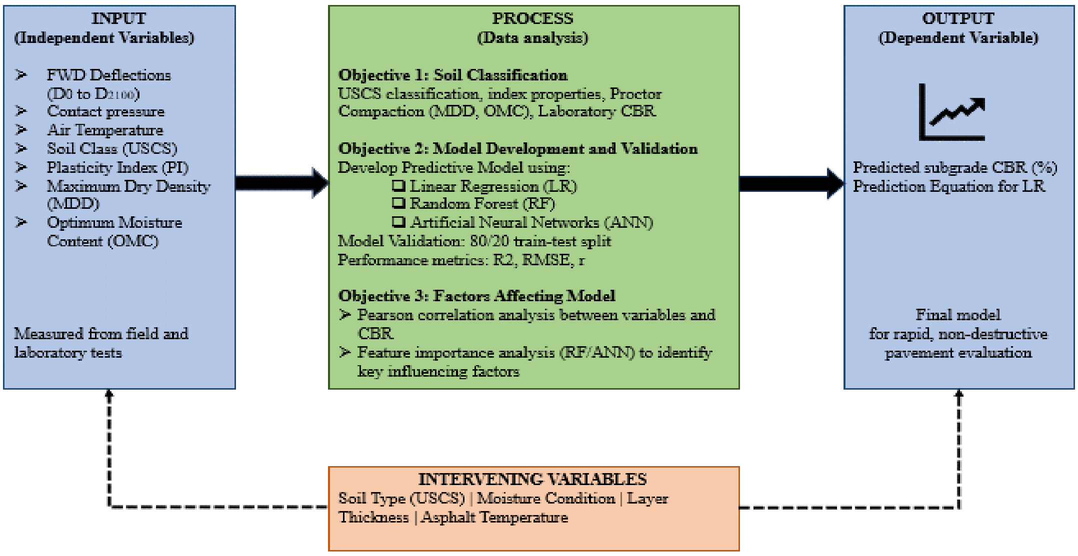

Figure 2.1: Conceptual Framework (Input-Process-Output)

The conceptual framework followed the input-process-output process: FWD deflection data (input) was processed through characterization, modelling, and factor analysis (process) to produce predicted subgrade CBR values (output), with soil type, moisture, layer thickness, and temperature acting as intervening variables.

CHAPTER THREE

MATERIALS AND METHODS

3.1 Overview

This chapter discusses the research design, study population and sampling technique, sources and types of data, equipment used, and methods of data collection and analysis. The chapter is organized according to the three specific objectives: characterization of subgrade materials, development and validation of predictive models for subgrade CBR from FWD data, and investigation of factors influencing the FWD-CBR relationship.

3.2 Research Design

Kothari (2004) defines a research design as the organization of conditions for data collection and analysis in a way that aims to combine the importance of the research purpose with economy. It is the conceptual arrangement within which research is carried out. This research employed a correlation research design by establishing a relationship between two related variables using existing data. In order to determine the relationship between variables, a correlation coefficient was used. The value of the correlation coefficient ranges between -1 and +1 whereby a coefficient of +1 indicates a positive relationship between two variables, while a value of -1 indicates a negative relationship.

3.3 Study Population and Sampling Technique

A sample of 18 road sections was selected from a group of 24 road sections covering various regions in Kenya using purposive sampling technique. Purposive sampling was preferred due to availability of data from recent pavement evaluation studies conducted by the Ministry of Roads and Transport. The selection criteria for the 18 road sections were: representation of common Kenyan subgrade soil types (black cotton clays, lateritic soils, and murram soils), and, availability of both FWD data and trenching data at the same locations. The 18 selected road sections are distributed across eight counties: Nairobi, Kiambu, Machakos, Kajiado, Nakuru, Uasin Gishu, Mombasa, and Kisumu. The specific locations of the 18 road sections are presented in Appendix 5. The study site locations are indicated in Figure 3-1.

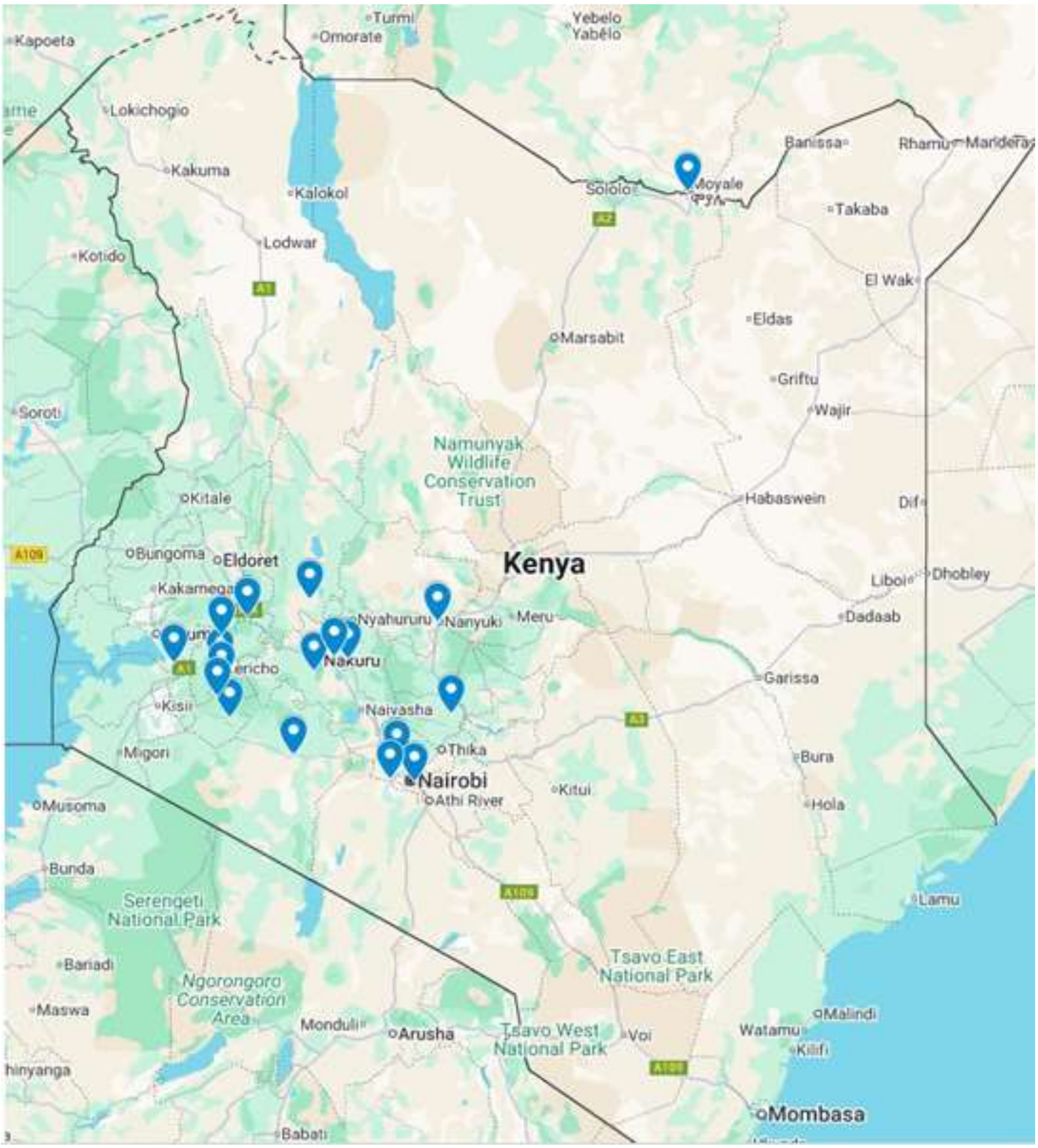

Figure 3.1: Map of Kenya Showing the Locations of the Study Sites

Figure 3-1 presents a map of Kenya with the 18 selected road sections marked. The blue markers indicate the specific test locations for each road section. The map shows the distribution of selected sections across the eight counties, with white labels identifying each road section by its assigned number (1 to 18).

3.4 Source and Type of Data

The study utilized secondary sources of data from the Ministry of Roads and Transport. The data included Falling Weight Deflectometer (FWD) data, trenching logs, laboratory test results, and construction data (including pavement layer thicknesses and material specifications).

3.5 Equipment

The following equipment was used to collect the required data: a Falling Weight Deflectometer (FWD) (Primax model, manufactured in Germany, meeting ASTM D4694-09 requirements) for field deflection measurements, a California Bearing Ratio (CBR) machine (ELE International model 36-3900) for determination of CBR of sampled soils in the laboratory, and a Dynamic Cone Penetrometer (DCP) for field determination of CBR during trenching. Additional equipment included a coring machine for pavement layer sampling and a plate bearing test apparatus. The equipment used for data collection is shown in Figures 3-2 through 3-7.

Figure 3.2: 9- and 14-geophone FWD (Primax, Germany)

Figure 3.3: Plate Bearing Test apparatus

Figure 3.4: Coring Machine

Figure 3.5: CBR Machine: (ELE International 36-3900)

Figure 3.6: DCP Equipment

Figure 3.7: Field Trenching

3.6 Data Collection and Analysis Methods by Objective

The data collection and analysis methods are organized according to the three specific objectives of the study.

3.6.1 Characterization of Subgrade Materials

To characterize subgrade materials from trench data, trenching and logging were carried out along the road sections at approximately 5 km intervals to confirm properties of the native subgrade. Trial pits were dug on the road shoulders to a depth of approximately 1.5 m below the finished road level.

Sample Preparation: The soil samples were sufficiently air dried to laboratory moisture conditions then sieved using a 5 mm sieve. To obtain a sample for sieve analysis, a riffle box was used where quartering of the sample was performed.

Index Properties: Several parameters including grain size distribution, Atterberg limits, and moisture content were considered in identifying the soil type and its likely engineering behavior in accordance with Das (2016). These parameters were important for classifying soils under the Unified Soil Classification System (USCS). The soil classification procedure involved the following steps. All data was compiled into a single spreadsheet capturing road name and location, trial pit number, depth of sample, chainage, density, moisture content, CBR, Atterberg limits, and particle size distribution. Values passing the 5 mm (No. 4) and 0.075 mm (No. 200) BS sieves were highlighted. Where more than 50 percent was retained on the No. 200 sieve, the soil was grouped under coarse-grained soils. Where 50 percent or more passed the No. 200 sieve, the soil was grouped under fine-grained soils. In this study, 167 samples were classified as fine-grained soils while 8 samples were classified as coarse-grained soils. Based on the Casagrande plasticity chart, a distinction was made between soils with liquid limit less than or greater than 50 (using symbol L for low and H for high) and between inorganic soil above the A-line. Using the plasticity chart, the point where values of plasticity index and liquid limit intersect was located, and the general group symbol was recorded (for example, MH or OH). Computations were performed to obtain gravel fraction, total coarse fraction, and sand fraction. Gravel fraction was computed as 100 minus the percentage passing the 5 mm sieve. Total coarse fraction was computed as 100 minus the percentage passing the 0.075 mm sieve. Sand fraction was computed as the total coarse fraction minus the gravel fraction divided by the total coarse fraction, multiplied by 100.

California Bearing Ratio (CBR): CBR, which is an empirical test that is widely used to estimate the strength of subgrade soils, has been found to be sensitive to soil type, compaction level and moisture condition (George et al., 2010), making it a practical yet variable indicator of subgrade performance. The CBR value of the materials used was obtained as follows: The mass of soil to be used in the CBR test was first determined using the Proctor compaction test. This was done by considering the maximum dry density (MDD) and optimum moisture content (OMC) as determined from the Proctor test. From this mass, the wet mass to use for three layers was determined. The actual mass of wet material per mould with an addition of 500 g was then determined. The dry mass per mould, which considered the total wet mass and the present moisture content, was determined. The water to be added when mixing was then determined as the product of the total dry mass and the difference between OMC and present moisture content (PMC). The measured-out sample was mixed with the determined amount of water. The soil sample was then placed in the mould in three uniform layers, with a filter paper placed at the bottom of the mould and on top of the sample. After compaction, the mould with the compacted soil was placed in a soaking tank for four days. The sample was removed after four days and allowed to drain water for approximately 15 minutes. The sample in the mould was then assembled in the loading machine, and penetration was carried out on both sides of the mould. The findings from the CBR test were used in this study to develop the prediction models. The other tested parameters (including particle size distribution, moisture content, field dry density, plasticity index, and soil class) were considered as intervening variables and were also used to explain the relationships in the prediction models.

3.6.2 Development and Validation of Predictive Models for Subgrade CBR Using FWD Data

Developing Predictive Models: Regression analysis was used to identify relationships between variables and to predict a variable. Regressions can be linear or non-linear. Regression can also be simple linear regression or multiple linear regression for identifying relationships for more variables (Hui, 2018). In this study, for the relationship $y = mx + c$, the values of m and c were determined by training a linear regression model using historical data. Y was the variable to predict (subgrade CBR), and x was the input variable (FWD deflections and back-calculated elastic modulus). FWD data from three points at the location of the trenches were obtained, and the average was computed. This data was used in developing the models. Multiple regression models were also developed by considering additional independent variables such as contact pressure, air temperature, MDD, OMC, plasticity index, and soil class. The contact pressure and air temperature values were recorded automatically by the FWD equipment. The CBR considered in developing the models was the actual CBR obtained from laboratory tests of materials from trenches. After training and testing the model, values of y were predicted by inputting values into x. In addition to regression models, other models were developed using machine learning tools, specifically Random Forest (RF) and Artificial Neural Networks (ANN).

FWD Data Collection: Data for deflection measurements was obtained from previous field surveys conducted using a Primax FWD which meets the requirements of ASTM D4694-09, using the test method defined in ASTM D4695-96. The deflection measurements were conducted on the Outer Wheel Path (OWP) at intervals of approximately 100 m. Readings were taken for nine geophones at each drop point. Normalization was conducted on FWD data from the test load to a standard load of 50 kN, which is equivalent to a standard pressure of 707 kPa. At each drop point, raw deflection readings were taken for the nine geophone points at offsets of 0, 200, 300, 600, 900, 1200, 1500, 1800, and 2000 mm, represented as D0, D200, D300, D600, D900, D1200, D1500, D1800, and D2000 respectively. Elastic modulus was obtained from back-calculated FWD data using RoSy design software. An average of three FWD readings was taken at the exact chainage where the trial pits were dug.

Validating Developed Predictive Models: Validation of the predictive models was performed to ensure that the models are accurate. External validation was carried out by splitting the dataset into two parts: a training (model development) sample and a test (model validation) sample using a random process. In this case, 80 percent of data from each road section was used for training the models, and the remaining 20 percent was used for testing the models. The R^2 score (coefficient of determination) and Root Mean Squared Error (RMSE) were used as measures of the models' predictive ability.

3.6.3 Investigation of Factors Influencing the FWD-CBR Relationship

Understanding and accounting for the factors that influence the relationship between FWD data and subgrade CBR is essential for accurately interpreting FWD data and predicting the CBR of subgrade soil in pavement design and maintenance practices. Some of the factors studied after developing the models included moisture content, degree of compaction (MDD), layer thickness for improved subgrade, temperature variations during field surveys, age and condition of pavement, environmental factors, and the FWD equipment used. The data was obtained from trench results and from FWD output data. Weather data relating to the specific days when the surveys were carried out was obtained from the FWD data captured during field surveys. The method of analysis was inferential statistics, where Pearson's correlation coefficient and p-value were used to determine relationships among measured variables. The Pearson correlation coefficient is a statistical measure that assesses variables importance by measuring the strength and direction of the linear relationship between each input variable and the target (CBR), where values closer to ±1 indicate stronger influence, and statistical significance is confirmed when the associated p-value is less than 0.05.

3.7 Data Processing and Analysis

Subgrade Surface Modulus Computation: Two formulas were used to compute the subgrade surface modulus. The first formula for subgrade surface modulus was applied on values at offset distances (E_n) as shown in equation 3.1:

Equation 3.1: Subgrade surface modulus (offset distances)

$$E_n = ((1 - 0.35^2) \times 150 \times 150 \times P) / (200 \times G_n) \text{ ………… Equation 3.1}$$

Where: P is the contact pressure in kPa; 150 mm is the radius of the load plate; and, G_n is the deflection at each offset distance from 200 mm to 2100 mm from the centre of the load plate. Poisson's ratio was taken as 0.35 for subgrade soils.

The second formula for subgrade surface modulus was applied on values taken at the load plate position (E_0) as shown in equation 3.2:

Equation 3.2: Subgrade Surface Modulus (load plate position)

$$E_0 = (2 \times (1 - 0.35^2) \times 150 \times P) / G_0 \text{ ………………….. Equation 3.2}$$

where G_0 is the deflection at the load plate position.

The subgrade modulus was of critical importance in determining the strength of the subgrade soil and the behaviour of the material, which then informed the model that would be developed.

Analysis Methods: The data was tabulated, interpreted, and analyzed using quantitative methods. Data was analyzed and displayed graphically using Microsoft Excel and Microsoft Word. Table 3.1 shows the standards used in carrying out the tests and the software for analysis. Table 3.2 shows the dependent and independent variables as well as the presentation of the data. Table 3.3 illustrates the data required for each objective, the method used, and the expected output.

Table 3.1: Analysis Software and Test Standards

Test	Relationship	Analysis Software	Test Standard
FWD	$E_r = \frac{P(1-\mu^2)}{\pi r D_r}$ ……*Equation 3.3* Where: D_r = surface deflection at offset r due to load P; P = point load; μ=Poisson's ratio; and, r = horizontal offset from the load.	RoSy, BAKFAA	ASTM D4694-09,1996 and ASTM D4695-03,2008
Lab CBR Test	CBR = (P_T/P_S) x 100 …….*Equation 3.4* Where: P_T = Corrected test load corresponding to the chosen penetration from the load penetration curve. P_S = Standard load for the same penetration	Ms Excel	BS1377-4:1990

Table 3.2: Methods of Data Analysis and Presentation

Objective	Variable Independent	Dependent	Method of analysis	Presentation
1. To characterize subgrade materials from the trench data	PSD, MC, FDD, PI, PM, RC, DCP CBR, Lab CBR	Subgrade Class	Mean, Percentages	Tables, Graphs
2. To develop and validate predictive models for subgrade CBR from FWD data	Deflections D600, contact pressure, air temperature, soil properties	CBR	Regression analysis, Machine learning, Statistical analysis, Correlation analysis	Tables, Graphs, Regression model, RF model, ANN model, R^2, RMSE, P-value, correlation coefficients
3. To investigate the factors that influence the relationship between FWD data and subgrade CBR	MDD, MC, MDD, PI, Soil Class, Lab CBR,	Predicted CBR	Pearson's correlation coefficient	Tables

Table 3.3: Data Source and Methodology for Each Objective

Objective	Data required	Source	Method	Expected Output
Characterization of materials	i) Grading to 0.075 mm sieve; ii) Atterberg limit tests; iii) Compaction tests (Standard compaction 2.5 kg rammer); and, iv) 4-days soak CBR	Lab data	i) UCS for classification iii) Percentages and means	i) Classified soils ii) Data sets
Predictive models and validation	i) Deflections at points of 0, 20, 30, 60, 90, 120, 150, 180 and 200 cm ii) Contact pressure and Air temperature from FWD data iii) MDD, OMC, PI, Soil Class	i) FWD data ii) Lab data	i) Regression analysis using Ms Excell and R-software; ii) Machine learning using Python software; iii) Inferential statistics iv) Back-calculation using Rosy and BAKFAA	i) Models showing input variables and output variables ii) R^2 index, iii) RMSE iv) Correlation coefficient, iv) P-value
Factors that influence relationship between FWD and CBR	i) Moisture content; ii) Degree of compaction; iii) Layer thickness for improved subgrade; iv) Temperature variations during field surveys;	i) Trench data ii) FWD data iii) Weather (Met) data iv) Construction data	Inferential statistics	i) Pearson's correlation coefficient ii) P-value

CHAPTER FOUR

RESULTS AND DISCUSSION

4.1 Overview

This chapter presents the results obtained for each objective and discusses the findings in relation to previous studies. The discussion is integrated within this chapter rather than presented separately. The chapter is organized according to the three specific objectives: characterization of subgrade materials, development and validation of predictive models for subgrade CBR from FWD data, and investigation of factors influencing the FWD-CBR relationship.

4.2 Characterization of Subgrade Materials

Soil classification was performed for 18 road sections selected from a group of 24 road sections. The initial group of 24 road sections was assessed for data availability and quality, from which 18 sections with complete datasets (both FWD and laboratory CBR data at matching chainages) were retained for analysis. Table 4.1 presents the soil classification results for the 18 selected road sections, showing the average plasticity index (PI), liquid limit (LL), optimum moisture content (OMC), maximum dry density (MDD), percentage passing No. 4 sieve, percentage passing No. 200 sieve, and Unified Soil Classification System (USCS) class. Raw data for individual trial pits is presented in Appendix 6. The values shown above are means for each road section. Figure 4-1 presents the percentage distribution of soil types from all trial pits.

Table 4.1: Soil Classification for 18 Road Sections (mean values)

Road No.	Location	Avg PI	Avg LL	Avg OMC	Avg MDD	Avg % Passing No.4	Avg. % Passing No. 200	Soil Class (UCS)
1	Nakuru/Nyandarua	23	55	24	1382	91	54	4MH, CH, CL
2	Rift Valley/Kisumu	13	40	14	1761	63	22	7ML, 3CL
3	Marsabit	23	55	16	1699	66	26	2MH, CL, GM, GH
4	Kericho, Bomet	22	52	23	1371	91	70	3MH, 2CH, CL &ML
5	Nakuru, Baringo	12	40	21	1428	94	56	4ML & 2CL
6	Nakuru, Narok	16	42	25	1305	95	52	4CL &2ML
7	Narok	16	42	25	1250	92	58	5ML, 4CL, MH & CH
8	Nakuru, Nyandarua, Laikipia	21	56	22	1354	91	68	5MH, CH, ML
9	Laikipia	20	48	21	1401	95	66	4MH, ML, CL
10	Baringo, Elgeyo Marakwet	22	49	21	1305	96	84	3CL, 2MH
11	Nairobi	27	55	30	1332	92	78	5CH, 3MH, CL
12	Nairobi	18	50	17	1559	76	56	2CL, MH, ML
13	Homa Bay	14	41	13	1801	87	30	3CL, MH, ML
14	Bomet, Kericho	16	50	19	1533	90	59	3MH, CL &ML
15	Kisumu	16	40	22	1563	83	42	2CL, ML
16	Kericho,Kericho	21	47	19	1779	64	32	3CL, 3ML, CH, MH
17	Murang'a	23	52	25	1419	86	52	9MH, 5CH, 7CL,
18	Kikuyu	23	47	27	1396	100	77	4CL, CH, MH

Lean clay (CL) was the predominant soil class, appearing in 34 percent of trial pits, followed by elastic silt (MH) at 33 percent. All road sections except Road No. 11 had at least one trial pit with soil classified as lean clay (CL). The average plasticity index ranged from 7 to 27 percent, OMC ranged from 12 to 30 percent, MDD ranged from 1250 to 1821 kg/m^3, and laboratory CBR ranged from 5 to 55 percent. These findings are consistent with Vasudeva Rao et al. (2019), who characterized subgrade soils for road expansion in Ethiopia using the AASHTO classification system and found predominantly silt and clay type materials. The presence of multiple soil types within individual road sections (as shown in Table 4.1) indicates the spatial variability of subgrade conditions in Kenya, which justifies the need for dense sampling and predictive modelling approaches.

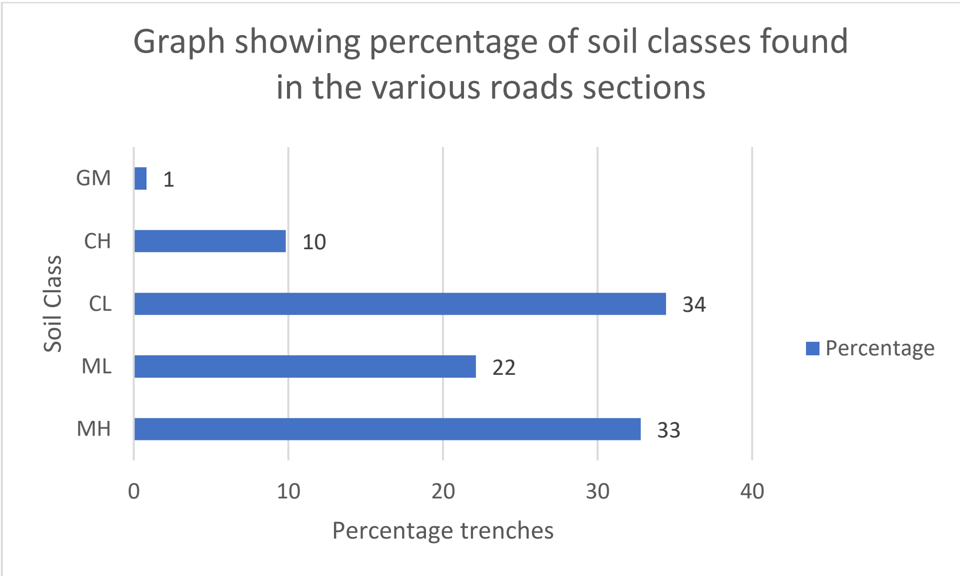

Figure 4.1: Distribution of Soil Types across all Trial Pits

Lean clay (CL) constituted 34 percent, elastic silt (MH) constituted 33 percent, silt with sand (ML) constituted 18 percent, fat clay (CH) constituted 12 percent, and other soils (GM, GC, SC) constituted 3 percent. This distribution confirms that fine-grained soils dominate Kenyan subgrade conditions, with clay and silt materials accounting for 97 percent of samples.

The engineering implications of this soil distribution are significant. Fine-grained soils, particularly those with high plasticity (CH and MH), are susceptible to moisture-induced volume changes and strength loss when saturated. Accurate characterization of these soils is therefore critical for pavement design. The wide range of OMC (12 to 30 percent) and MDD (1250 to 1821 kg/m³) reflects the diversity of compaction characteristics across different geological regions of Kenya, from the volcanic soils of the Rift Valley and Central to the calcaric soils of Nanyuki region.

4.3 Development and Validation of Predictive Models for Subgrade CBR

4.3.1 Deflection Characteristics

Deflection measurements were recorded using nine geophones at offsets ranging from 0 mm to 2100 mm from the centre of the loading plate. Table 4.2 presents the mean deflections for each road section. Complete deflection data for all 18 road sections is presented in Appendix 7.

Table 4.2: Mean Deflections in µm at Nine Geophone Offsets (selected road sections)

Rd No.	D0	D200	D300	D600	D900	D1200	D1500	D1800	D2100
1	657	400	274	119	70	48	36	31	26
2	367	145	126	98	90	74	61	48	31
3	532	456	314	206	124	78	62	49	30
5	1139	888	734	445	303	226	188	167	154
7	671	453	349	164	111	82	67	57	48
16	786	379	250	144	96	66	54	45	39

The deflection values varied substantially across road sections, with mean peak deflections (D0) ranging from 367 µm (Road 2) to 1139 µm (Road 5). This variation reflects differences in pavement structural capacity, subgrade strength, and pavement age. Higher deflections generally indicate weaker pavement structures or softer subgrade conditions.

4.3.2 Deflection Bowls and Material Behaviour

Deflection bowls were developed for all road sections to study deflection behaviour and identify the appropriate model type (linear or non-linear). Figure 4-2 presents deflection bowls for road sections 1 to 18.

4.3.2.1 Deflection Bowls

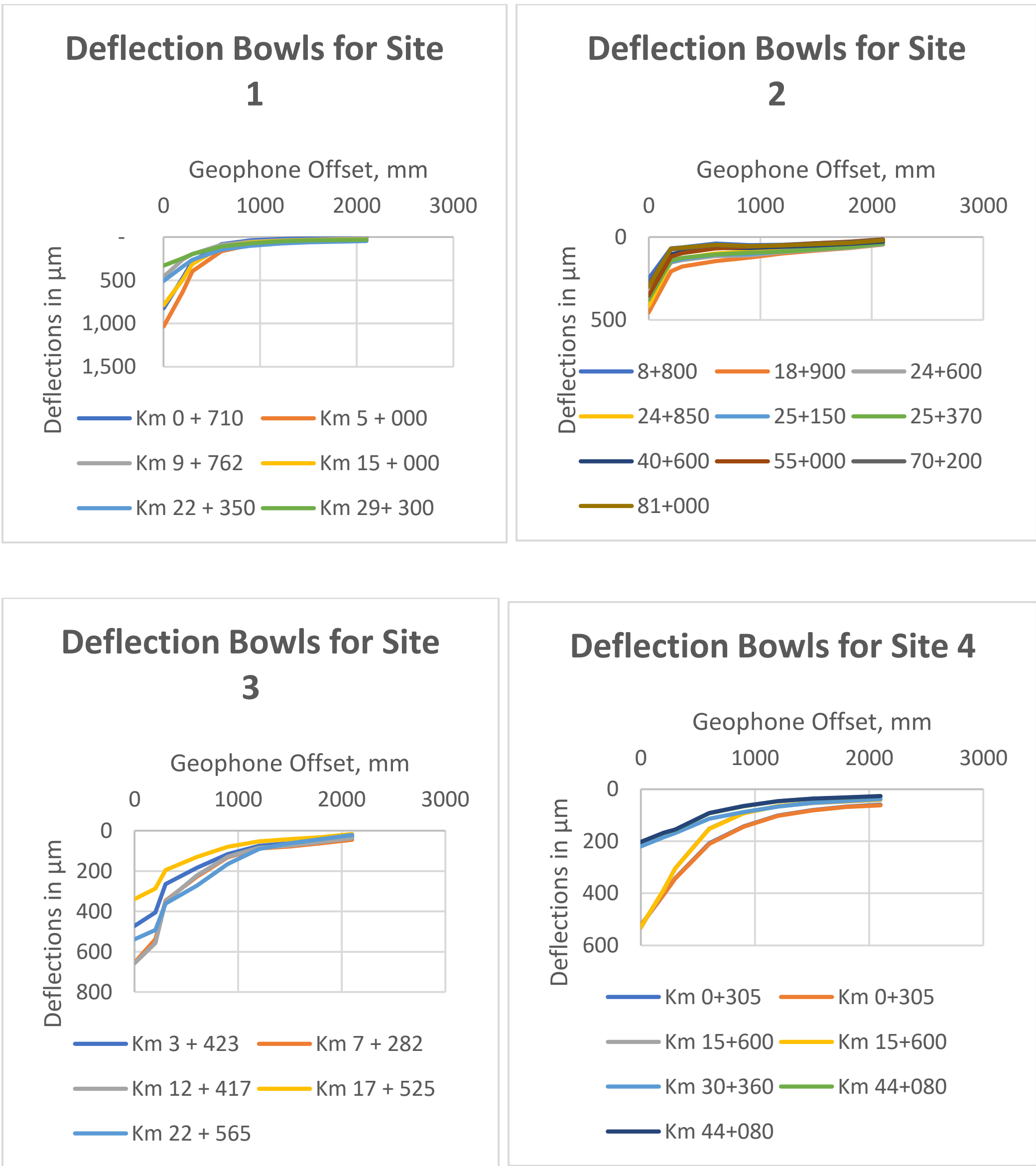

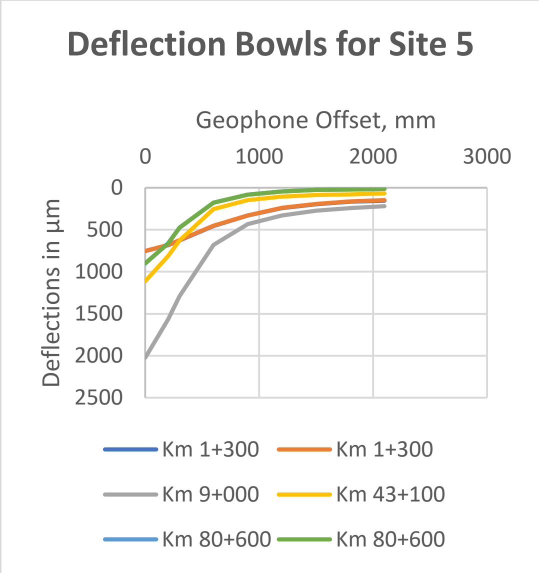
Deflection Bowls for Site 5
Geophone Offset, mm
0
1000
2000
3000
0
500
1000
1500
2000
2500
Deflections in µm
Km 1+300
Km 1+300
Km 9+000
Km 43+100
Km 80+600
Km 80+600

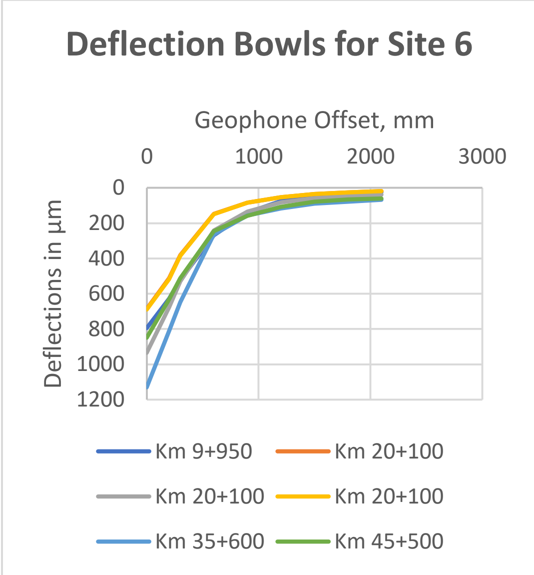
Deflection Bowls for Site 6
Geophone Offset, mm
0
1000
2000
3000
0
200
400
600
800
1000
1200
Deflections in µm
Km 9+950
Km 20+100
Km 20+100
Km 20+100
Km 35+600
Km 45+500

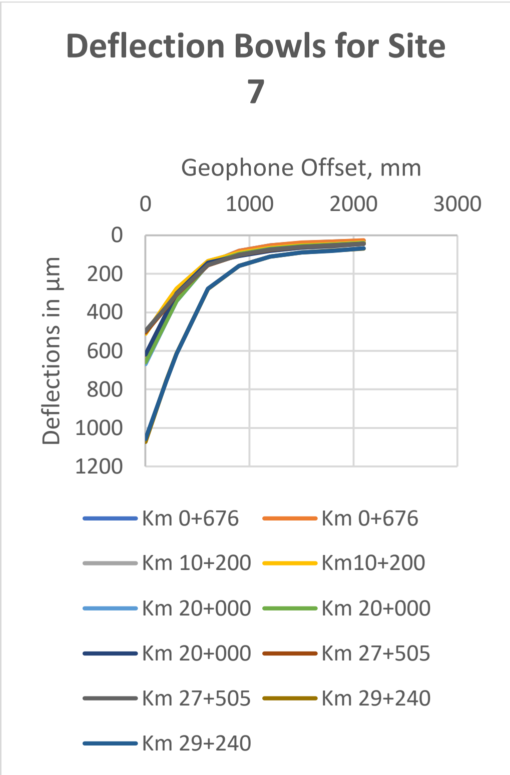
Deflection Bowls for Site 7
Geophone Offset, mm
0
1000
2000
3000
0
200
400
600
800
1000
1200
Deflections in µm
Km 0+676
Km 0+676
Km 10+200
Km10+200
Km 20+000
Km 20+000
Km 20+000
Km 27+505
Km 27+505
Km 29+240
Km 29+240

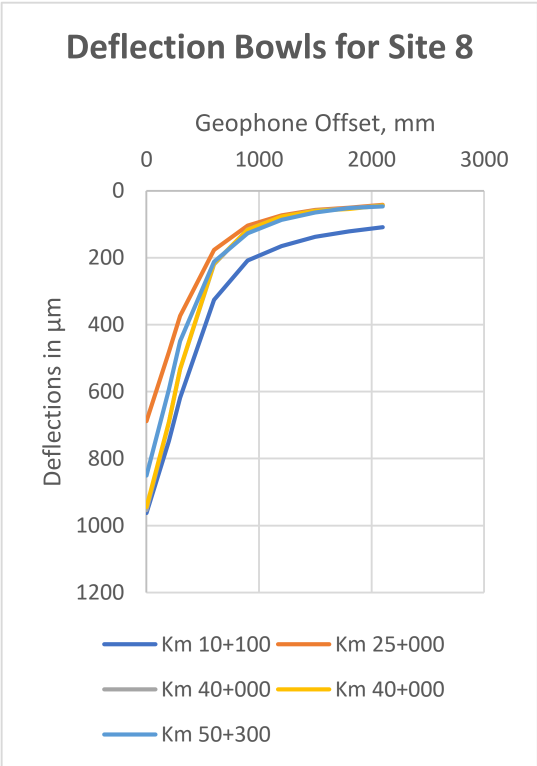
Deflection Bowls for Site 8
Geophone Offset, mm
0
1000
2000
3000
0
200
400
600
800
1000
1200
Deflections in µm
Km 10+100
Km 25+000
Km 40+000
Km 40+000
Km 50+300

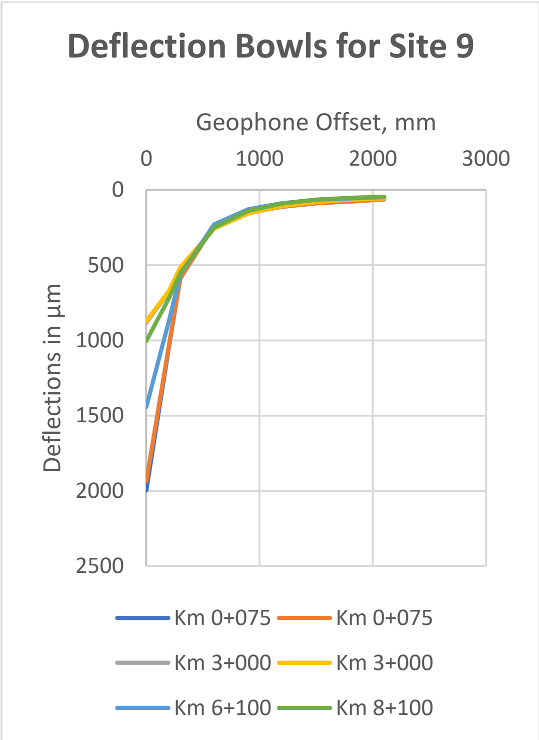
Deflection Bowls for Site 9
Geophone Offset, mm
0
1000
2000
3000
0
500
1000
1500
2000
2500
Deflections in µm
Km 0+075
Km 0+075
Km 3+000
Km 3+000
Km 6+100
Km 8+100

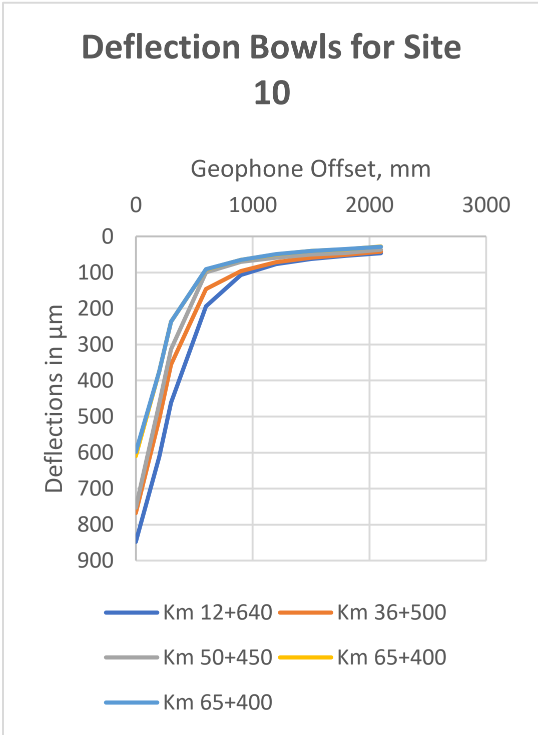
Deflection Bowls for Site 10
Geophone Offset, mm
0
1000
2000
3000
0
100
200
300
400
500
600
700
800
900
Deflections in µm
Km 12+640
Km 36+500
Km 50+450
Km 65+400
Km 65+400

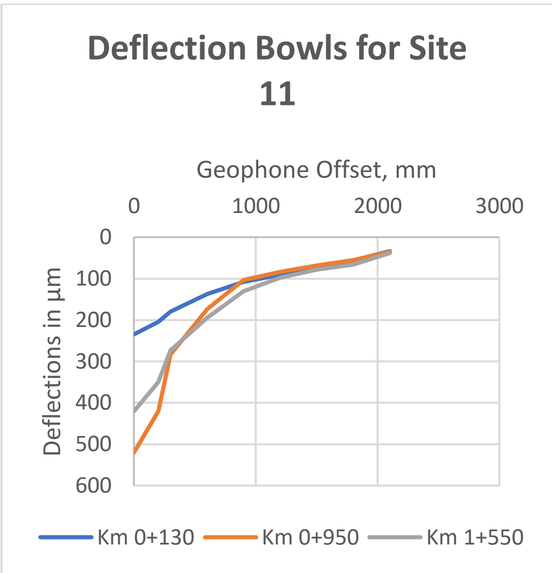
Deflection Bowls for Site 11
Geophone Offset, mm
0
1000
2000
3000
0
100
200
300
400
500
600
Deflections in µm
Km 0+130
Km 0+950
Km 1+550

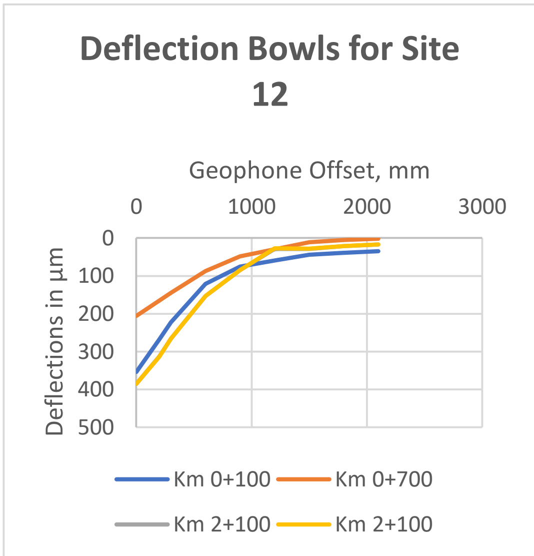
Deflection Bowls for Site 12
Geophone Offset, mm
0
1000
2000
3000
0
100
200
300
400
500
Deflections in µm
Km 0+100
Km 0+700
Km 2+100
Km 2+100

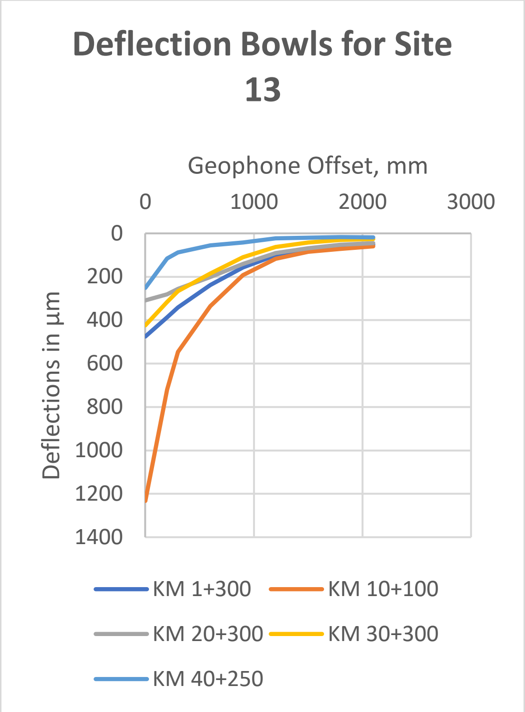
Deflection Bowls for Site 13
Geophone Offset, mm
0
1000
2000
3000
Deflections in µm
0
200
400
600
800
1000
1200
1400
KM 1+300
KM 10+100
KM 20+300
KM 30+300
KM 40+250

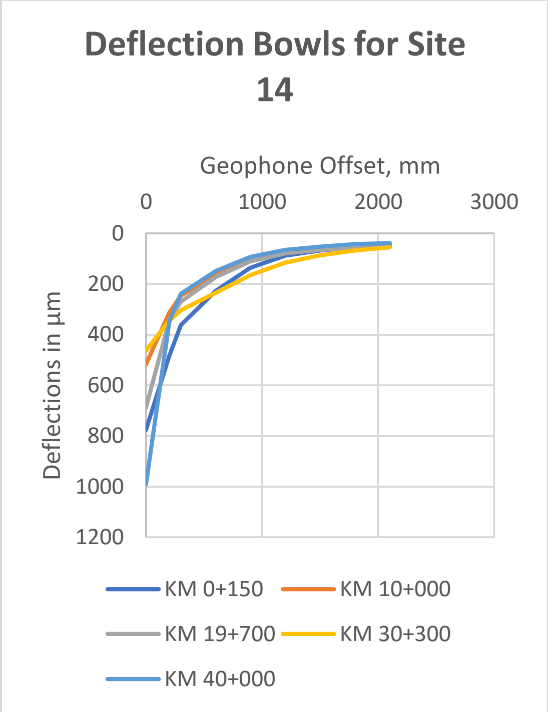
Deflection Bowls for Site 14
Geophone Offset, mm
0
1000
2000
3000
Deflections in µm
0
200
400
600
800
1000
1200
KM 0+150
KM 10+000
KM 19+700
KM 30+300
KM 40+000

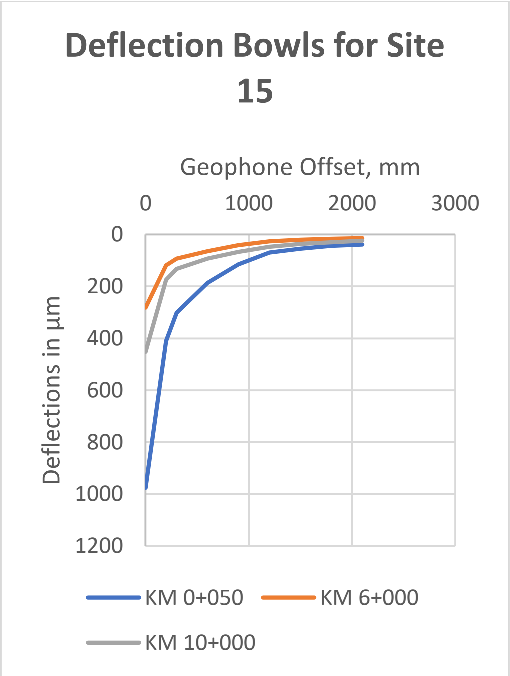
Deflection Bowls for Site 15
Geophone Offset, mm
0
1000
2000
3000
Deflections in µm
0
200
400
600
800
1000
1200
KM 0+050
KM 6+000
KM 10+000

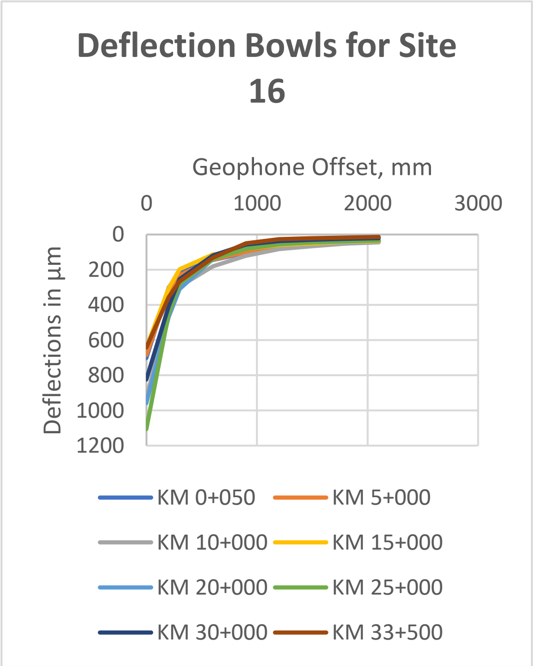
Deflection Bowls for Site 16
Geophone Offset, mm
0
1000
2000
3000
Deflections in µm
0
200
400
600
800
1000
1200
KM 0+050
KM 5+000
KM 10+000
KM 15+000
KM 20+000
KM 25+000
KM 30+000
KM 33+500

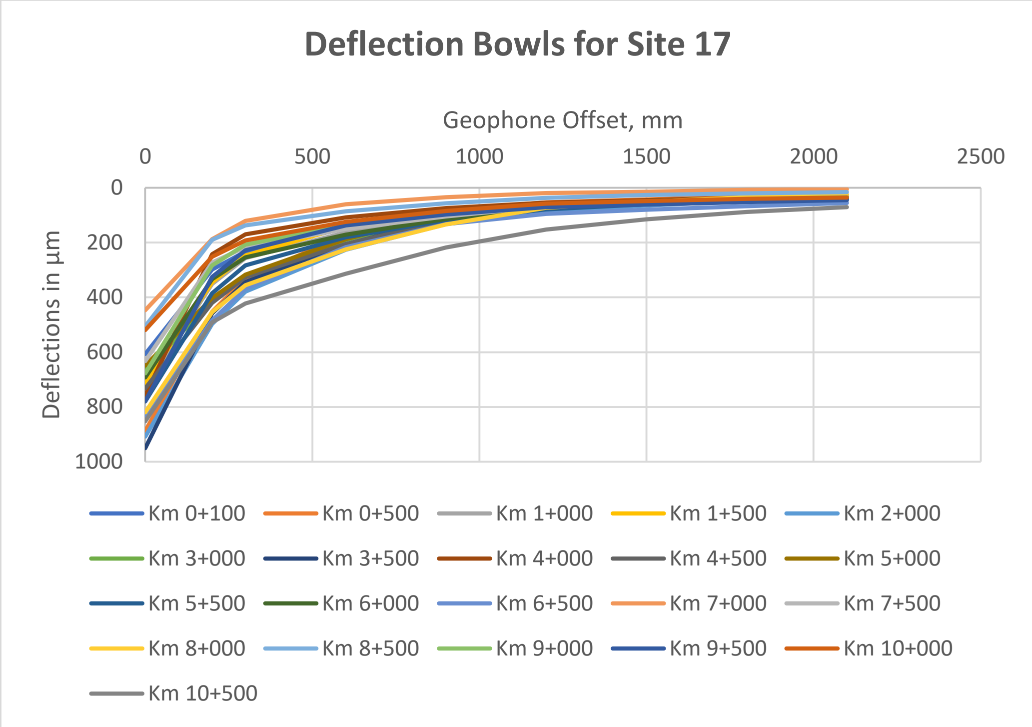

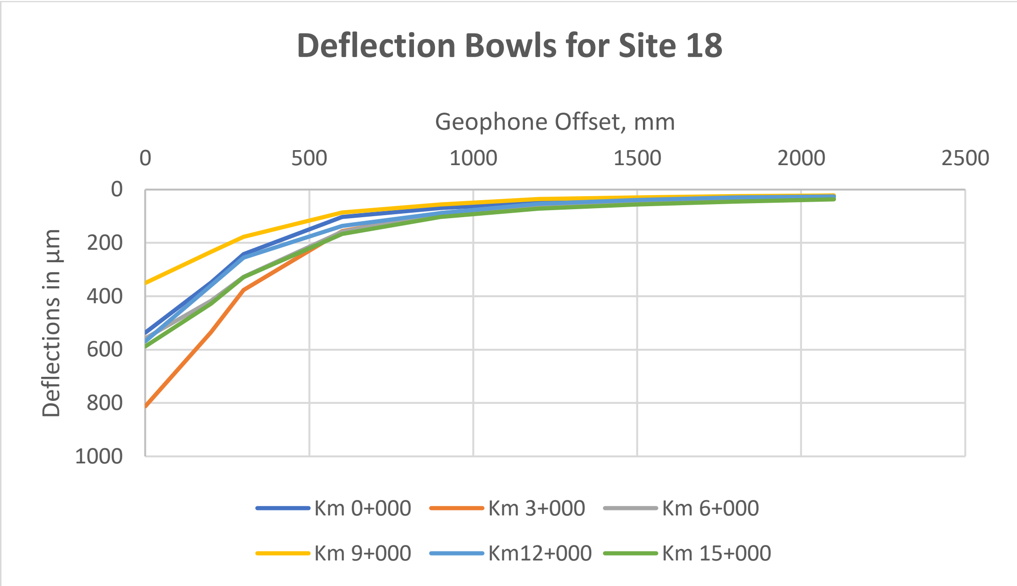

Figure 4.2: Deflection Bowls for Road Site 1 to Road 18

Figure 4-2 shows the deflection bowl profiles for 18 road sections. The deflection bowls exhibit a characteristic shape with peak deflection at the centre (D0) and decreasing deflections with increasing radial distance from the load. Road section 5 shows the highest deflections across all geophone positions, indicating a relatively weak pavement structure or soft subgrade. Road section 2 shows the lowest deflections, indicating a stiffer pavement structure. The rate of decay of the deflection bowl from D0 to D200 is steepest for Road 2, suggesting a stiff asphalt layer over a relatively weaker lower section, while Road 5 shows a more gradual decay, indicating a more uniform stiffness distribution.

4.3.2.2 Deflection Ratios

The deflection ratios (DR) were computed to assess the linearity or non-linearity of material behaviour. Table 4.3 presents the mean deflection ratios across all road sections. Complete deflection ratios for all 18 road sections are presented in Appendix 8.

Table 4.3: Mean Deflection Ratios across Selected Road Sections

Rd No	**D0/D200**	**D200/D300**	**D300/D600**	**D600/D900**	**D900/D1200**	**D1200/D1500**	**D1500/D1800**	**D1800/D2100**
1	1.60	1.45	2.41	1.71	1.47	1.36	1.16	1.24
2	3.03	1.13	1.33	1.02	1.16	1.22	1.27	1.69
3	1.17	1.50	1.47	1.67	1.58	1.23	1.31	1.69
5	1.26	1.25	2.09	1.73	1.57	1.38	1.21	1.23
7	1.43	1.28	2.16	1.59	1.42	1.26	1.15	1.21
16	2.14	1.48	1.86	1.77	1.52	1.24	1.22	1.17

The deflection ratios for D600/D900 (mean of 1.45 across all roads) and D900/D1200 (mean of 2.41) showed notable variance. This variance indicates non-linear behaviour of the pavement materials, suggesting that a linear regression model alone may not fully capture the relationship between FWD deflections and subgrade CBR. This finding is consistent with Chai et al. (2013), who observed similar non-linearity in thin bituminous pavements in Australia. The implication for model development is that machine learning approaches (Random Forest and Artificial Neural Networks), which can capture non-linear relationships, should be considered alongside linear regression.

4.3.3 Subgrade Surface Modulus

The subgrade surface modulus was computed at each geophone offset using Equation 3.1. Table 4.4 presents the mean subgrade surface modulus values across selected road sections. Figure 4-3 shows the graphical representation of the subgrade surface modulus for selected road sites. Complete surface modulus and graphical representation for all 18 road sections is presented in Appendix 9 and 10 respectively.

Table 4.4: Mean Subgrade Surface Modulus in MPa at Geophone Offsets (selected road sections)

Rd No	E0	E200	E300	E600	E900	E1200	E1500	E1800	E2100
1	341	200	185	221	255	272	286	261	278
2	540	686	517	371	233	200	196	210	306
3	372	163	164	119	133	155	149	167	250
5	197	90	77	83	105	146	186	209	232
7	311	172	149	160	164	171	173	167	176
16	213	173	169	154	172	198	199	208	209

Figure 4-3 shows the graphical representation of the subgrade surface modulus for selected road sites.

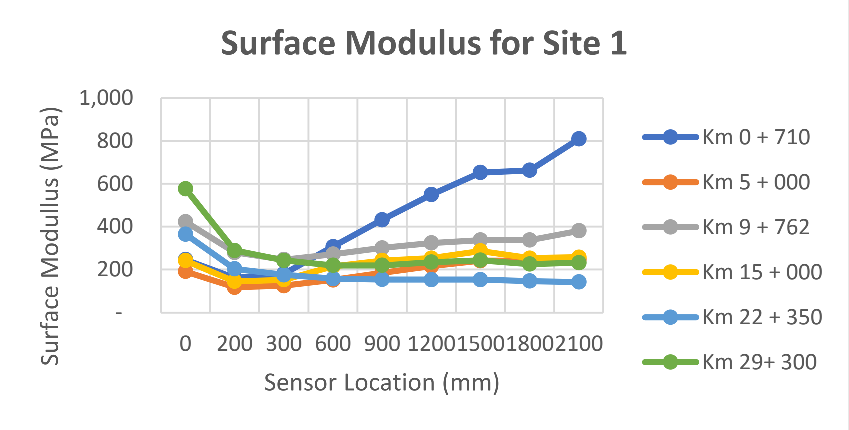

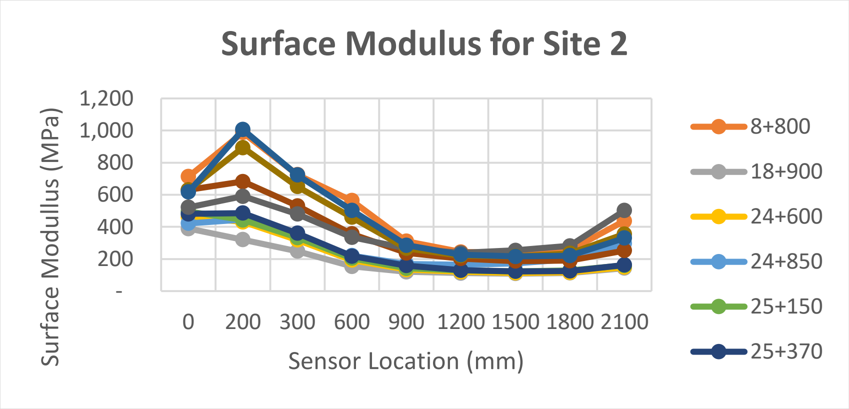

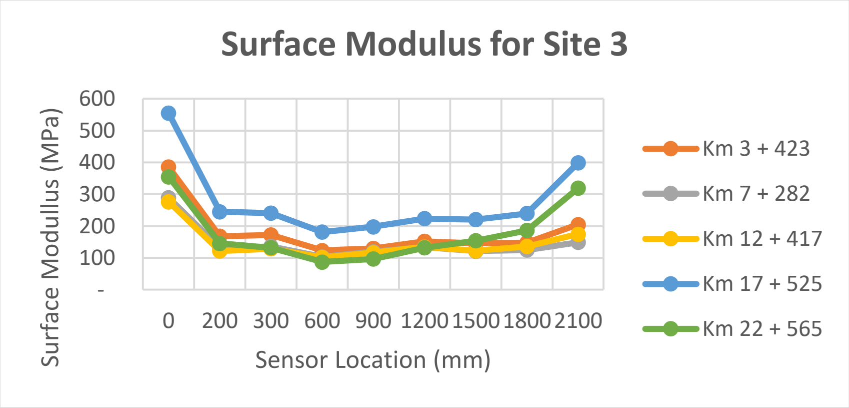

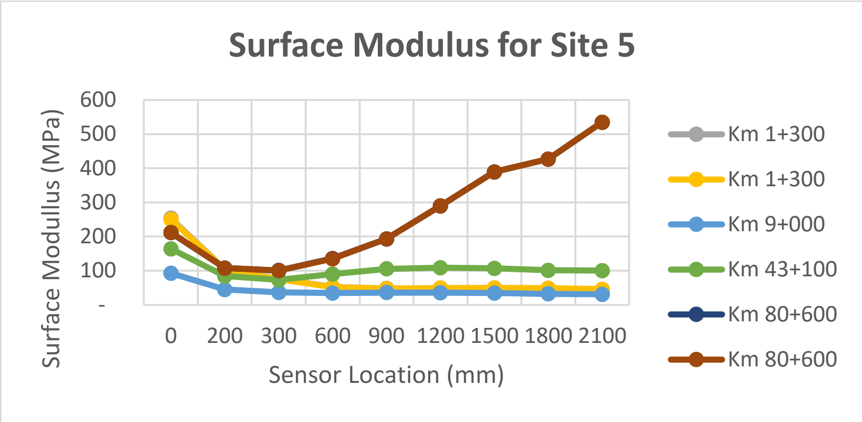

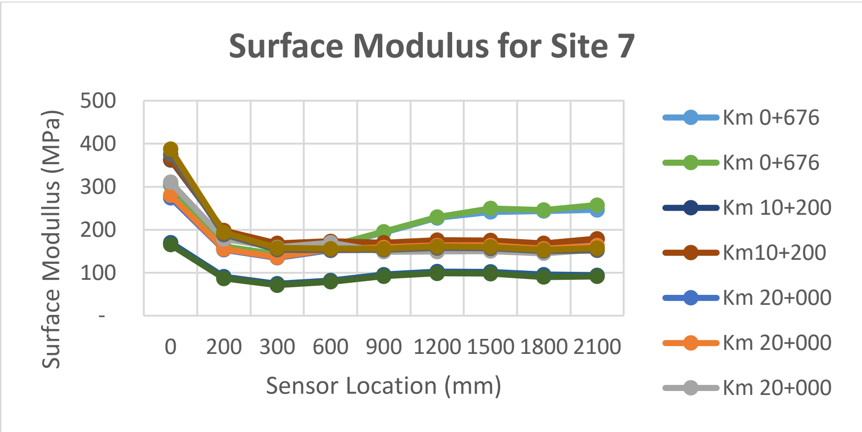

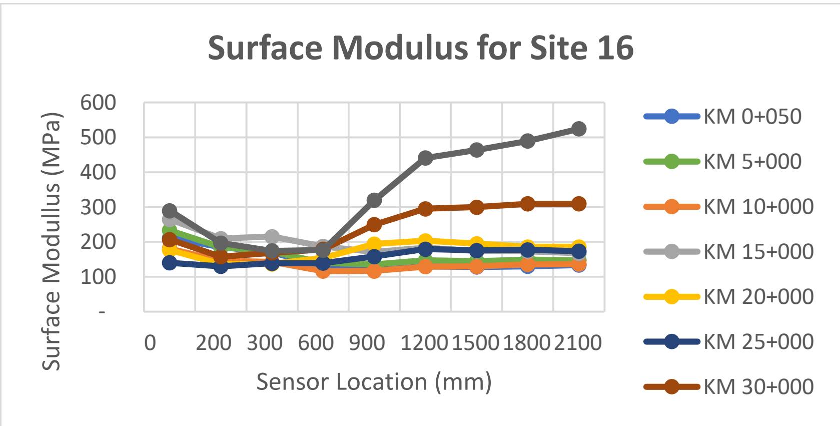

Figure 4.3: Subgrade Surface Modulus

The subgrade surface modulus decreased as the distance from the load plate increased up to approximately 600 mm (E600). Beyond 600 mm, the modulus began to increase as the distance increased. This behaviour is consistent with the findings of Chai et al. (2013), who observed that surface modulus decreased with stress level up to a distance of about 450 mm from the centre of the loading plate, after which the modulus increased as stress level decreased. This phenomenon indicates non-linear stress-dependent behaviour of the subgrade and pavement materials, where the material stiffness varies with the applied stress level. The engineering implication is that deflection measurements at the 600 mm offset (D600) are particularly informative for subgrade characterization, as this represents the transition point in material behaviour.

4.3.4 Model Development

Eleven predictive models were developed using three techniques: Linear Regression (LR), Random Forest (RF), and Artificial Neural Networks (ANN). The models were categorized into four groups based on the independent variables used, as shown in Table 4.5. The dataset of 70 paired observations was split into 80 percent for training (56 observations) and 20 percent for testing (14 observations). Figure 4-4 illustrates the predictions made using all models and Figure 4-5 shows the predictions made from LR model 5. The detailed predicted values are presented in Appendix 11.

Table 4.5: Summary of Developed Models

Model Group	Model No.	Technique	Independent Variables	Dependent Variable
1	1, 2, 3	RF, LR, ANN	D600, Contact Pressure, Air Temperature	CBR
2	4, 5, 6	RF, LR, ANN	D600, Contact Pressure, Air Temperature, MDD, OMC	CBR
3	7, 8, 9	RF, LR, ANN	D600, Contact Pressure, Air Temperature, MDD, OMC, Soil Class, PI	CBR
4	10, 11	RF, LR	D600 only	CBR

Numerical soil classes were allocated for ease of analysis as follows: MH – 1, ML – 2, CL – 3, CH – 4 and GM - 5

Table 4.6: Statistical Performance of Developed Models

Model Group	**Model No.**	**Technique**	**Pearson's r**	**R^2 Score**	**RMSE (%)**
A	1	RF	0.600	0.300	9.35
A	2	LR	0.112	0.006	11.14
A	3	ANN	-0.080	-0.157	12.02
B	4	RF	0.823	0.575	7.29
B	5	LR	0.844	0.611	6.97
B	6	ANN	0.813	0.592	7.14
C	7	RF	0.830	0.596	7.10
C	8	LR	0.824	0.582	7.23
C	9	ANN	0.807	0.554	7.46
D	10	RF	0.235	-0.050	11.45
D	11	LR	0.133	0.014	11.10

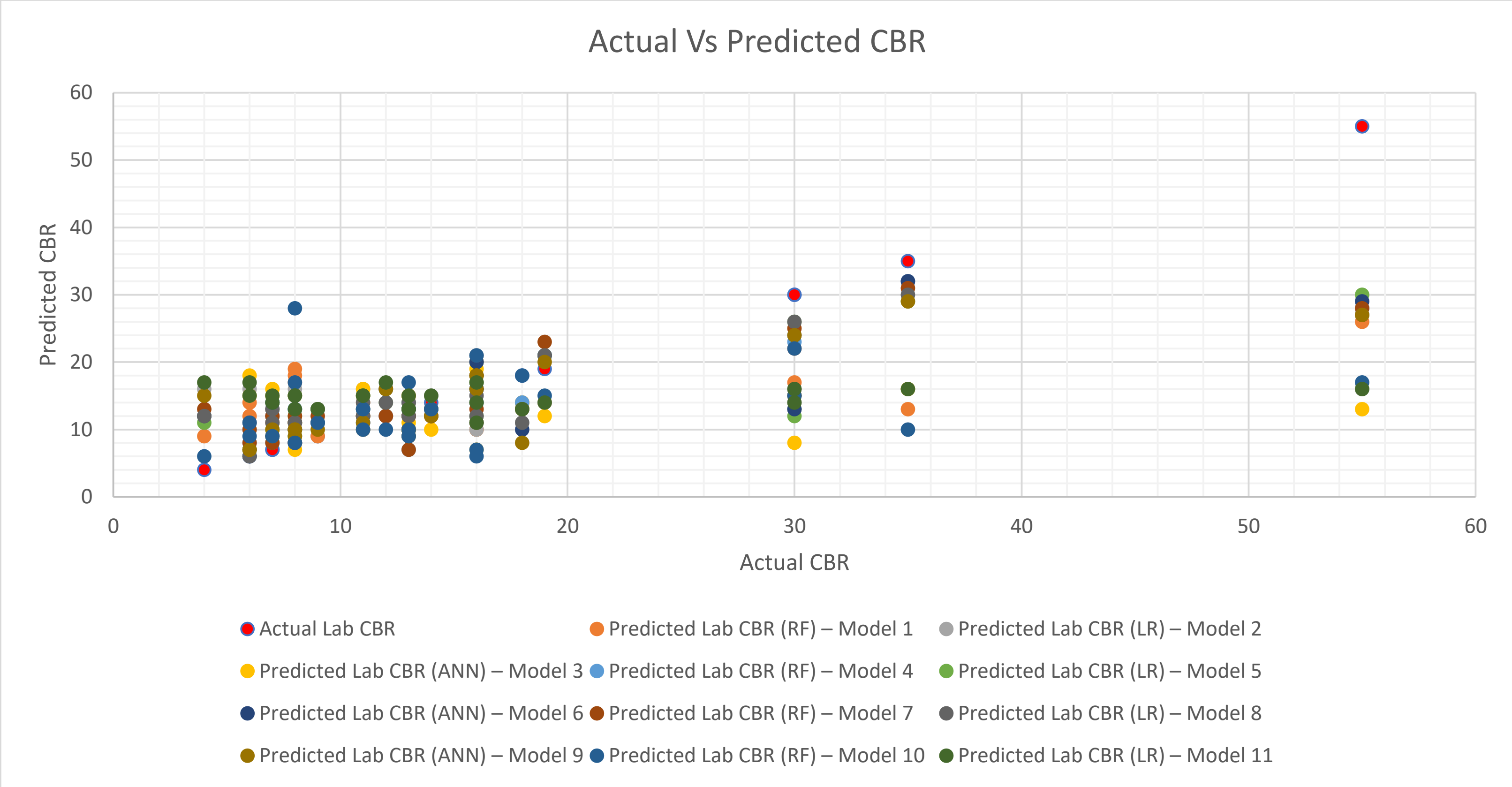

Figure 4.4: Predicted vs. Measured CBR for Model 1 to 11

4.3.5 Model Performance Analysis

Models in Group 2 (incorporating D600, contact pressure, air temperature, MDD, and OMC) demonstrated the best overall performance. Model 5 (Linear Regression) achieved the highest R^2 score of 0.611 and the lowest RMSE of 6.97 percent, indicating that it explained 61.1 percent of the variance in laboratory CBR values with an average prediction error of approximately 7 percent. The Pearson correlation coefficient of 0.844 for Model 5 indicates a strong positive correlation between predicted and laboratory CBR values.

Models in Group 1, which excluded MDD and OMC, performed poorly with R^2 values below 0.3 and high RMSE values above 9 percent. This finding highlights the critical importance of MDD and OMC as input variables for accurate CBR prediction. Models in Group 3, which added soil class and plasticity index, did not show substantial improvement over Group 2 models, suggesting that the additional soil property variables did not add significant predictive power beyond MDD and OMC.

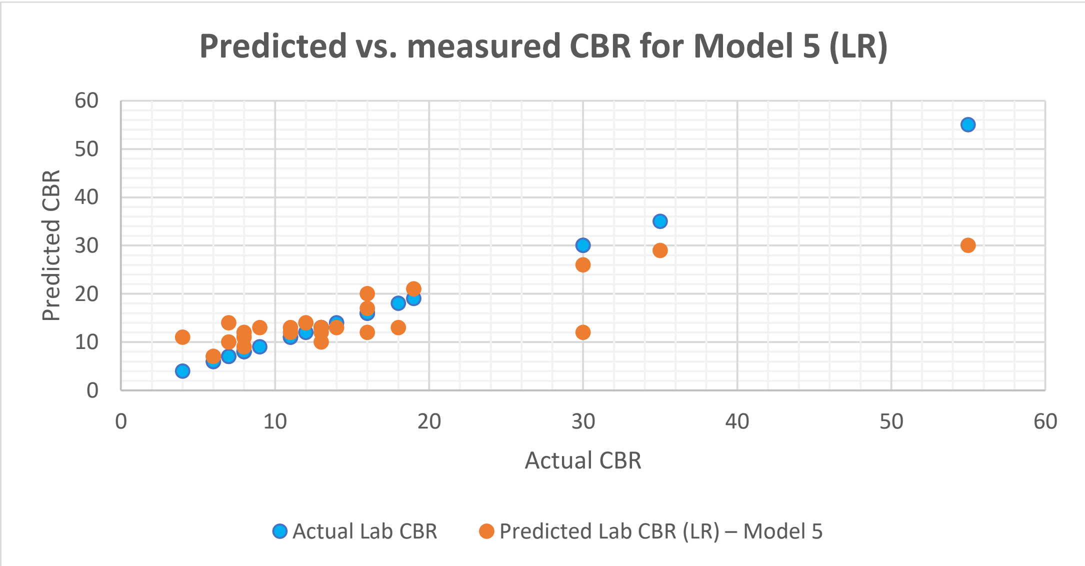

Figure 4.5: Predicted vs. Measured CBR for Model 5 (Linear Regression)

Figure 4-5 presents a scatter plot of predicted CBR values from Model 5 against laboratory-measured CBR values. Most data points cluster around the actual CBR values, with deviations increasing at higher CBR values (above 30 percent). The plot confirms the strong correlation ($r = 0.844$) and reasonable predictive accuracy, though the model tends to under-predict very high CBR values (above 40 percent) and over-predict very low CBR values (below 10 percent).

The finding that machine learning models (RF and ANN) performed comparably to linear regression (R^2 of 0.575 to 0.596 for RF and ANN vs. 0.611 for LR) suggests that for this dataset, the additional complexity of non-linear models did not yield substantial improvements. This may be due to the relatively small dataset size (70 observations) or the inherent near-linearity of the FWD-CBR relationship when MDD and OMC are included. However, RF and ANN models remain valuable alternatives, particularly for larger datasets or when non-linear relationships are expected.

The final predictive model (Model 5) is expressed as:

Equation 4.1: Final Predictive Model for Subgrade CBR

$$CBR = 5.2215 + (-0.0036 \times D600) + (-0.0144 \times P_c) + (-0.2522 \times T_{air}) + (0.0233 \times MDD) + (-0.3732 \times OMC)$$

Where:

CBR = predicted subgrade California Bearing Ratio (percent)

D600 = normalized deflection at 600 mm from load centre (µm)

P_c = contact pressure (kPa)

T_{air} = air temperature during FWD testing (°C)

MDD = maximum dry density of subgrade soil (kg/m^3)

OMC = optimum moisture content of subgrade soil (percent)

To use this model, an engineer would collect FWD deflection data (specifically D600), record contact pressure and air temperature during testing, and obtain MDD and OMC values for the subgrade soil. MDD and OMC can be obtained from construction records, project specifications, or from non-destructive methods such as Ground Penetrating Radar (GPR), Nuclear Density Gauge (NDG), or Light Weight Deflectometers (LWD) calibrated for the specific soil type.

4.3.6 Comparison with other Prediction Techniques

The predictive performance of Model 5 (R^2 = 0.611, RMSE = 6.97%) compares favourably with existing FWD-CBR prediction models. Chai et al. (2013) reported an R^2 of 0.58 for their model using D450 deflections on thin bituminous pavements in Australia. Nazzal and Mohammad (2010) reported correlation coefficients ranging from 0.51 to 0.81 for their FWD back-calculation models, depending on the software used. The present model's performance is therefore within the range of published models, while being specifically validated for Kenyan subgrade conditions.

4.4 Factors Influencing the FWD-CBR Relationship

The Pearson correlation coefficient, denoted as 'r, was used to measure the strength and direction of linear relationships between predicted CBR and various factors. Values ranged from -1 to +1. A value of +1 indicated a perfect positive correlation, -1 indicated a perfect negative correlation, while 0 indicated no correlation. Table 4.7 summarizes the correlation coefficients for each model group.

Table 4.7: Pearson Correlation Coefficients by Model Group

Model Group	Independent Variables	RF	LR	ANN
1	D600, Contact Pressure, Air Temperature	0.600	0.112	-0.080
2	Group 1 + MDD, OMC	0.823	0.844	0.813
3	Group 2 + Soil Class, PI	0.830	0.824	0.807
4	D600 only	0.235	0.133	-

Models in Group 2 and Group 3 showed strong positive correlations (r > 0.80) between predicted and laboratory CBR, while Group 1 models showed weak correlations (r < 0.60) and Group 4 models showed very weak correlations (r < 0.24). This indicates that MDD and OMC are the most critical intervening variables in the FWD-CBR relationship.

Figure 4-6 presents the feature importance ranking from the Random Forest models showing the various dependent variables used in developing the models.

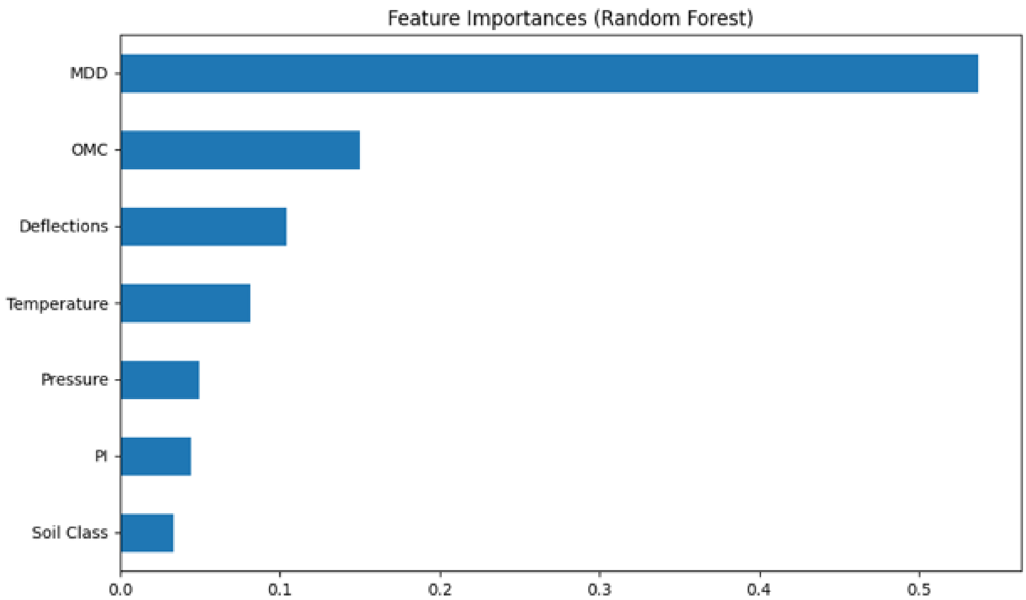

Figure 4.6: Feature Importance for Random Forest Models

Figure 4-6 showed that MDD (maximum dry density) was the most important predictor, followed by OMC (optimum moisture content), then D600 deflection, air temperature, and contact pressure. Plasticity index and soil class showed lower importance. This ranking confirms that subgrade compaction characteristics (MDD and OMC) have the greatest influence on the FWD-CBR relationship, while soil type and plasticity have secondary importance.

The engineering implication of this finding is that accurate prediction of subgrade CBR from FWD data requires knowledge of subgrade compaction properties. Engineers cannot rely solely on FWD deflection measurements; they must obtain MDD and

OMC values either from construction records or from complementary non-destructive testing methods. The relatively low importance of soil class and plasticity index suggests that the model may be applicable across different soil types, provided MDD and OMC are known.

The negative correlation between air temperature and CBR (coefficient of -0.2522 in Equation 4.1) indicates that higher temperatures lead to lower predicted CBR. This is consistent with Obafemi (2004), who found that temperature affects the resilient modulus of subgrade soils by influencing both surface tension and matric suction. The practical implication is that FWD testing should preferably be conducted within a consistent temperature range, or temperature corrections should be applied.

CHAPTER FIVE

CONCLUSIONS AND RECOMMENDATIONS

5.1 Overview

This chapter presents the conclusions drawn from the study findings, organized according to the three specific objectives. Recommendations for practical application and for further research are then provided.

5.2 Conclusions

5.2.1 Subgrade Material Characterization

The characterization of subgrade materials from trench data revealed that lean clay (CL) and elastic silt (MH) are the predominant soil types on Kenyan flexible pavements, together accounting for 67 percent of all samples. The average plasticity index ranged from 7 to 23% percent, optimum moisture content ranged from 12 to 27 %, maximum dry density ranged from 1250 to 1821 kg/m^3, and laboratory CBR ranged from 5 to 31 % across the 18 road sections. The presence of multiple soil types within individual road sections confirms the spatial variability of subgrade conditions in Kenya, which justifies the need for predictive modelling approaches that can provide dense spatial coverage.

5.2.2 Predictive Model Development and Validation

The study successfully developed and validated predictive models for subgrade CBR from FWD deflection parameters. Among the eleven models developed, Model 5 (Linear Regression using D600 deflection, contact pressure, air temperature, MDD, and OMC) performed best, achieving an R^2 of 0.611, a Pearson correlation coefficient of 0.844, and a root mean square error of 6.97 percent. This model explains 61 percent of the variance in laboratory CBR values and shows a strong positive correlation between predicted and measured CBR. The model is expressed in Equation 4.1 as:

$$CBR = 5.2215 - 0.0036(D600) - 0.0144(P_c) - 0.2522(T_{air}) + 0.0233(MDD) - 0.3732(OMC)$$

Where:

D4 are the normalized deflections in µm recorded on the 4^{th} geophone which is 600mm from the centre of the loading plate;

P_c is Contact pressure is recorded in the FWD file in kPa;

T_{air} is air temperature is recorded in the FWD file during the study in ^oC;

MDD is the material Maximum Dry Density; and,

OMC is the Optimum Moisture Content.

The inclusion of MDD and OMC as input variables was found to be critical for accurate prediction; models excluding these variables performed poorly ($R^2 < 0.3$). Machine learning models (Random Forest and Artificial Neural Networks) performed comparably to linear regression, indicating that the additional complexity of non-linear models did not yield substantial improvements for this dataset.

5.2.3 Factors Influencing the FWD-CBR Relationship

The investigation of factors influencing the FWD-CBR relationship confirmed that maximum dry density and optimum moisture content are the most important intervening variables, with feature importance rankings showing MDD as the most influential predictor, followed by OMC. Air temperature and contact pressure showed moderate importance, while plasticity index and soil class showed lower importance. The strong correlation ($r > 0.80$) observed when MDD and OMC are included, compared to weak correlation ($r < 0.60$) when they are excluded, demonstrates that subgrade compaction characteristics are essential for accurate CBR prediction from FWD data. Temperature was found to have a negative influence on predicted CBR, consistent with existing literature.

5.4 Recommendations

5.4.1 Recommendations from the Study

1. Engineers conducting pavement evaluation in Kenya can use the developed Model 5 (Equation 4.1) to estimate subgrade CBR from FWD deflection data, as it provides a validated, locally-calibrated alternative to the plate bearing test correlations currently provided in the Road Design Manual. This recommendation is based on the model's strong correlation ($r = 0.844$) and acceptable prediction error (RMSE = 6.97%).
2. When using the predictive model, engineers must obtain accurate values for subgrade maximum dry density and optimum moisture content, either from construction records or from non-destructive testing methods such as Ground Penetrating Radar or Nuclear Density Gauges. This recommendation is based on the finding that models excluding MDD and OMC performed poorly ($R^2 < 0.3$).
3. FWD testing for subgrade evaluation should be conducted under consistent temperature conditions, preferably during the dry season when temperatures are stable. Where temperature varies substantially, temperature corrections should be applied or air temperature should be included as an input variable as shown in the model. This recommendation is based on the negative correlation between air temperature and CBR (coefficient of -0.2522).
4. For routine pavement evaluations where destructive testing is already planned, engineers should collect D600 deflection data alongside DCP or laboratory CBR tests to continuously validate and refine the predictive model for local conditions. This recommendation is based on the need for ongoing model validation across different sites and seasons.

5.4.2 Recommendations for further Research

1. Further research should validate the developed model on road sections outside the thirteen counties covered in this study (Nairobi, Kiambu, Nakuru, Uasin Gishu, Marsabit, Kericho, Baringo, Narok, Laikipia, Nyandarua, Homabay,

Bomet and Kisumu) to assess its generalizability across all 47 counties of Kenya. This recommendation arises from the limitation of the current study whose target sample size did not capture all Kenyan subgrade diversity.

2. The effect of subgrade depth (depth from pavement surface to the subgrade layer) on the FWD-CBR relationship should be investigated, as this variable was not consistently available in the secondary data used for this study. This recommendation is based on the finding by Kumar et al. (2015) that depth of testing influences CBR correlations across different countries.
3. The feasibility of using non-destructive methods (GPR, NDG, LWD) to estimate MDD and OMC should be investigated, as these parameters are critical inputs to the predictive model but are currently obtained through destructive laboratory tests. This recommendation is based on the finding that MDD and OMC are the most important predictors in the model, yet they require time-consuming laboratory testing to determine.

REFERENCES

AASHTO. (2017). *Standard practice for falling weight deflectometer testing*. American Association of State Highway and Transportation Officials.

ASTM International. (2008). *Standard guide for general pavement deflection measurements* (ASTM D4695-03(2008)). ASTM International.

ASTM International. (2020). *Standard test method for deflections with a falling-weight-type impulse load device* (ASTM D4694-20). ASTM International.

British Standards Institution. (1990). *Methods of test for soils for civil engineering purposes* (BS 1377-4:1990). BSI.

Central Intelligence Agency. (2025). *The world factbook: Roadways*. CIA.

Chai, G., Kelly, G., & Chowdhury, S. (2013). Prediction of subgrade CBR using FWD for thin bituminous pavements. *International Journal of Pavement Engineering*, 14(3), 231-240.

Das, B. M. (2015). *Principles of foundation engineering* (8th ed.). Cengage Learning.

Das, B. M. (2016). *Principles of geotechnical engineering* (9th ed.). Cengage Learning.

George, K. P. (2004). *Prediction of subgrade strength from FWD deflections* (Report No. FHWA/MS-DOT-RD-04-170). University of Mississippi.

George, V., Kumar, A., & Sivakumar, N. (2010). Factors affecting CBR of subgrade soils. *Geotechnical Engineering Journal*, 41(3), 45-52.

Government of Kenya. (2025a). *Pavement evaluation and rehabilitation guidelines*. Ministry of Roads and Transport.

Government of Kenya. (1987). *Road design manual Part III: Pavements*. Ministry of Transport and Infrastructure.

Government of Kenya. (2017). *Road design manual Part 3: Pavements* (Rev. ed.). Ministry of Transport, Infrastructure, Housing and Urban Development.

Government of Kenya. (2025b). *Road design manual Volume 3: Materials and pavement design*. Ministry of Roads and Transport.

Harrell, F. E. (2015). *Regression modeling strategies: With applications to linear models, logistic and ordinal regression, and survival analysis* (2nd ed.). Springer.

Hasan, M. A., Praveen, B. S., Bag, R., & Ramu, B. (2024). *The state-of-the-art review on prediction of subgrade CBR: Past and present trends.* Indian Geotechnical Journal. Retieved from https://doi.org/10.1007/s40098-024-01113-2)

Hoffman, M. S., & Thompson, M. R. (1981). *Mechanistic interpretation of non-destructive pavement testing deflections* (Report No. FHWA/IL/UI-201). University of Illinois.

Horak, E. (2008). *Benchmarking of structural pavement deflection parameters*. CSIR Built Environment.

Huang, Y. H. (2004). *Pavement analysis and design* (2nd ed.). Pearson Prentice Hall.

Hui, C. (2018). *Data science for civil engineers*. World Scientific Publishing.

Kenya Investment Authority. (2024). *Infrastructure sector report 2024*. Kenya Investment Authority.

Kenya National Bureau of Statistics. (2026). *Economic survey 2026*. Kenya National Bureau of Statistics.

Kenya National Highways Authority. (2022). *Pavement evaluation and asset management report*. KeNHA.

Kenya Roads Board. (2023). *Annual public roads statistics report 2022-2023*. Kenya Roads Board.

Kenya Roads Board. (2024). *Annual public roads statistics report 2023-2024*. Kenya Roads Board.

Kenya Urban Roads Authority. (2023). *Standard specifications for road works*. KURA.

Kim, Y. R., Ranjithan, S. R., & Lee, S. (2010). FWD back-calculation for subgrade modulus using artificial neural networks. *Journal of Transportation Engineering*, 136(5), 420-428.

Kothari, C. R. (2004). *Research methodology: Methods and techniques* (2nd ed.). New Age International Publishers.

Kumar, A., Sharma, R., & Jain, P. K. (2015). Relationship between subgrade strength and DCP data for Indian national highways. *Indian Geotechnical Journal*, 45(2), 156-165.

Magg, C., Biljecki, F., & Koelle, R. (2024). Road pavedness as a proxy for human development index. *Nature Communications*, 15(1), 234-245.

Mwangi, J. K., & Mwea, S. K. (2016). Premature pavement failure in Nairobi urban roads: Causes and mitigation. *East African Journal of Engineering*, 3(2), 45-58.

Nazzal, M. D., & Mohammad, L. N. (2010). Regression models for resilient modulus of subgrade soils from FWD back-calculated modulus. *Journal of Materials in Civil Engineering*, 22(8), 785-793.

Ndagea, M. (2011). *Impact of axle overloading on pavement deterioration in Kenya*. Unpublished PhD Thesis, Pretoria: University of Pretoria.

Obafemi, A. (2004). Temperature effects on subgrade resilient modulus in cold regions. *Cold Regions Science and Technology*, 39(2), 101-112.

Odero, J. O., Ochieng, P. O., & Nyakundi, R. M. (2021). Subgrade characterization for road construction in Kenya. *Journal of Civil Engineering Research*, 11(4), 78-89.

Powell, W. D., Potter, J. F., Mayhew, H. C., & Nunn, M. E. (1986). *The structural design of bituminous roads* (TRRL Report LR 1132). Transport and Road Research Laboratory.

Rahman, M. S., Khan, M. A., & Hossain, M. I. (2011). Subgrade strength and its impact on pavement performance. *International Journal of Pavement Engineering*, 12(6), 521-534.

Rodrigue, J. P. (2020). *The geography of transport systems* (5th ed.). Routledge.

Scullion, T., & Stokoe, K. H. (1997). *Non-destructive testing of pavements: Back-calculation and analysis* (NCHRP Synthesis 253). Transportation Research Board.

Transport Research Laboratory. (2002). *A guide to the structural design of bitumen-surfaced roads in tropical and sub-tropical countries* (Overseas Road Note 31). TRL.

U.S. Department of Transportation. (2023). *Highway statistics 2023*. Federal Highway Administration.

Vasudeva Rao, A. V., Reddy, K. S., & Mohanty, S. (2019). Characterization and mapping of subgrade soils for road expansion in Ethiopia. *International Journal of Geotechnical Engineering*, 13(2), 145-156.

WION News. (2024, December 8). Which country has the largest road network. *WION News*. Retrieved from https://www.wionews.com)

World Bank. (2022). *China's transport infrastructure development report 2022*. World Bank Group.

Yoder, E. J., & Witczak, M. W. (1975). *Principles of pavement design* (2nd ed.). John Wiley & Sons.

APPENDICES

Appendix I: Publications

Certificate of Publication

IJAER

ISSN 2643-

International Journal of Academic Engineering Research (IJAER)

This is to certify that our Editorial, Advisory, and Review Board Accepted Research Paper of

Dr/Mr/Ms: Catherine Mugai, Kepha Abongo and Brian Jacks Odero

Topic:-Prediction of Subgrade California Bearing Ratio Using Falling Weight Deflectometer for Pavement Evaluation in Kenya

Published in Vol. 9 Issue: 8 August 2025

The Research Paper is Original and Innovative. It is Peer-Reviewed.

IJARW

Washington DC, USA
http://www.ijeais.org/ijaer
ijaerchiefeditor@gmail.com

IJAER Editor-in-Chief

African Journal of Engineering Research and Innovation. Volume 3. No. 3, September 2025

Characterization of Subgrade Soils in Prediction Modelling of Subgrade CBR using Falling Weight Deflectometer (FWD) for Pavement Evaluation in Kenya

C. Mugai[1*] K. Abongo[2], B. J. Odero[3]

1. Department of Civil, Construction & Environmental Engineering, Jomo Kenyatta University of Agriculture & Technology, P.O Box 62000-00200, Nairobi, Kenya

2.Department of Civil, Construction & Environmental Engineering, Jomo Kenyatta University of Agriculture & Technology, P.O Box 62000-00200, Nairobi, Kenya

3. Department of Civil, Construction & Environmental Engineering, Jomo Kenyatta University of Agriculture & Technology, P.O Box 62000-00200, Nairobi, Kenya

*Corresponding author: cwmugai@gmail.com

Certificate of Publication

IJAER

ISSN 2643-9085

International Journal of Academic Engineering Research (IJAER)

This is to certify that our Editorial, Advisory, and Review Board Accepted Research Paper of Dr/Mr/Ms : Eng. Catherine Mugai Dr. Kepha Abongo, Dr. Brian Jacks Odero

Topic:-Assessment of Linear and Nonlinear Subgrade Behavior Using FWD Deflection Ratios: Implications for Pavement Modelling

Published in Vol. 10 Issue: 1 January 2026

The Research Paper is Original and Innovative. It is Peer-Reviewed.

IJARW

Washington DC, USA

IJAER Editor-in-Chief

Appendix II: Plagiarism Report

Plagiarism Detector v. 2867 - Originality Report 04/09/2025 15:58:38

Analyzed document: Rev 1 - Catherine Mugai Msc Thesis - August 2025.docx Licensed to: Jomo Kenyatta University of Agriculture and Technology

Comparison Preset: Rewrite Detected language: En

Check type: Internet Check

TEE and encoding: DocX n/a

Detailed document body analysis:

Relation chart:

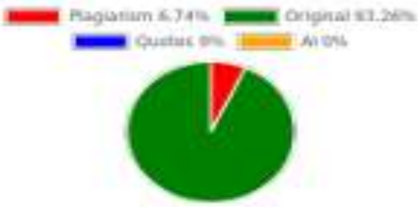

Distribution graph:

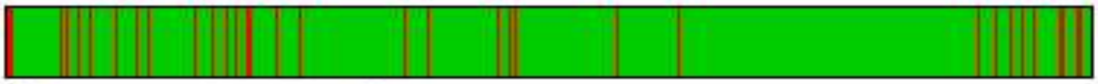

Top sources of plagiarism: 41

17%	2949	1.	https://link.springer.com/article/10.1007/s40808-025-02512-x
12%	2073	2.	https://link.springer.com/article/10.1007/s40288-025-01297-1
12%	2006	3.	https://link.springer.com/article/10.1007/s42107-025-01389-w

Processed resources details: 170 - Ok / 12 - Failed

Important notes:

Wikipedia:	Google Books:	Ghostwriting services:	Anti-cheating:
[not detected]	[not detected]	[not detected]	[not detected]

UACE: UniCode Anti-Cheat Engine report:

1. Status: Analyzer On Normalizer On character similarity set to **100%**
2. Detected UniCode contamination percent:0% with limit of: 4%
3. Document not normalized: percent not reached 5%
4. All suspicious symbols will be marked in purple color: Abcd...
5. Invisible symbols found: 0

Appendix III: Research Approval Letter

JOMO KENYATTA UNIVERSITY
OF
AGRICULTURE AND TECHNOLOGY

OFFICE OF THE DIRECTOR, GRADUATE SCHOOL

P.O. BOX 62000, 00200 • NAIROBI •KENYA•TEL: (067)-5870001-4• Email: director@bps.jkuat.ac.ke

REF: JKU/2/11/ENC311-2233/2021 5TH SEPTEMBER, 2024

CATHERINE MUGAI WAMBUI
C/o SCEGE
JKUAT

Dear, Catherine

RE: APPROVAL OF RESEARCH PROPOSAL AND APPOINTMENT OF SUPERVISORS

Kindly note that your MSc. research proposal entitled: **"PREDICTION OF SUBGRADE CBR USING FALLING WEIGHT DEFLECTOMETER (FWD) FOR PAVEMENT EVALUATION IN KENYA''**, has been approved. The following are your approved supervisors:-

1. Dr. Kepha Abongo - JKUAT
2. Dr. Brian Odero - JKUAT

Please be advised that you are expected to publish your research outputs in quality and indexed journals.

Yours sincerely

PROF. FRANCIS K. NJONGE, Ph.D
DIRECTOR, GRADUATE SCHOOL
Copy to: Dean, SCEGE

JKUAT is ISO 9001:2015 and ISO 14001:2015 Certified
Setting Trends in Higher Education, Research, Innovation and Entrepreneurship

Appendix IV: National Commission for Science, Technology & Innovation (NACOSTI) Research Permit

REPUBLIC OF KENYA

NATIONAL COMMISSION FOR SCIENCE, TECHNOLOGY & INNOVATION

Ref No: 720206

Date of Issue: 24/September/2024

RESEARCH LICENSE

This is to Certify that Ms.. Catherine Mugai of Jomo Kenyatta University of Agriculture and Technology, has been licensed to conduct research as per the provision of the Science, Technology and Innovation Act, 2013 (Rev.2014) in Baringo, Bomet, Elgeyo-Marakwet, Kericho, Kilifi, Kwale, Laikipia, Machakos, Marsabit, Meru, Mombasa, Muranga, Nairobi, Nakuru, Narok, Nyandarua, Nyeri, Tharaka Nithi, Uasin-Gishu on the topic: PREDICTION OF SUBGRADE CBR USING FALLING WEIGHT DEFLECTOMETER (FWD) FOR PAVEMENT EVALUATION IN KENYA for the period ending : 24/September/2025.

License No: NACOSTI/P/24/40179

720206

Applicant Identification Number

Director General
NATIONAL COMMISSION FOR SCIENCE, TECHNOLOGY & INNOVATION

Verification QR Code

NOTE: This is a computer generated License. To verify the authenticity of this document, Scan the QR Code using QR scanner application.

See overleaf for conditions

Appendix V: Specific Roads Selected for the Study

Road No.	Location
1	Nakuru/Nyandarua
2	Rift Valley/Kisumu
3	Marsabit
4	Kericho, Bomet
5	Nakuru, Baringo
6	Nakuru, Narok
7	Narok
8	Nakuru, Nyandarua, Laikipia
9	Laikipia
10	Baringo, Elgeyo Marakwet
11	Nairobi
12	Nairobi
13	Homa Bay
14	Bomet, Kericho
15	Kisumu
16	Kericho,Kericho
17	Murang'a
18	Kikuyu

Appendix VI: Raw Data for Individual Trial Pits

Road No. & Location	TP No.	Chainage	Depth	Layer	Lane	Thickness mm	Max. Dry Density gcc	Optimum Moisture Content (%)	PI %	LL %	% Pass. BS Sieve 5mm (No.4)	% Pass. BS Sieve 2mm	% Pass. BS Sieve 0.425mm	% Pass. BS Sieve 0.075mm (No.200)	Gravel Fraction	Total Coarse Fraction	Sand Fraction	No.200 Retained	Coarse/Fine Grained	Plasticity Chart	Group Symbol	Soil Classification
1. Nakuru/Nyandarua	1	0+710	290	TSG	RHS	150	1470	18.0	23	55	89	79	51	25	11	75	85	26	Fine-grained	MH/OH	MH	Elastic Silt with Sand
	2	5+000	400	TSG	LHS	150	1355	27.0	26	58	91	86	75	67	9	33	73	8	Fine-grained	MH/OH	MH	Elastic Silt
	3	9+762	345	TSG	RHS	150	1385	22.4	24	55	85	81	70	66	15	34	56	4	Fine-grained	MH/OH	MH	Elastic Silt
	4	15+000	390	SG	LHS	150	1270	29.4	26	69	100	84	76	64	0	36	100	12	Fine-grained	MH/OH	MH	Elastic Silt
	5	22+350	430	TSG	LHS	150	1380	22.8	23	51	94	90	78	65	6	35	83	13	Fine-grained	CH/OH	CH	Fat Clay
	6	29+300	370	TSG	RHS	150	1430	22.6	18	41	86	75	50	37	14	63	78	13	Fine-grained	CL/OL	CL	Lean Clay
2. Rift Valley/Kisumu	1	8+800	450	TSG	LHS	300	1826	12.0	15	40	69	50	26	21	31	79	61	5	Fine-grained	CL/ML	CL	Lean Clay
	2	18+900	460	TSG	RHS	330	1785	11.8	14	44	56	42	34	17	44	83	47	17	Fine-grained	CL/OL	CL	Lean Clay with Sand
	3	24+600	450	TSG	LHS	280	1851	11.0	14	40	55	40	35	18	45	82	45	17	Fine-grained	ML/OL	ML	Silt with sand
	4	24+850	440	TSG	RHS	450	1835	12.5	16	45	56	44	36	20	44	80	45	16	Fine-grained	ML/OL	ML	Silt with sand
	5	25+150	510	TSG	LHS	150	1475	19.9	13	40	64	50	32	19	36	81	56	13	Fine-grained	ML/OL	ML	Silt
	6	25+370	450	TSG	RHS	170	1863	10.6	13	45	62	45	21	13	38	87	56	8	Fine-grained	ML/OL	ML	Silt
	7	40+600	450	TSG	LHS	170	1698	16.7	10	39	70	55	32	24	30	76	61	8	Fine-grained	ML/OL	ML	Silt
	8	55+000	400	TSG	RHS	160	1831	10.8	8	26	76	60	34	25	24	75	68	9	Fine-grained	CL/OL	CL	Lean Clay
	9	70+200	500	TSG	LHS	280	1642	16.4	16	48	60	55	45	28	40	72	44	17	Fine-grained	ML/OL	ML	Silt with sand
	10	81+000	490	TSG	RHS	230	1803	15.1	10	35	65	64	50	30	35	70	50	20	Fine-grained	ML/OL	ML	Silt with sand
3. Marsabit	1	3+423	305	TSG	LHS	150	1690	15.4	20	42	86	75	56	39	14	61	77	17	Fine-grained	CL/OL	CL	Lean Clay with Sand
	2	7+282	357	TSG	RHS	250	1770	14.6	24	62	61	43	24	19	39	81	52	5	Fine-grained	MH/OH	MH	Elastic Silt
	3	12+417	375	TSG	RHS	200	1480	23.0	26	67	73	58	38	30	27	70	61	8	Fine-grained	MH/OH	MH	Elastic Silt
	4	17+525	365	TSG	LHS	200	1900	11.5	21	50	49	31	16	12	51	88	42	4	Coarse-grained	MH/OH	GM	Silty Gravel
	5	22+565	370	SG	RHS	280	1655	16.7	25	54	63	49	36	31	37	69	46	5	Fine-grained	CH/OH	CH	Gravelly Fat Clay
4. Kericho, Bomet	1	0+305	390	TSG	RHS	150	1460	15.6	18	46	78	72	62	45	22	55	60	17	Fine-grained	ML/OL	ML	Silt with Sand
	1	0+305	540	BSG	RHS	200	1170	31.2	24	53	95	94	92	87	5	13	62	5	Fine-grained	CH/OH	CH	Fat Clay
	2	15+600	480	TSG	LHS	190	1400	20.3	21	52	89	85	78	75	11	25	56	3	Fine-grained	MH/OH	MH	Elastic Silt
	2	15+600	670	BSG	LHS	300	1380	22.8	24	61	95	89	78	74	5	26	81	4	Fine-grained	MH/OH	MH	Elastic Silt
	3	30+360	525	SG	RHS	300	1280	25.6	23	56	94	90	76	69	6	31	81	7	Fine-grained	MH/OH	MH	Elastic Silt
	4	44+080	455	TSG	LHS	150	1465	23.0	20	46	90	84	76	71	10	29	66	5	Fine-grained	CL/OL	CL	Lean Clay
	4	44+080	605	BSG	LHS	200	1445	21.7	24	51	93	89	77	70	7	30	77	7	Fine-grained	CH/OH	CH	Fat Clay
5. Nakuru, Baringo	1	1+300	411	TSG	RHS	200	1250	24.2	12	42	94	88	70	53	6	47	87	17	Fine-grained	ML/OL	ML	Silt with sand
	1	1+300	611	BSG	RHS	300	1250	24.4	10	47	95	87	62	46	5	54	91	16	Fine-grained	ML/OL	ML	Silt with sand
	2	9+000	345	SG	LHS	400	1200	25.6	8	44	96	88	74	58	4	42	90	16	Fine-grained	ML/OL	ML	Silt with sand
	3	43+100	340	SG	LHS	300	1450	18.9	17	37	97	94	80	64	3	36	92	16	Fine-grained	CL/OL	CL	Lean Clay with Sand
	4	80+600	390	TSG	RHS	200	1700	15.0	16	44	85	78	65	54	15	46	67	11	Fine-grained	ML/OL	ML	Silt
	4	80+600	590	BSG	RHS	200	1720	17.6	11	26	98	95	76	62	2	38	95	14	Fine-grained	CL/OL	CL	Lean Clay
6. Nakuru, Narok	1	9+950	368	SG	LHS	400	1310	24.2	13	35	92	82	71	60	8	40	80	11	Fine-grained	CL/OL	CL	Lean Clay
	2	20+100	305	TSG	RHS	150	1310	21.0	16	35	98	93	75	63	2	37	95	12	Fine-grained	CL/OL	CL	Lean Clay
	2	20+100	455	BSG	RHS	300	1380	20.4	20	47	97	87	61	47	3	53	94	14	Fine-grained	CL/OL	CL	Lean Clay
	2	20+100	755	NS	RHS	300	1080	29.0	15	46	97	90	64	45	3	55	95	19	Fine-grained	ML/OL	ML	Silt with sand
	3	35+600	330	SG	LHS	500	1355	33.6	14	43	92	81	59	44	8	56	86	15	Fine-grained	ML/OL	ML	Silt with sand
	3	45+500	360	SG	RHS	460	1395	24.0	18	43	92	84	69	54	8	46	83	15	Fine-grained	CL/OL	CL	Lean Clay with Sand
7. Narok	1	0+676	300	TSG	RHS	200	1285	23.4	14	44	88	75	58	45	12	55	78	13	Fine-grained	ML/OL	ML	Silt
	1	0+676	570	BSG	RHS	200	1245	24.2	14	36	89	75	56	44	11	56	80	12	Fine-grained	CL/OL	CL	Lean Clay
	2	10+200	405	TSG	LHS	200	1300	19.8	18	37	90	79	68	56	10	44	77	12	Fine-grained	CL/OL	CL	Lean Clay
	2	10+200	605	BSG	LHS	300	1180	26.2	14	35	99	96	83	71	1	29	97	12	Fine-grained	CL/OL	CL	Lean Clay
	3	20+000	415	TSG	RHS	200	1320	24.5	13	41	91	80	64	51	9	49	82	13	Fine-grained	ML/OL	ML	Silt
	3	20+000	615	BSG	RHS	200	1310	24.2	14	40	90	80	70	61	10	39	74	9	Fine-grained	ML/OL	ML	Silt
	3	20+000	815	NS	RHS	300	1060	30.6	24	55	89	79	69	59	11	41	73	10	Fine-grained	MH/OH	MH	Elastic Silt
	4	27+505	525	TSG	LHS	250	1255	26.8	14	41	93	84	72	61	7	39	82	11	Fine-grained	ML/OL	ML	Silt
	4	27+505	775	BSG	LHS	200	1310	24.3	17	40	92	82	71	60	8	40	80	11	Fine-grained	CL/OL	CL	Lean Clay
	5	29+240	340	TSG	LHS	200	1195	23.1	13	39	92	84	75	65	8	35	77	10	Fine-grained	ML/OL	ML	Silt
	5	29+240	540	NS	LHS	200	1284	24.6	24	51	93	81	70	59	7	41	83	11	Fine-grained	CH/OH	CH	Fat Clay
8. Nakuru,	1	10+100	430	TSG	RHS	300	1310	15.7	24	53	96	90	67	61	4	39	90	6	Fine-grained	CH/OH	CH	Fat Clay
	1	10+100	730	NS	RHS	300	1000	23.3	10	59	78	58	29	26	22	74	70	3	Fine-grained	MH/OH	MH	Elastic Silt
	2	25+000	480	SG	LHS	300	1410	25.6	24	60	99	98	95	93	1	7	86	2	Fine-grained	MH/OH	MH	Elastic Silt

Road No. & Location	TP No.	Chainage	Depth	Layer	Lane	Thickness mm	Max. Dry Density gcc	Optimum Moisture Content (%)	PI %	LL %	% Pass. BS Sieve 5mm (No.4)	% Pass. BS Sieve 2mm	% Pass. BS Sieve 0.425mm	% Pass. BS Sieve 0.075mm (No.200)	Gravel Fraction	Total Coarse Fraction	Sand Fraction	No.200 Retained	Coarse/Fine Grained	Plasticity Chart	Group Symbol	Soil Classification
Nyandarua,	3	40+000	330	TSG	LHS	150	1430	20.3	24	57	93	90	83	77	7	23	70	6	Fine-grained	MH/OH	MH	Elastic Silt
Laikipia	3	40+000	480	BSG	LHS	150	1380	26.8	25	58	92	87	81	74	8	26	69	7	Fine-grained	MH/OH	MH	Elastic Silt
	3	40+000	630	NS	LHS	200	1570	16.8	18	46	77	70	59	51	23	49	53	8	Fine-grained	ML/OL	ML	Silt
	4	50+300	340	SG	RHS	300	1380	26.8	24	57	100	99	97	95	0	5	100	2	Fine-grained	MH/OH	MH	Elastic Silt
	1	0+075	370	TSG	LHS	200	1433	20.4	18	45	84	77	65	58	16	42	62	7	Fine-grained	ML/OL	ML	Silt
	1	0+075	570	BSG	LHS	300	1385	23.6	20	52	95	93	80	68	5	32	84	12	Fine-grained	MH/OH	MH	Elastic Silt
9.	2	3+000	380	TSG	RHS	200	1380	22.0	16	43	98	94	84	67	2	33	94	17	Fine-grained	MH/OH	MH	Elastic Silt with sand
Laikipia	2	3+000	580	BSG	RHS	200	1350	21.6	20	50	95	93	76	60	5	40	88	16	Fine-grained	MH/OH	MH	Elastic Silt with sand
	3	6+100	335	SG	LHS	300	1510	15.2	19	42	97	92	82	62	3	38	92	20	Fine-grained	CL/OL	CL	Lean Clay with Sand
	4	8+100	377	SG	RHS	300	1345	23.6	24	55	100	99	93	81	0	19	100	12	Fine-grained	MH/OH	MH	Elastic Silt
	1	12+640	390	SG	LHS	300	1445	21.4	23	46	96	91	87	79	4	21	81	8	Fine-grained	CL/OL	CL	Lean Clay
10.	2	36+500	300	SG	RHS	150	1490	20.8	18	37	92	88	84	75	8	25	68	9	Fine-grained	CL/OL	CL	Lean Clay
Baringo, Elgeyo	3	50+450	270	SG	LHS	270	1155	25.4	24	48	98	97	96	92	2	8	75	4	Fine-grained	CL/OL	CL	Lean Clay
Marakwet	4	65+400	275	TSG	RHS	200	1325	18.4	22	55	95	93	86	78	5	22	77	8	Fine-grained	MH/OH	MH	Elastic Silt
	4	65+400	475	BSG	RHS	200	1110	20.0	23	58	99	98	97	96	1	4	75	1	Fine-grained	MH/OH	MH	Elastic Silt
	1	0+300	500	SG	LHS	300	1380	31.5	28	54	95	91	87	86	5	14	64	1	Fine-grained	CH/OH	CH	Fat Clay
	2	1+180	520	SG	RHS	300	1455	28.9	28	57	70	53	33	16	30	84	64	17	Fine-grained	CH/OH	CH	Fat clay with sand
	3	2+207	320	SG	RHS	150	1365	27.2	29	53	97	94	91	89	3	11	73	2	Fine-grained	CH/OH	CH	Fat Clay
11.	4	2+207	470	BSG	RHS	300	1315	31.1	28	53	99	98	96	94	1	6	83	2	Fine-grained	CH/OH	CH	Fat Clay
Nairobi	5	0+130		BSG	RHS		1310	29.8	26	57	99	98	96	93	1	7	86	3	Fine-grained	MH/OH	MH	Elastic Silt
	6	0+950		BSG	LHS		1345	31.8	24	56	89	78	75	74	11	26	58	1	Fine-grained	MH/OH	MH	Elastic Silt
	7	1+550		BSG	RHS		1245	32.6	23	56	98	97	95	94	2	6	67	1	Fine-grained	MH/OH	MH	Elastic Silt
	8	2+052		BSG	LHS		1390	22.5	27	48	81	74	68	64	19	36	47	4	Fine-grained	CL/OL	CL	Lean Clay
	9	2+500		BSG	LHS		1180	37.6	32	62	99	98	97	96	1	4	75	1	Fine-grained	CH/OH	CH	Fat Clay
	1	0+100		SG	LHS		1555	18.2	14	38	88	78	58	48	12	52	77	10	Fine-grained	CL/OL	CL	Lean Clay
12.	2	0+700		BSG	RHS		1255	28.3	31	82	100	98	94	88	0	12	100	6	Fine-grained	MH/OH	MH	Elastic Silt
Nairobi	3	2+100		TSG	LHS		1700	11	14	48	76	56	38	33	24	67	64	5	Fine-grained	ML/OL	ML	Silt
	3	2+100		BSG	LHS		1725	9.5	12	30	41	23	2	1	59	99	40	1	Coarse-grained	CL/OL	CL	Lean Clay
	1	1+300		SG	RHS		1475	20.4	18	45	85	69	45	31	15	69	78	14	Fine-grained	ML/OL	CL	Lean Clay
13.	2	10+100		SG	RHS		1915	10.4	9	29	85	70	45	26	15	74	80	19	Fine-grained	CL/OL	CL	Lean Clay with sand
Homabay	3	20+300		SG	LHS		1850	11.6	15	44	89	68	37	28	11	72	85	9	Fine-grained	ML/OL	ML	Silt
	4	30+300		SG	LHS		1880	12.0	16	51	90	72	41	27	10	73	86	14	Fine-grained	MH/OH	MH	Elastic Silt
	5	40+250		SG	RHS		1885	10.8	14	35	86	69	54	36	14	64	78	18	Fine-grained	CL/OL	CL	Lean Clay with sand
	1	0+150		SG	LHS		1445	18.6	17	41	88	70	55	48	12	52	77	7	Fine-grained	CL/OL	CL	Lean Clay
14.	2	10+000		SG	RHS		1880	12.0	19	59	85	69	48	36	15	64	77	12	Fine-grained	MH/OH	MH	Elastic Silt
Bomet, Kericho	3	19+700		SG	LHS		1360	25.5	18	55	95	91	85	79	5	21	76	6	Fine-grained	MH/OH	MH	Elastic Silt
	4	30+300		SG	LHS		1535	16.6	11	39	90	82	81	64	10	36	72	17	Fine-grained	ML/OL	ML	Silt with sand
	5	40+000		SG	LHS		1445	20.6	17	54	94	89	81	70	6	30	80	11	Fine-grained	MH/OH	MH	Elastic Silt
15.	1	0+050	345	SG	LHS	150	1385	28.6	16	39	84	67	57	45	16	55	71	12	Fine-grained	CL/OL	CL	Lean Clay
Kisumu	2	6+000	350	SG	RHS	150	1650	18.6	16	42	71	54	35	25	29	75	61	10	Fine-grained	ML/OL	ML	Silt
	3	10+000	331	SG	LHS	150	1655	18.5	15	38	93	84	69	56	7	44	84	13	Fine-grained	CL/OL	CL	Lean Clay
	1	0+050	248	SG	LHS	253	1650	18.2	22	37	82	78	64	52	18	48	63	12	Fine-grained	CL/OL	CL	Lean Clay
	2	5+000	450	SG	RHS	200	1535	28.2	28	53	81	75	50	38	19	62	69	12	Fine-grained	CH/OH	CH	Fat Clay
	3	10+000	260	SG	LHS	240	1725	20	18	48	46	42	31	16	54	84	36	15	Coarse-grained	ML/OL	ML	Silt with sand
16.	4	15+000	250	SG	RHS	250	2070	15.2	24	49	47	41	34	24	53	76	30	10	Coarse-grained	CL/OL	CL	Lean Clay
Kericho,Kericho	5	20+000	400	SG	LHS	170	1775	19.2	20	54	50	44	34	28	50	72	31	6	Fine-grained	MH/OH	MH	Elastic Silt
	6	25+000	242	SG	RHS	480	1685	19.8	16	44	67	60	46	24	33	76	57	22	Fine-grained	ML/OL	ML	Silt with sand
	7	30+000	220	SG	LHS	375	1895	14.2	22	44	69	60	46	36	31	64	52	10	Fine-grained	CL/OL	CL	Lean Clay
	8	33+500	205	SG	RHS	360	1900	18.2	18	46	69	57	42	41	31	59	47	1	Fine-grained	ML/OL	ML	Silt
	1	0+100	360	SG	LHS	300	1500	21.6	22	58	78	58	36	27	22	73	70	9	Fine-grained	MH/OH	MH	Elastic Silt
	2	0+500	345	SG	RHS	150	1470	26.4	31	60	94	80	70	67	6	33	82	3	Fine-grained	CH/OH	CH	Fat Clay
	3	1+000	350	SG	LHS	150	1565	18.6	22	41	91	62	44	40	9	60	85	4	Fine-grained	CL/OL	CL	Lean Clay
17.	4	1+500	285	SG	RHS	175	1350	32.2	25	62	93	88	83	74	7	26	73	9	Fine-grained	MH/OH	MH	Elastic Silt
Murang'a	5	2+000	330	SG	LHS	100	1200	31.5	24	53	100	98	96	95	0	5	100	1	Fine-grained	CH/OH	CH	Fat Clay
	6	3+000	240	SG	LHS	150	1560	22.0	18	43	84	71	52	43	16	57	72	9	Fine-grained	CL/OL	CL	Lean Clay
	7	3+500	335	SG	RHS	300	1410	23.9	24	55	73	50	41	30	27	70	61	11	Fine-grained	MH/OH	MH	Elastic Silt
	8	4+000	340	SG	LHS	300	1510	19.6	21	54	72	49	37	24	28	76	63	13	Fine-grained	MH/OH	MH	Elastic Silt

Road No. & Location	TP No.	Chainage	Depth	Layer	Lane	Thickness mm	Max. Dry Density gcc	Optimum Moisture Content (%)	PI %	LL %	% Pass. BS Sieve 5mm (No.4)	% Pass. BS Sieve 2mm	% Pass. BS Sieve 0.425mm	% Pass. BS Sieve 0.075mm (No.200)	Gravel Fraction	Total Coarse Fraction	Sand Fraction	No.200 Retained	Coarse/Fine Grained	Plasticity Chart	Group Symbol	Soil Classification
	9	4+500	278	SG	RHS	300	1690	16.4	20	41	71	51	30	22	29	78	63	8	Fine-grained	CL/OL	CL	Lean Clay
	10	5+000	410	SG	LHS	300	1225	33.8	23	50	99	98	96	88	1	12	92	8	Fine-grained	CL/OL	CL	Lean Clay
	11	5+500	350	SG	RHS	300	1610	18.5	19	44	74	56	37	28	26	72	64	9	Fine-grained	CL/OL	CL	Lean Clay
	12	6+000	339	SG	LHS	150	1270	29.2	19	50	80	63	30	26	20	74	73	4	Fine-grained	MH/OH	MH	Elastic Silt
	13	6+500	335	SG	RHS	100	1395	23.0	26	56	99	91	80	75	1	25	96	5	Fine-grained	CH/OH	CH	Fat Clay
	14	7+000	450	SG	LHS	300	1565	21.2	22	41	77	56	35	25	23	75	69	10	Fine-grained	CL/OL	CL	Lean Clay
	15	7+500	268	SG	RHS	300	1495	22.0	23	55	73	61	40	30	27	70	61	10	Fine-grained	MH/OH	MH	Elastic Silt
	16	8+000	330	SG	LHS	150	1165	24.8	29	61	100	99	91	86	0	14	100	5	Fine-grained	MH/OH	MH	Elastic Silt
	17	8+500	605	SG	RHS	300	1225	25.3	26	55	98	96	86	84	2	16	88	2	Fine-grained	CH/OH	CH	Fat Clay
	18	9+000	383	SG	LHS	150	1340	32.0	26	59	94	92	90	84	6	16	63	6	Fine-grained	MH/OH	MH	Elastic Silt
	19	9+500	334	SG	RHS	300	1255	28.6	28	54	95	91	81	73	5	27	81	8	Fine-grained	CH/OH	CH	Fat Clay
	20	10+000	340	SG	LHS	150	1490	27.7	18	40	80	63	40	30	20	70	71	10	Fine-grained	CL/OL	CL	Lean Clay
	21	10+500	295	SG	RHS	170	1500	24.0	20	51	88	75	54	37	12	63	81	17	Fine-grained	MH/OH	MH	Elastic Silt with sand
	1	0+000		SG	LHS		1310	32.1	23	56	100	100	89	86	0	14	100	3	Fine-grained	MH/OH	MH	Elastic Silt
	2	3+000		SG	LHS		1440	24.2	27	56	100	89	84	78	0	22	100	6	Fine-grained	CH/OH	CH	Fat Clay
18.	3	6+000		SG	RHS		1445	25.9	22	45	100	72	66	59	0	41	100	7	Fine-grained	CL/OL	CL	Lean Clay
Kikuyu	4	9+000		SG	LHS		1485	23.0	20	41	100	89	84	77	0	23	100	7	Fine-grained	CL/OL	CL	Lean Clay
	5	12+000		SG	RHS		1390	25.0	21	41	100	88	84	80	0	20	100	4	Fine-grained	CL/OL	CL	Lean Clay
	6	15+000		SG	LHS		1305	30.9	22	44	100	88	86	84	0	16	100	2	Fine-grained	CL/OL	CL	Lean Clay

Appendix VII: Deflections Recorded at 9 Geophones

Road No.	Chainage	Deflections in µm at the 9 Geophone Offsets (mm) 0	200	300	600	900	1200	1500	1800	2100	Soil Class
1	Km 0 + 710	823	470	282	82	39	23	16	13	9	MH
	Km 5 + 000	1033	631	396	163	89	57	41	34	29	MH
	Km 9 + 762	459	260	197	89	54	37	29	24	18	MH
	Km 15 + 000	787	492	312	110	66	47	33	31	26	MH
	Km 22 + 350	508	341	264	147	100	75	60	53	47	CH
	Km 29+ 300	329	246	195	108	72	51	39	35	29	CL
2	Km 8+800	250	68	62	40	48	46	38	29	15	CL
	Km 18+900	455	207	178	144	123	99	81	65	44	CL
	Km 24+600	383	153	138	114	110	92	78	63	42	ML
	Km 24+850	417	148	128	99	87	67	51	37	21	ML
	Km 25+150	354	149	132	107	103	85	71	57	39	ML
	Km 25+370	378	140	126	105	95	87	74	60	40	ML
	Km 40+600	299	104	89	66	66	58	50	41	27	ML
	Km 55+000	354	117	96	69	58	48	36	27	13	CL
	Km 70+200	282	74	68	48	56	50	41	31	18	ML
	Km 81+000	301	69	64	46	54	51	43	35	20	ML
3	Km 3 + 423	472	405	264	184	117	75	62	51	32	CL
	Km 7 + 282	654	538	348	228	132	89	78	63	45	MH
	Km 12 + 417	656	557	351	222	129	84	74	55	37	MH
	Km 17 + 525	339	287	195	130	79	52	43	33	17	GM
	Km 22 + 565	537	492	362	273	165	90	62	43	21	CH
4	Km 0+305	524	405	343	207	143	101	80	67	60	ML
	Km 0+305	522	406	343	210	144	102	82	68	62	CH
	Km 15+600	533	388	305	151	92	65	53	47	42	MH
	Km 15+600	530	386	305	152	92	65	52	46	39	MH
	Km 30+360	220	185	169	113	87	66	52	45	37	MH
	Km 44+080	203	168	156	93	65	46	36	32	26	CL
	Km 44+080	203	168	155	92	65	46	36	32	26	CH
5	Km 1+300	751	683	626	455	331	243	194	165	152	ML
	Km 1+300	751	681	624	452	327	239	190	161	147	ML
	Km 9+000	2021	1569	1291	679	433	329	272	241	217	ML
	Km 43+100	1112	813	626	254	145	105	86	75	65	CL
	Km 80+600	901	661	473	175	82	41	24	19	13	ML
	Km 80+600	898	663	474	176	82	41	24	19	13	CL
6	Km 9+950	795	628	520	268	139	75	45	32	24	CL
	Km 20+100	686	511	381	148	83	52	36	26	18	CL
	Km 20+100	934	677	529	242	134	83	58	47	39	CL
	Km 20+100	689	516	384	149	84	53	35	26	18	ML
	Km 35+600	1131	811	647	264	155	116	89	78	68	ML
	Km 45+500	848	632	512	246	158	108	79	65	60	CL
7	Km 0+676	625	445	334	146	82	52	39	32	27	ML
	Km 0+676	624	443	332	147	81	52	38	32	26	CL
	Km 10+200	511	354	278	135	91	66	54	46	37	CL
	Km10+200	511	351	276	134	91	66	53	46	37	CL
	Km 20+000	670	449	341	151	97	71	57	50	42	ML
	Km 20+000	659	447	340	149	97	71	56	49	40	ML
	Km 20+000	619	404	302	141	108	80	64	55	45	MH
	Km 27+505	504	375	308	155	103	75	60	52	44	ML
	Km 27+505	496	372	305	154	103	75	60	52	44	CL
	Km 29+240	1073	754	613	279	159	111	90	79	69	ML
	Km 29+240	1058	757	616	277	159	111	89	81	68	CH
8	Km 10+100	963	747	619	326	209	165	137	121	109	MH
	Km 25+000	688	482	374	177	104	74	57	51	42	MH
	Km 40+000	954	692	533	220	116	77	59	53	44	MH
	Km 40+000	944	691	532	217	116	77	60	54	44	MH
	Km 50+300	850	594	449	212	127	87	65	52	46	MH
9	Km 0+075	1998	1040	589	232	151	111	88	76	62	ML
	Km 0+075	1935	1027	586	234	152	110	89	76	62	MH
	Km 3+000	883	675	517	256	156	106	78	64	57	MH
	Km 3+000	870	669	514	256	156	106	79	64	56	MH
	Km 6+100	1442	868	563	228	128	88	65	55	47	CL
	Km 8+100	1003	719	551	248	139	91	65	51	45	MH
10	Km 12+640	848	612	462	194	107	77	63	53	46	CL
	Km 36+500	768	507	355	146	96	71	59	51	42	CL
	Km 50+450	752	465	313	100	71	59	50	45	37	CL
	Km 65+400	609	375	237	92	65	50	40	35	28	MH
	Km 65+400	598	375	237	91	65	49	40	35	28	MH
11	Km 0+130	235	204	179	137	107	91	71	55	33	MH
	Km 0+950	520	420	284	173	103	84	68	55	35	MH
	Km 1+550	420	350	273	194	130	98	78	66	38	MH
12	Km 0+100	354	267	223	121	76	59	44	39	35	CL
	Km 0+700	206	165	145	88	48	29	11	5	2	MH
	Km 2+100	385	312	265	153	85	29	29	21	17	ML
	Km 2+100	385	313	266	154	85	27	28	22	17	CL
13	KM 1+300	475	387	342	239	157	101	76	58	53	CL

Road No.	Chainage	Deflections in μm at the 9 Geophone Offsets (mm)									Soil Class
		0	200	300	600	900	1200	1500	1800	2100	
	KM 10+100	1233	720	547	335	193	118	86	71	60	CL
	KM 20+300	310	281	257	201	141	92	69	53	45	ML
	KM 30+300	423	317	267	185	110	62	42	31	26	MH
	KM 40+250	251	115	88	56	43	23	20	18	19	CL
14	KM 0+150	776	483	362	227	137	88	68	55	48	CL
	KM 10+000	517	312	245	164	108	73	60	50	43	MH
	KM 19+700	688	343	270	173	111	79	66	57	51	MH
	KM 30+300	463	344	304	234	165	116	87	68	55	ML
	KM 40+000	991	348	238	149	93	66	53	42	39	MH
15	KM 0+050	976	410	301	187	114	70	54	44	38	CL
	KM 6+000	282	119	93	64	41	26	20	16	14	ML
	KM 10+000	452	174	132	93	66	47	36	29	23	CL
16	KM 0+050	701	301	217	144	104	71	58	48	40	CL
	KM 5+000	684	323	231	143	98	68	55	44	39	CH
	KM 10+000	931	433	295	181	120	82	65	52	44	ML
	KM 15+000	642	304	198	114	83	58	49	41	36	CL
	KM 20+000	958	468	310	138	73	52	43	38	33	MH
	KM 25+000	1105	447	279	139	82	54	44	36	32	ML
	KM 30+000	824	405	252	119	57	36	28	23	20	CL
	KM 33+500	642	354	267	132	49	26	20	16	13	ML
17	Km 0+100	607	298	233	147	95	71	57	45	34	MH
	Km 0+500	888	453	331	172	82	53	42	30	24	CH
	Km 1+000	725	350	257	163	114	76	61	50	44	CL
	Km 1+500	713	346	247	141	84	63	54	43	36	MH
	Km 2+000	908	497	379	226	132	87	65	46	39	CH
	Km 3+000	665	414	322	189	102	71	52	40	32	CL
	Km 3+500	951	459	344	206	112	72	53	43	36	MH
	Km 4+000	758	242	170	108	74	54	44	35	30	MH
	Km 4+500	733	420	327	204	119	73	51	39	32	CL
	Km 5+000	649	403	318	187	93	60	48	40	32	CL
	Km 5+500	780	385	283	181	118	79	60	48	39	CL
	Km 6+000	692	334	254	170	113	72	48	37	32	MH
	Km 6+500	838	484	368	217	132	95	80	67	55	CH
	Km 7+000	447	187	121	60	34	19	14	8	5	CL
	Km 7+500	633	273	217	150	104	68	52	41	32	MH
	Km 8+000	820	454	355	225	134	73	50	34	26	MH
	Km 8+500	505	190	137	86	56	36	26	20	16	CH
	Km 9+000	678	283	207	135	92	63	52	41	34	MH
	Km 9+500	779	325	228	137	97	70	61	52	45	CH
	Km 10+000	519	252	192	124	84	58	48	40	35	CL
	Km 10+500	852	491	422	313	217	152	114	88	71	MH
18	Km 0+000	537	349	243	103	70	50	38	29	26	MH
	Km 3+000	813	535	377	155	91	66	52	40	35	CH
	Km 6+000	558	418	327	158	89	56	42	30	23	CL
	Km 9+000	350	234	177	86	56	36	30	25	23	CL
	Km12+000	569	360	256	137	89	54	39	30	27	CL
	Km 15+000	587	428	329	167	104	72	57	46	38	CL

Appendix VIII: FWD Deflection Ratios

Road No.	Chainage	FWD Deflection Ratio (DR)							
		D0/ D200	**D200/ D300**	**D300/ D600**	**D600/ D900**	**D900/ D1200**	**D1200/ D1500**	**D1500/ D1800**	**D1800/ D2100**
1	Km 0 + 710	1.752	1.668	3.416	2.111	1.694	1.483	1.220	1.423
	Km 5 + 000	1.637	1.593	2.431	1.830	1.555	1.394	1.200	1.196
	Km 9 + 762	1.764	1.322	2.204	1.661	1.436	1.300	1.200	1.316
	Km 15 + 000	1.600	1.577	2.823	1.687	1.396	1.412	1.063	1.185
	Km 22 + 350	1.488	1.293	1.797	1.465	1.329	1.246	1.151	1.128
	Km 29+ 300	1.336	1.259	1.811	1.500	1.423	1.300	1.111	1.200
	Mean	**1.596**	**1.452**	**2.414**	**1.709**	**1.472**	**1.356**	**1.157**	**1.241**
2	Km 8+800	3.692	1.102	1.553	0.826	1.045	1.222	1.286	2.000
	Km 18+900	2.193	1.166	1.234	1.171	1.245	1.221	1.242	1.476
	Km 24+600	2.497	1.107	1.213	1.038	1.195	1.176	1.233	1.500
	Km 24+850	2.814	1.157	1.287	1.146	1.302	1.313	1.371	1.750
	Km 25+150	2.379	1.129	1.228	1.041	1.213	1.194	1.241	1.459
	Km 25+370	2.693	1.114	1.206	1.097	1.094	1.181	1.220	1.513
	Km 40+600	2.886	1.167	1.343	1.000	1.136	1.157	1.214	1.556
	Km 55+000	3.017	1.221	1.397	1.193	1.188	1.333	1.333	2.077
	Km 70+200	3.789	1.092	1.413	0.868	1.104	1.231	1.300	1.765
	Km 81+000	4.348	1.078	1.391	0.852	1.059	1.186	1.229	1.750
	Mean	**3.031**	**1.133**	**1.326**	**1.023**	**1.158**	**1.221**	**1.267**	**1.685**
3	Km 3 + 423	1.164	1.535	1.433	1.579	1.562	1.197	1.220	1.613
	Km 7 + 282	1.216	1.547	1.522	1.731	1.489	1.139	1.234	1.391
	Km 12 + 417	1.177	1.585	1.583	1.714	1.537	1.139	1.333	1.500
	Km 17 + 525	1.179	1.472	1.504	1.638	1.509	1.233	1.303	1.941
	Km 22 + 565	1.093	1.360	1.323	1.660	1.820	1.459	1.452	2.000
	Mean	**1.166**	**1.500**	**1.473**	**1.665**	**1.583**	**1.233**	**1.309**	**1.689**
4	Km 0+305	1.294	1.183	1.653	1.453	1.418	1.256	1.200	1.121
	Km 0+305	1.288	1.181	1.634	1.459	1.410	1.250	1.200	1.094
	Km 15+600	1.375	1.273	2.013	1.645	1.409	1.222	1.125	1.143
	Km 15+600	1.372	1.268	2.000	1.649	1.424	1.245	1.128	1.175
	Km 30+360	1.190	1.095	1.487	1.299	1.318	1.269	1.156	1.216
	Km 44+080	1.210	1.077	1.685	1.415	1.413	1.278	1.125	1.231
	Km 44+080	1.214	1.084	1.685	1.415	1.413	1.278	1.125	1.231

Road No.	Chainage	FWD Deflection Ratio (DR)							
		D0/ D200	**D200/ D300**	**D300/ D600**	**D600/ D900**	**D900/ D1200**	**D1200/ D1500**	**D1500/ D1800**	**D1800/ D2100**
	Mean	**1.277**	**1.166**	**1.737**	**1.477**	**1.401**	**1.257**	**1.151**	**1.173**
5	Km 1+300	1.100	1.091	1.376	1.376	1.363	1.253	1.172	1.090
	Km 1+300	1.102	1.092	1.382	1.382	1.369	1.255	1.178	1.101
	Km 9+000	1.288	1.215	1.901	1.568	1.316	1.212	1.128	1.110
	Km 43+100	1.368	1.300	2.466	1.754	1.379	1.226	1.135	1.156
	Km 80+600	1.362	1.397	2.704	2.131	2.000	1.680	1.316	1.462
	Km 80+600	1.354	1.398	2.694	2.143	2.000	1.680	1.316	1.462
	Mean	**1.263**	**1.249**	**2.087**	**1.725**	**1.571**	**1.384**	**1.207**	**1.230**
6	Km 9+950	1.265	1.207	1.940	1.928	1.865	1.644	1.406	1.333
	Km 20+100	1.342	1.342	2.576	1.775	1.589	1.474	1.357	1.474
	Km 20+100	1.379	1.280	2.186	1.809	1.617	1.421	1.239	1.211
	Km 20+100	1.334	1.345	2.583	1.773	1.571	1.514	1.370	1.421
	Km 35+600	1.394	1.253	2.452	1.699	1.339	1.298	1.151	1.141
	Km 45+500	1.342	1.236	2.081	1.560	1.456	1.373	1.203	1.095
	Mean	**1.343**	**1.277**	**2.303**	**1.757**	**1.573**	**1.454**	**1.288**	**1.279**
7	Km 0+676	1.404	1.332	2.282	1.795	1.566	1.325	1.212	1.179
	Km 0+676	1.408	1.332	2.267	1.807	1.566	1.359	1.182	1.222
	Km 10+200	1.446	1.271	2.067	1.473	1.379	1.222	1.174	1.243
	Km10+200	1.453	1.272	2.060	1.473	1.379	1.245	1.152	1.243
	Km 20+000	1.492	1.315	2.262	1.552	1.371	1.250	1.143	1.195
	Km 20+000	1.474	1.315	2.277	1.542	1.371	1.250	1.143	1.225
	Km 20+000	1.532	1.337	2.137	1.315	1.337	1.258	1.158	1.239
	Km 27+505	1.345	1.218	1.987	1.510	1.368	1.246	1.151	1.178
	Km 27+505	1.333	1.219	1.981	1.500	1.377	1.242	1.148	1.200
	Km 29+240	1.423	1.229	2.197	1.756	1.431	1.239	1.128	1.147
	Km 29+240	1.398	1.228	2.227	1.745	1.433	1.238	1.105	1.188
	Mean	**1.428**	**1.279**	**2.159**	**1.588**	**1.416**	**1.261**	**1.154**	**1.205**
8	Km 10+100	1.289	1.207	1.898	1.563	1.261	1.204	1.132	1.110
	Km 25+000	1.429	1.289	2.114	1.697	1.416	1.283	1.132	1.205
	Km 40+000	1.380	1.297	2.426	1.901	1.494	1.306	1.127	1.196
	Km 40+000	1.366	1.298	2.454	1.862	1.506	1.283	1.111	1.227
	Km 50+300	1.432	1.321	2.119	1.667	1.465	1.344	1.255	1.109
	Mean	**1.379**	**1.283**	**2.202**	**1.738**	**1.428**	**1.284**	**1.152**	**1.169**

Road No.	Chainage	FWD Deflection Ratio (DR)							
		D0/ D200	D200/ D300	D300/ D600	D600/ D900	D900/ D1200	D1200/ D1500	D1500/ D1800	D1800/ D2100
9	Km 0+075	1.920	1.766	2.540	1.534	1.364	1.259	1.164	1.217
	Km 0+075	1.884	1.754	2.507	1.534	1.383	1.244	1.162	1.233
	Km 3+000	1.307	1.306	2.020	1.638	1.476	1.355	1.226	1.127
	Km 3+000	1.302	1.300	2.008	1.639	1.476	1.346	1.238	1.125
	Km 6+100	1.662	1.540	2.476	1.772	1.460	1.359	1.185	1.174
	Km 8+100	1.395	1.304	2.218	1.787	1.533	1.394	1.269	1.130
	Mean	**1.578**	**1.495**	**2.295**	**1.651**	**1.449**	**1.326**	**1.207**	**1.168**
10	Km 12+640	1.385	1.326	2.376	1.814	1.395	1.227	1.179	1.143
	Km 36+500	1.513	1.427	2.435	1.515	1.347	1.220	1.157	1.214
	Km 50+450	1.617	1.485	3.146	1.411	1.197	1.173	1.106	1.237
	Km 65+400	1.624	1.584	2.576	1.414	1.296	1.256	1.132	1.267
	Km 65+400	1.596	1.584	2.604	1.391	1.327	1.238	1.135	1.233
	Mean	**1.547**	**1.481**	**2.627**	**1.509**	**1.312**	**1.223**	**1.142**	**1.219**
11	Km 0+130	1.150	1.138	1.310	1.275	1.182	1.283	1.277	1.679
	Km 0+950	1.239	1.481	1.634	1.686	1.229	1.228	1.239	1.586
	Km 1+550	1.201	1.281	1.408	1.495	1.329	1.254	1.189	1.710
	Mean	**1.197**	**1.300**	**1.451**	**1.485**	**1.247**	**1.255**	**1.235**	**1.658**
12	Km 0+100	1.325	1.199	1.844	1.600	1.270	1.340	1.146	1.108
	Km 0+700	1.244	1.143	1.652	1.816	1.633	2.727	2.200	2.500
	Km 2+100	1.235	1.176	1.733	1.809	2.967	1.000	1.364	1.222
	Km 2+100	1.231	1.176	1.732	1.805	3.107	0.966	1.318	1.294
	Mean	**1.259**	**1.174**	**1.740**	**1.757**	**2.244**	**1.508**	**1.507**	**1.531**
13	KM 1+300	1.230	1.130	1.432	1.519	1.560	1.333	1.313	1.091
	KM 10+100	1.712	1.317	1.633	1.738	1.633	1.380	1.203	1.180
	KM 20+300	1.103	1.094	1.275	1.427	1.539	1.333	1.295	1.189
	KM 30+300	1.336	1.188	1.439	1.685	1.769	1.486	1.346	1.182
	KM 40+250	2.175	1.311	1.574	1.306	1.895	1.118	1.133	0.938
	Mean	**1.511**	**1.208**	**1.471**	**1.535**	**1.679**	**1.330**	**1.258**	**1.116**
14	KM 0+150	1.606	1.337	1.591	1.664	1.545	1.305	1.229	1.143
	KM 10+000	1.658	1.272	1.496	1.517	1.483	1.224	1.195	1.171
	KM 19+700	2.004	1.270	1.563	1.560	1.400	1.204	1.149	1.119
	KM 30+300	1.346	1.130	1.301	1.419	1.418	1.338	1.283	1.233
	KM 40+000	2.845	1.463	1.598	1.608	1.411	1.244	1.250	1.091

Road No.	Chainage	FWD Deflection Ratio (DR)							
		D0/ D200	D200/ D300	D300/ D600	D600/ D900	D900/ D1200	D1200/ D1500	D1500/ D1800	D1800/ D2100
	Mean	**1.892**	**1.294**	**1.510**	**1.553**	**1.451**	**1.263**	**1.221**	**1.151**
15	KM 0+050	2.383	1.361	1.614	1.629	1.644	1.283	1.243	1.156
	KM 6+000	2.368	1.284	1.451	1.545	1.571	1.313	1.231	1.182
	KM 10+000	2.599	1.315	1.421	1.407	1.421	1.310	1.208	1.263
	Mean	**2.450**	**1.320**	**1.495**	**1.527**	**1.546**	**1.302**	**1.227**	**1.200**
16	KM 0+050	2.331	1.385	1.512	1.380	1.460	1.235	1.214	1.200
	KM 5+000	2.120	1.394	1.623	1.452	1.448	1.234	1.237	1.152
	KM 10+000	2.150	1.466	1.634	1.505	1.473	1.254	1.255	1.175
	KM 15+000	2.112	1.540	1.740	1.370	1.431	1.186	1.194	1.125
	KM 20+000	2.046	1.512	2.244	1.896	1.396	1.200	1.143	1.167
	KM 25+000	2.474	1.601	2.008	1.703	1.510	1.225	1.212	1.138
	KM 30+000	2.032	1.606	2.119	2.096	1.576	1.269	1.238	1.167
	KM 33+500	1.813	1.328	2.024	2.717	1.840	1.316	1.267	1.250
	Mean	**2.135**	**1.479**	**1.863**	**1.765**	**1.517**	**1.240**	**1.220**	**1.172**
17	Km 0+100	2.036	1.279	1.589	1.550	1.333	1.250	1.263	1.310
	Km 0+500	1.959	1.367	1.932	2.085	1.543	1.278	1.385	1.238
	Km 1+000	2.068	1.366	1.577	1.429	1.492	1.245	1.225	1.143
	Km 1+500	2.064	1.398	1.748	1.691	1.333	1.159	1.257	1.207
	Km 2+000	1.828	1.313	1.676	1.713	1.521	1.340	1.395	1.188
	Km 3+000	1.608	1.285	1.699	1.866	1.439	1.357	1.313	1.231
	Km 3+500	2.073	1.331	1.669	1.849	1.550	1.364	1.222	1.200
	Km 4+000	3.136	1.420	1.579	1.462	1.354	1.231	1.258	1.192
	Km 4+500	1.746	1.285	1.599	1.722	1.617	1.429	1.313	1.231
	Km 5+000	1.613	1.268	1.699	2.000	1.560	1.250	1.212	1.222
	Km 5+500	2.027	1.361	1.564	1.529	1.500	1.308	1.268	1.206
	Km 6+000	2.073	1.312	1.493	1.505	1.565	1.512	1.281	1.185
	Km 6+500	1.730	1.314	1.699	1.645	1.390	1.185	1.204	1.200
	Km 7+000	2.389	1.552	2.000	1.778	1.800	1.364	1.833	1.500
	Km 7+500	2.319	1.258	1.444	1.448	1.526	1.295	1.294	1.259
	Km 8+000	1.807	1.277	1.578	1.682	1.833	1.463	1.464	1.333
	Km 8+500	2.660	1.383	1.597	1.532	1.567	1.364	1.294	1.308
	Km 9+000	2.394	1.369	1.530	1.474	1.444	1.227	1.257	1.207
	Km 9+500	2.396	1.426	1.664	1.413	1.379	1.160	1.163	1.162

Road No.	Chainage	FWD Deflection Ratio (DR)							
		D0/ D200	**D200/ D300**	**D300/ D600**	**D600/ D900**	**D900/ D1200**	**D1200/ D1500**	**D1500/ D1800**	**D1800/ D2100**
	Km 10+000	2.062	1.314	1.544	1.471	1.458	1.200	1.212	1.138
	Km 10+500	1.737	1.162	1.349	1.440	1.434	1.326	1.296	1.246
	Mean	**2.082**	**1.335**	**1.630**	**1.633**	**1.507**	**1.300**	**1.305**	**1.234**
18	Km 0+000	1.540	1.437	2.351	1.480	1.389	1.333	1.286	1.105
	Km 3+000	1.519	1.418	2.427	1.705	1.375	1.280	1.282	1.147
	Km 6+000	1.337	1.276	2.072	1.769	1.592	1.324	1.423	1.300
	Km 9+000	1.498	1.318	2.066	1.520	1.563	1.185	1.227	1.100
	Km12+000	1.579	1.408	1.869	1.544	1.646	1.371	1.296	1.125
	Km 15+000	1.372	1.301	1.966	1.615	1.444	1.260	1.250	1.212
	Mean	**1.474**	**1.360**	**2.125**	**1.606**	**1.501**	**1.292**	**1.294**	**1.165**

Appendix IX: Subgrade Modulus for all Road Sections

Road No.	Chainage	Subgrade Surface Modulus (E_0 0 to 2100)								
		0	200	300	600	900	1200	1500	1800	2100
1	Km 0 + 710	246	162	180	307	432	549	652	663	808
	Km 5 + 000	191	118	125	152	185	216	241	241	247
	Km 9 + 762	423	280	247	272	301	324	337	337	380
	Km 15 + 000	242	145	153	215	242	253	286	253	257
	Km 22 + 350	365	203	175	158	154	153	153	147	142
	Km 29+ 300	577	289	242	219	219	234	244	226	232
2	Km 8+800	713	987	725	563	310	243	238	255	437
	Km 18+900	389	320	249	153	120	112	109	113	143
	Km 24+600	460	431	318	193	134	120	113	116	149
	Km 24+850	422	445	343	221	169	165	173	198	297
	Km 25+150	496	442	333	204	142	129	123	127	159
	Km 25+370	480	485	360	217	159	130	123	125	162
	Km 40+600	630	682	530	356	237	202	187	189	252
	Km 55+000	521	590	480	335	267	238	253	282	501
	Km 70+200	629	893	651	460	266	220	217	235	355
	Km 81+000	617	1006	723	503	286	227	215	220	330
3	Km 3 + 423	386	168	172	123	130	152	146	148	205
	Km 7 + 282	289	132	136	103	119	133	121	125	149
	Km 12 + 417	276	122	129	102	117	134	122	136	175
	Km 17 + 525	555	245	241	181	198	224	221	240	399
	Km 22 + 565	355	146	132	87	97	132	154	186	320
4	Km 0+305	346	168	132	109	106	113	113	113	109
	Km 0+305	366	177	139	114	111	117	117	117	110
	Km 15+600	353	182	155	156	171	180	176	165	162
	Km 15+600	357	184	155	155	171	182	182	171	172
	Km 30+360	843	376	275	204	177	175	177	171	178
	Km 44+080	911	413	297	250	236	250	256	240	253
	Km 44+080	918	418	302	254	240	254	260	244	257
5	Km 1+300	253	105	76	52	48	49	49	48	45
	Km 1+300	250	103	75	52	48	49	49	49	46
	Km 9+000	93	45	36	35	36	36	35	32	31
	Km 43+100	164	84	73	90	105	109	107	101	100
	Km 80+600	211	108	101	136	193	290	389	427	535
	Km 80+600	212	108	100	135	193	290	389	427	535
6	Km 9+950	232	110	89	86	110	155	203	238	272
	Km 20+100	285	143	128	165	195	233	274	310	392
	Km 20+100	213	110	94	103	124	150	171	176	183
	Km 20+100	259	129	116	150	177	209	253	289	352
	Km 35+600	155	81	68	83	94	94	98	94	92

Road No.	Chainage	Subgrade Surface Modulus (E_o 0 to 2100)								
		0	200	300	600	900	1200	1500	1800	2100
	Km 45+500	231	116	96	100	104	113	124	125	117
7	Km 0+676	303	160	142	162	194	228	241	244	246
	Km 0+676	305	161	143	162	195	230	250	246	257
	Km 10+200	363	197	167	172	169	175	171	167	178
	Km10+200	364	198	168	173	170	176	175	168	179
	Km 20+000	274	154	135	152	157	162	162	154	158
	Km 20+000	280	155	136	155	159	163	163	156	163
	Km 20+000	311	178	159	170	149	149	150	145	154
	Km 27+505	375	189	153	152	153	157	157	150	152
	Km 27+505	388	194	157	156	156	161	160	153	157
	Km 29+240	170	91	74	82	96	103	102	96	94
	Km 29+240	165	87	71	79	92	99	98	90	92
8	Km 10+100	193	93	75	71	74	70	68	64	61
	Km 25+000	283	152	130	138	156	166	170	160	166
	Km 40+000	204	106	91	111	140	157	164	154	158
	Km 40+000	196	101	87	107	133	150	154	142	150
	Km 50+300	215	116	102	108	120	132	142	148	141
9	Km 0+075	90	65	76	97	99	101	102	99	103
	Km 0+075	93	66	77	97	99	103	102	99	105
	Km 3+000	205	101	88	88	97	107	116	118	114
	Km 3+000	212	103	90	90	98	109	117	121	117
	Km 6+100	133	83	85	105	124	136	148	146	147
	Km 8+100	188	98	86	95	113	130	145	153	149
10	Km 12+640	232	120	106	126	153	160	157	154	151
	Km 36+500	248	141	134	163	165	166	162	157	163
	Km 50+450	256	155	154	241	227	204	191	176	187
	Km 65+400	329	200	211	272	257	250	251	236	257
	Km 65+400	329	197	208	271	251	250	247	234	247
11	Km 0+130	671	290	220	144	122	108	111	118	170
	Km 0+950	299	139	137	112	126	116	114	118	160
	Km 1+550	358	161	138	97	97	96	97	96	140
12	Km 0+100	557	277	221	204	218	207	222	212	202
	Km 0+700	921	430	327	270	327	401	875	1604	3437
	Km 2+100	508	235	184	160	192	428	343	389	408
	Km 2+100	494	228	179	155	186	434	336	369	409
13	KM 1+300	326	150	113	81	82	96	103	112	105
	KM 10+100	125	80	71	58	67	82	90	91	92
	KM 20+300	499	206	151	96	91	106	113	121	124
	KM 30+300	367	184	146	105	118	156	186	208	211
	KM 40+250	618	504	441	347	302	429	384	362	291
14	KM 0+150	209	126	112	89	99	115	120	123	120

Road No.	Chainage	Subgrade Surface Modulus (E_o 0 to 2100)								
		0	200	300	600	900	1200	1500	1800	2100
	KM 10+000	296	184	156	117	118	131	129	128	129
	KM 19+700	222	167	142	111	115	121	116	111	107
	KM 30+300	315	159	120	78	74	78	84	90	95
	KM 40+000	160	171	167	133	143	151	150	157	147
15	KM 0+050	162	144	131	106	115	142	145	150	149
	KM 6+000	528	469	402	291	300	354	371	381	386
	KM 10+000	336	327	287	204	191	204	214	215	233
16	KM 0+050	211	185	171	129	119	130	128	130	134
	KM 5+000	233	185	172	140	135	147	145	149	147
	KM 10+000	181	146	142	116	117	129	129	135	136
	KM 15+000	265	210	215	187	171	184	174	173	167
	KM 20+000	177	136	137	154	194	203	195	186	186
	KM 25+000	140	130	139	139	158	179	176	177	173
	KM 30+000	207	158	169	179	250	295	300	309	309
	KM 33+500	290	197	174	176	320	441	464	490	525
17	Km 0+100	260	198	169	134	139	139	139	146	164
	Km 0+500	181	133	121	117	163	188	192	222	236
	Km 1+000	204	158	144	113	108	121	120	123	120
	Km 1+500	212	164	153	134	151	151	140	147	152
	Km 2+000	168	115	101	84	96	110	118	137	139
	Km 3+000	226	136	117	99	123	133	145	158	167
	Km 3+500	163	127	113	94	116	135	147	150	154
	Km 4+000	216	254	241	190	185	188	185	194	199
	Km 4+500	208	136	116	93	107	130	148	162	171
	Km 5+000	239	145	122	104	138	162	162	164	171
	Km 5+500	206	156	142	111	113	127	133	141	146
	Km 6+000	231	179	157	117	117	138	167	178	181
	Km 6+500	180	117	103	87	96	100	94	95	97
	Km 7+000	332	297	307	307	364	492	536	820	1054
	Km 7+500	247	214	180	130	125	144	149	160	173
	Km 8+000	186	126	108	85	95	131	153	187	214
	Km 8+500	308	308	284	227	231	272	297	320	359
	Km 9+000	234	210	192	147	144	156	153	161	166
	Km 9+500	197	177	168	140	132	136	127	123	122
	Km 10+000	298	230	202	156	153	167	160	162	158
	Km 10+500	176	114	89	60	57	62	66	71	76
18	Km 0+000	249	144	138	162	160	166	177	190	180
	Km 3+000	221	126	119	144	164	169	173	185	182
	Km 6+000	291	146	124	129	152	181	192	228	254
	Km 9+000	471	264	232	240	243	285	270	276	261
	Km12+000	291	173	162	151	156	192	211	228	220

Road No.	Chainage	Subgrade Surface Modulus (E_o 0 to 2100)								
		0	**200**	**300**	**600**	**900**	**1200**	**1500**	**1800**	**2100**
	Km 15+000	278	143	124	122	131	142	144	150	155

Appendix X: Graphical Representation of the Subgrade Surface Modulus for all Road Sites

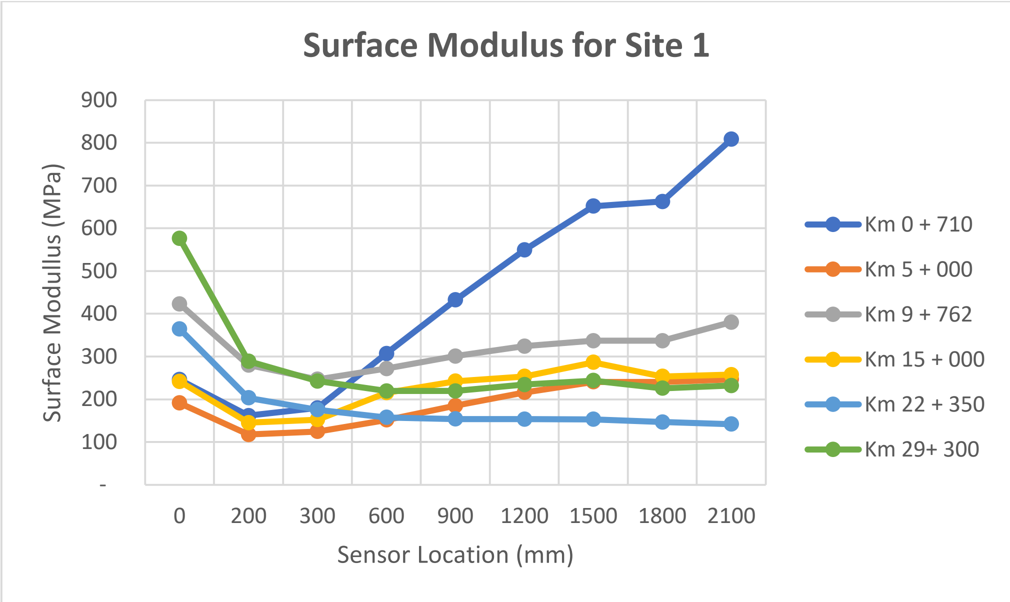

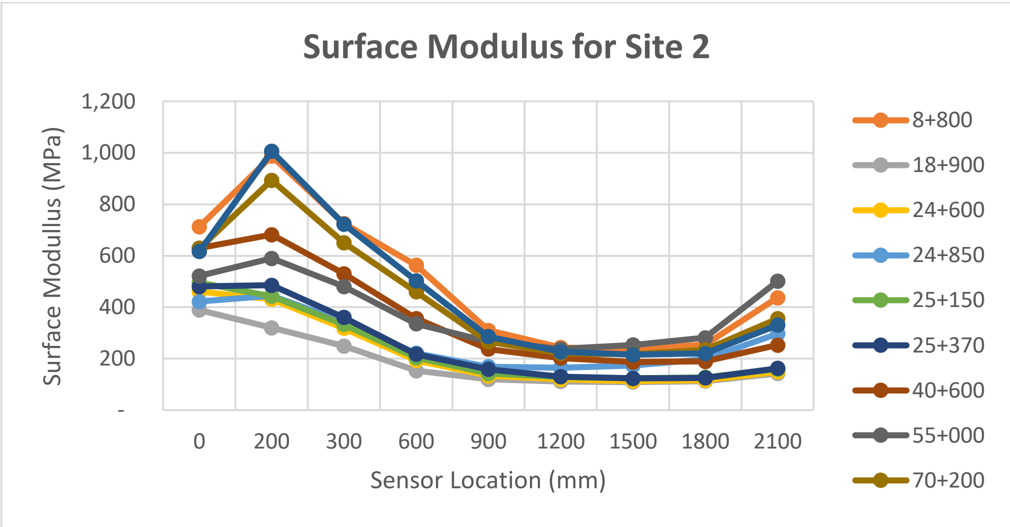

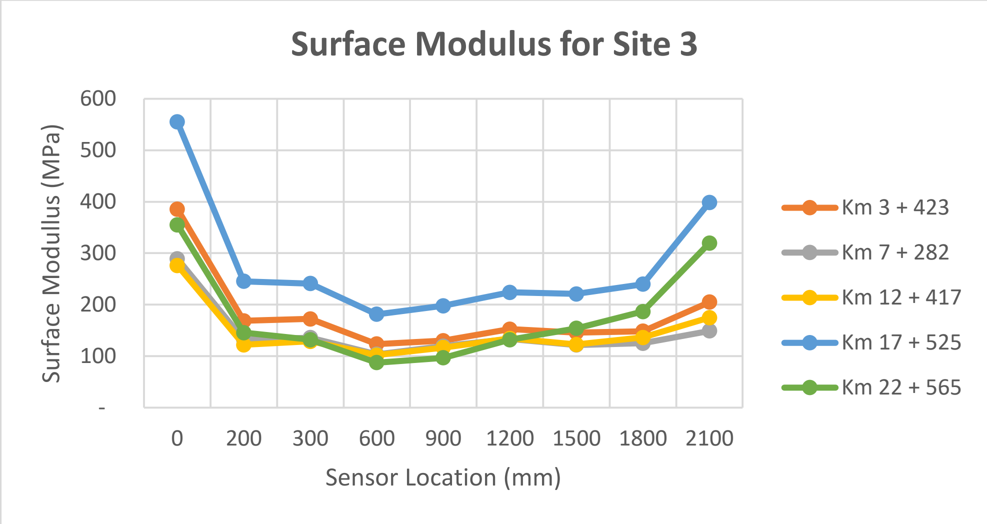

Surface Modulus for Site 3
Surface Modullus (MPa)
600
500
400
300
200
100
-
0
200
300
600
900
1200
1500
1800
2100
Sensor Location (mm)
Km 3 + 423
Km 7 + 282
Km 12 + 417
Km 17 + 525
Km 22 + 565

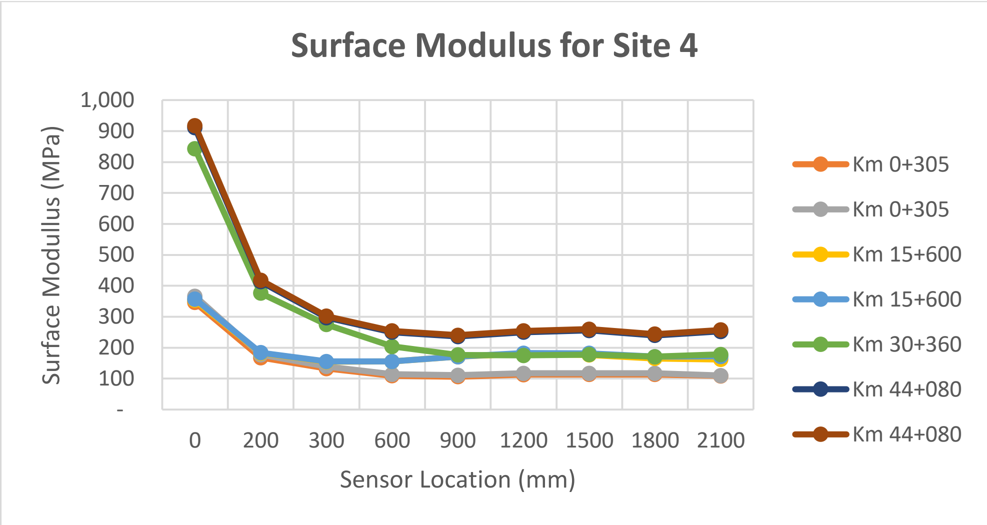

Surface Modulus for Site 4
Surface Modullus (MPa)
1,000
900
800
700
600
500
400
300
200
100
-
0
200
300
600
900
1200
1500
1800
2100
Sensor Location (mm)
Km 0+305
Km 0+305
Km 15+600
Km 15+600
Km 30+360
Km 44+080
Km 44+080

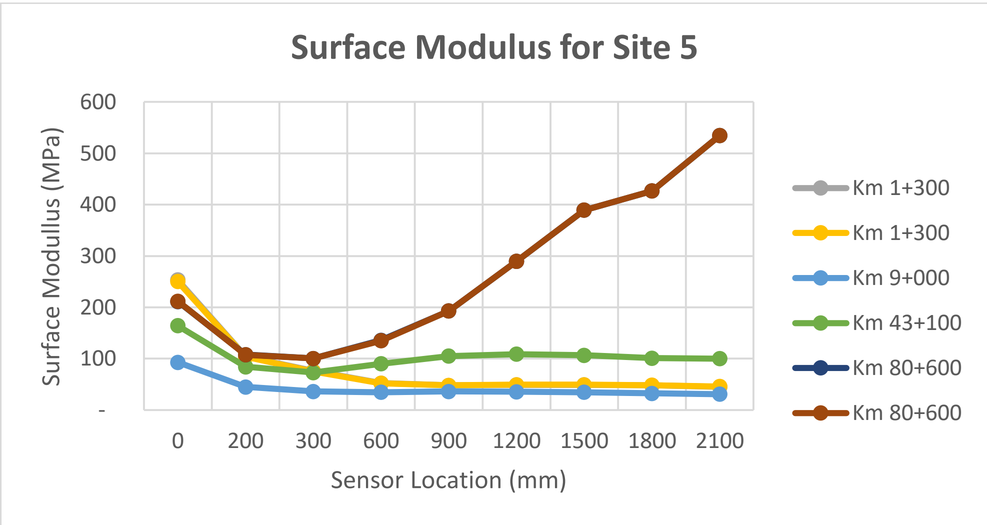

Surface Modulus for Site 5
Surface Modullus (MPa)
600
500
400
300
200
100
-
0
200
300
600
900
1200
1500
1800
2100
Sensor Location (mm)
Km 1+300
Km 1+300
Km 9+000
Km 43+100
Km 80+600
Km 80+600

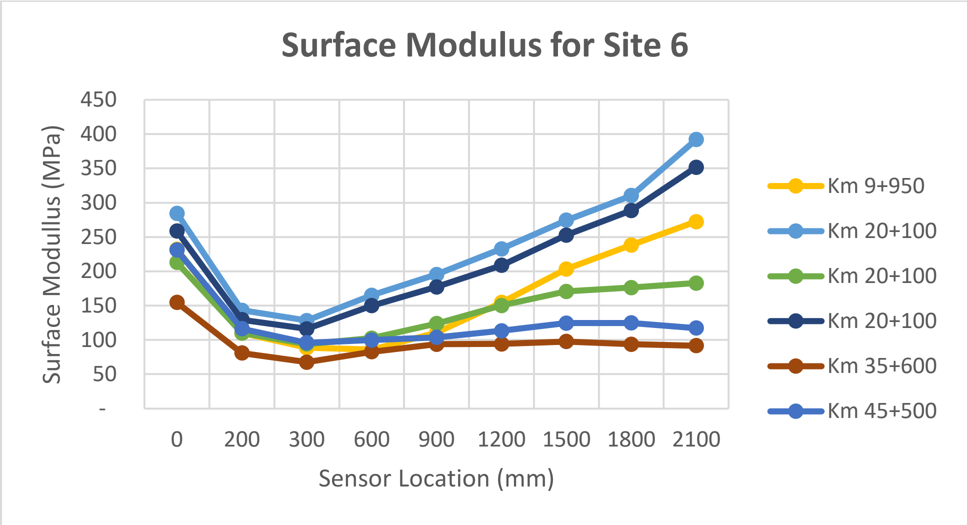
Surface Modulus for Site 6
Surface Modullus (MPa)
450
400
350
300
250
200
150
100
50
-
0
200
300
600
900
1200
1500
1800
2100
Sensor Location (mm)
Km 9+950
Km 20+100
Km 20+100
Km 20+100
Km 35+600
Km 45+500

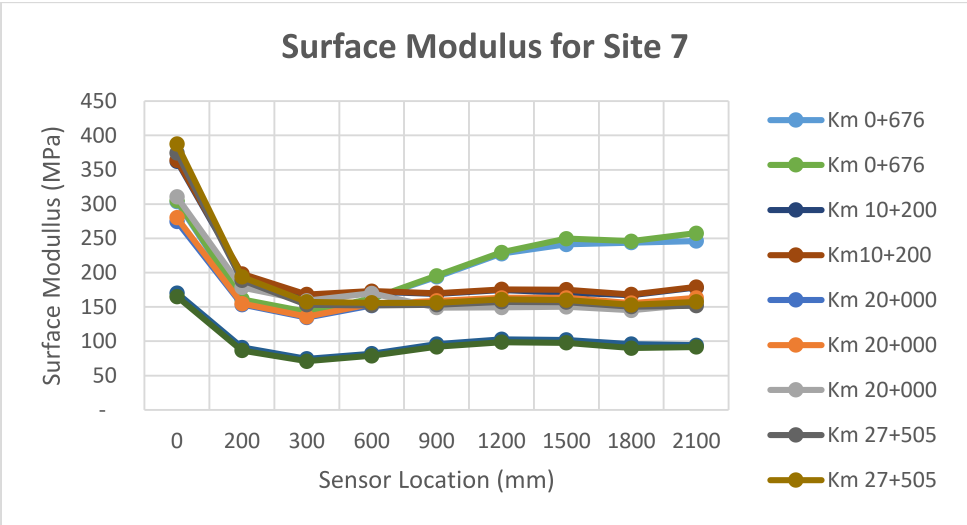
Surface Modulus for Site 7
Surface Modullus (MPa)
450
400
350
300
250
200
150
100
50
-
0
200
300
600
900
1200
1500
1800
2100
Sensor Location (mm)
Km 0+676
Km 0+676
Km 10+200
Km10+200
Km 20+000
Km 20+000
Km 20+000
Km 27+505
Km 27+505

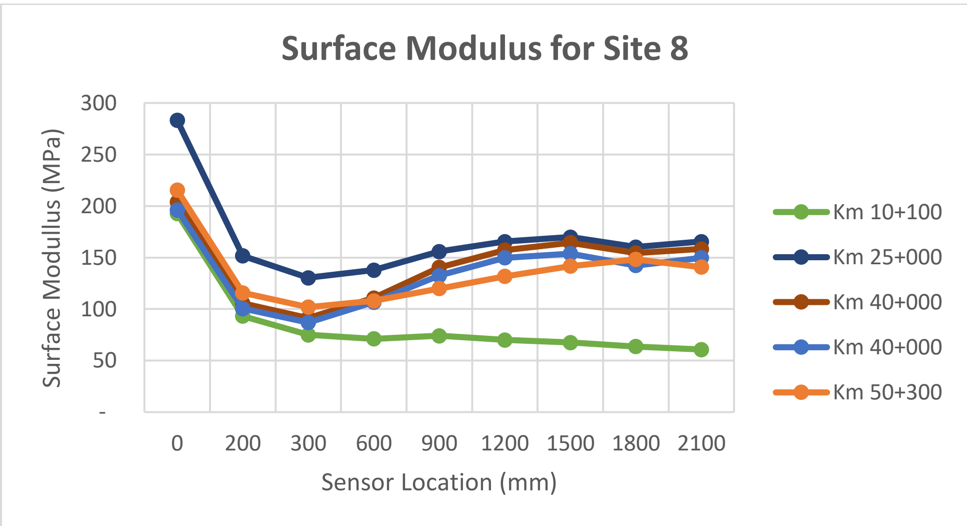
Surface Modulus for Site 8
Surface Modullus (MPa)
300
250
200
150
100
50
-
0
200
300
600
900
1200
1500
1800
2100
Sensor Location (mm)
Km 10+100
Km 25+000
Km 40+000
Km 40+000
Km 50+300

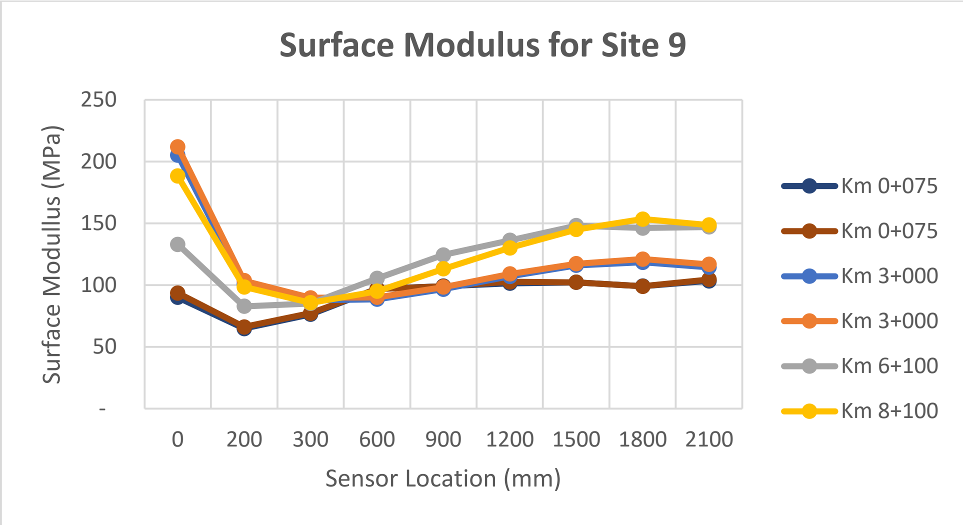
Surface Modulus for Site 9
Surface Modullus (MPa)
250
200
150
100
50
-
0
200
300
600
900
1200
1500
1800
2100
Sensor Location (mm)
Km 0+075
Km 0+075
Km 3+000
Km 3+000
Km 6+100
Km 8+100

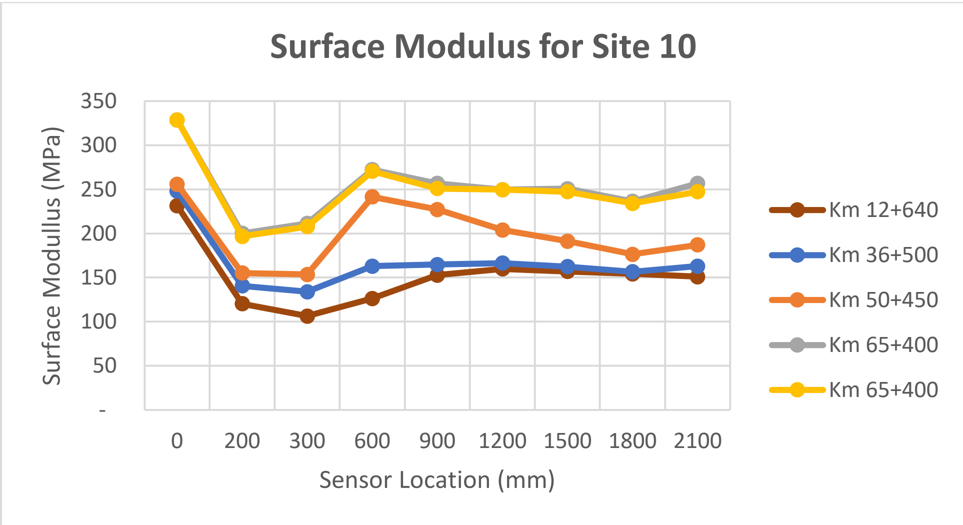
Surface Modulus for Site 10
Surface Modullus (MPa)
350
300
250
200
150
100
50
-
0
200
300
600
900
1200
1500
1800
2100
Sensor Location (mm)
Km 12+640
Km 36+500
Km 50+450
Km 65+400
Km 65+400

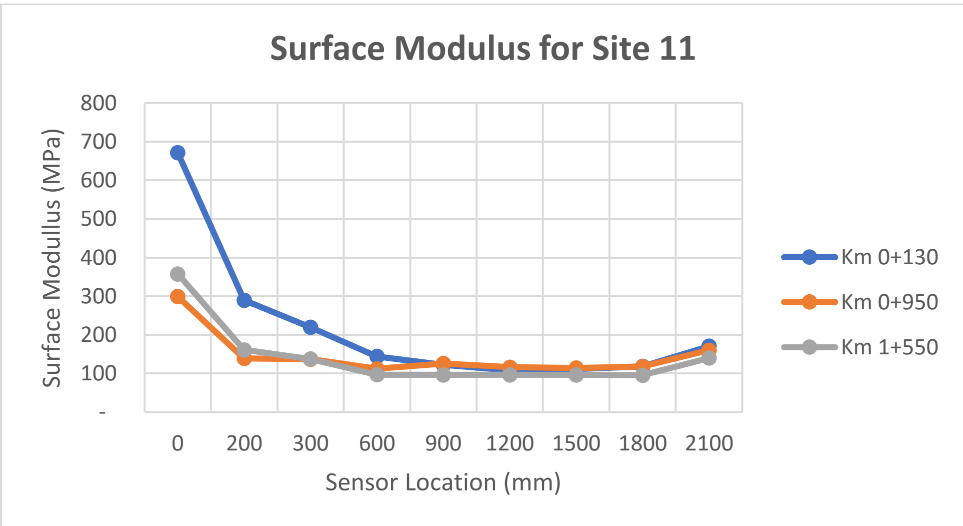
Surface Modulus for Site 11
Surface Modullus (MPa)
800
700
600
500
400
300
200
100
-
0
200
300
600
900
1200
1500
1800
2100
Sensor Location (mm)
Km 0+130
Km 0+950
Km 1+550

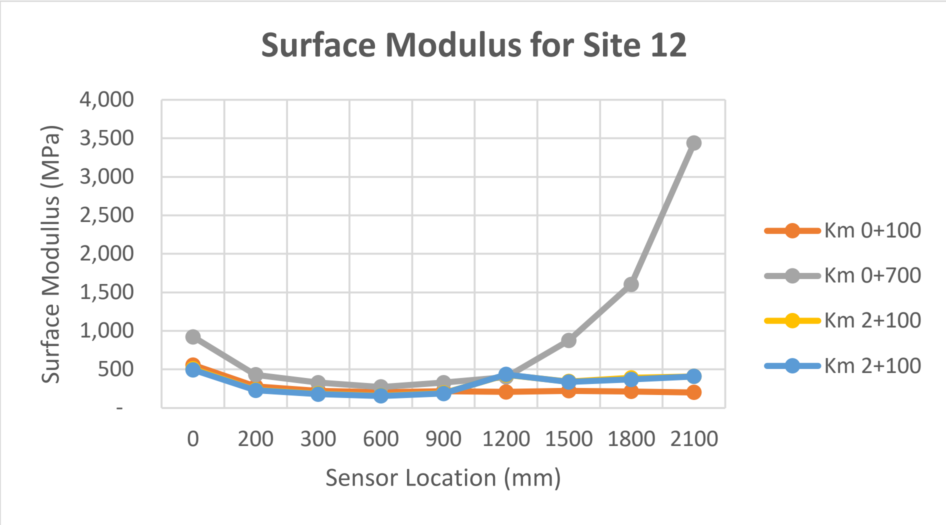
Surface Modulus for Site 12
Surface Modullus (MPa)
4,000
3,500
3,000
2,500
2,000
1,500
1,000
500
-
0
200
300
600
900
1200
1500
1800
2100
Sensor Location (mm)
Km 0+100
Km 0+700
Km 2+100
Km 2+100

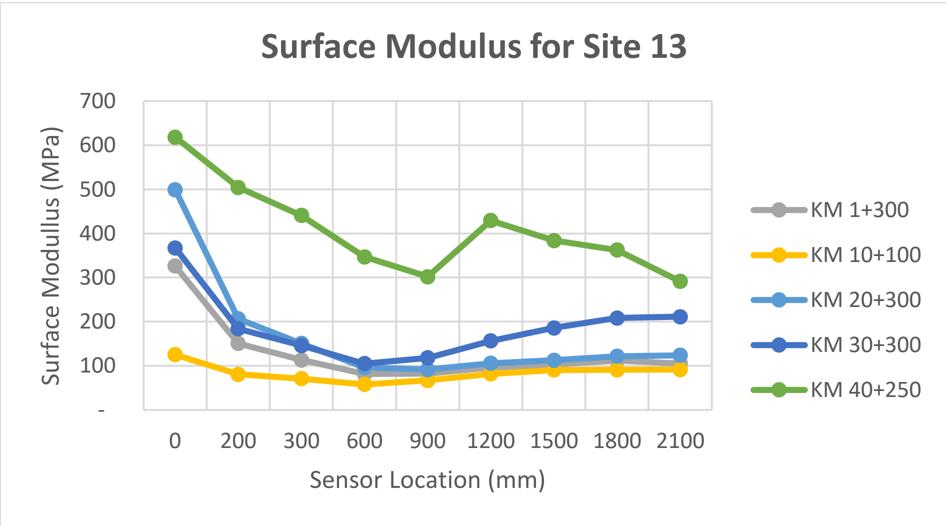
Surface Modulus for Site 13
Surface Modullus (MPa)
700
600
500
400
300
200
100
-
0
200
300
600
900
1200
1500
1800
2100
Sensor Location (mm)
KM 1+300
KM 10+100
KM 20+300
KM 30+300
KM 40+250

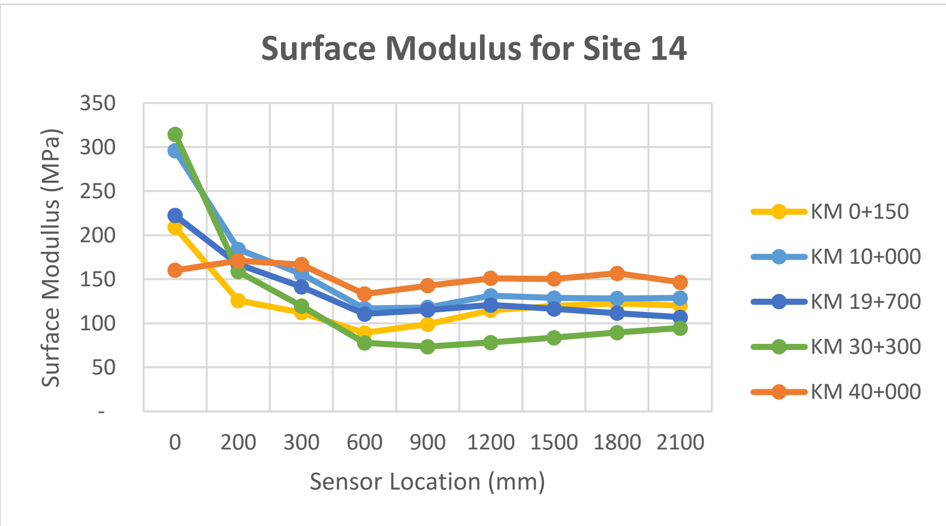
Surface Modulus for Site 14
Surface Modullus (MPa)
350
300
250
200
150
100
50
-
0
200
300
600
900
1200
1500
1800
2100
Sensor Location (mm)
KM 0+150
KM 10+000
KM 19+700
KM 30+300
KM 40+000

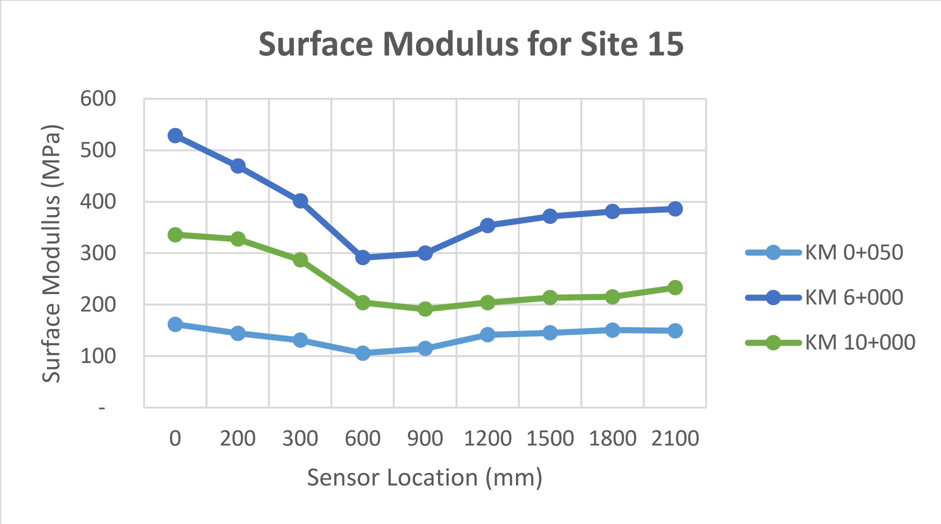
Surface Modulus for Site 15
Surface Modullus (MPa)
600
500
400
300
200
100
-
0
200
300
600
900
1200
1500
1800
2100
Sensor Location (mm)
KM 0+050
KM 6+000
KM 10+000

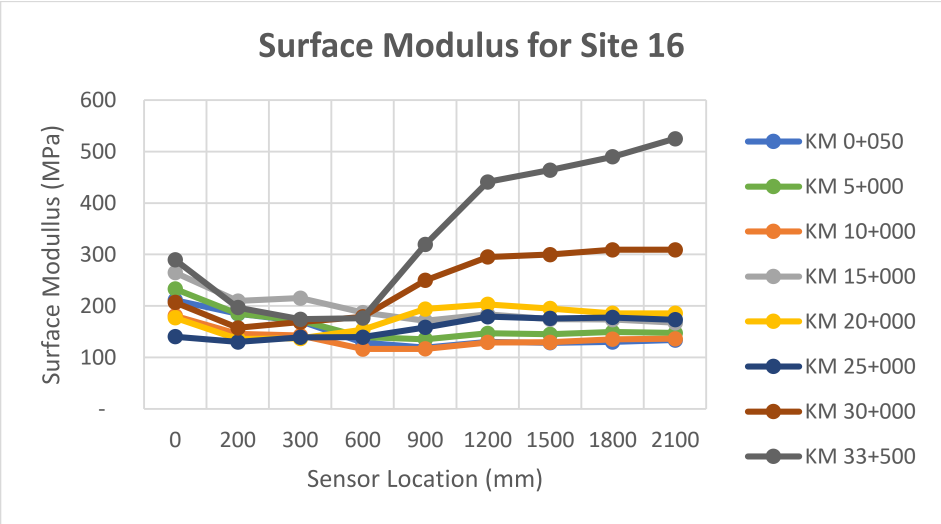
Surface Modulus for Site 16
Surface Modullus (MPa)
600
500
400
300
200
100
-
0
200
300
600
900
1200
1500
1800
2100
Sensor Location (mm)
KM 0+050
KM 5+000
KM 10+000
KM 15+000
KM 20+000
KM 25+000
KM 30+000
KM 33+500

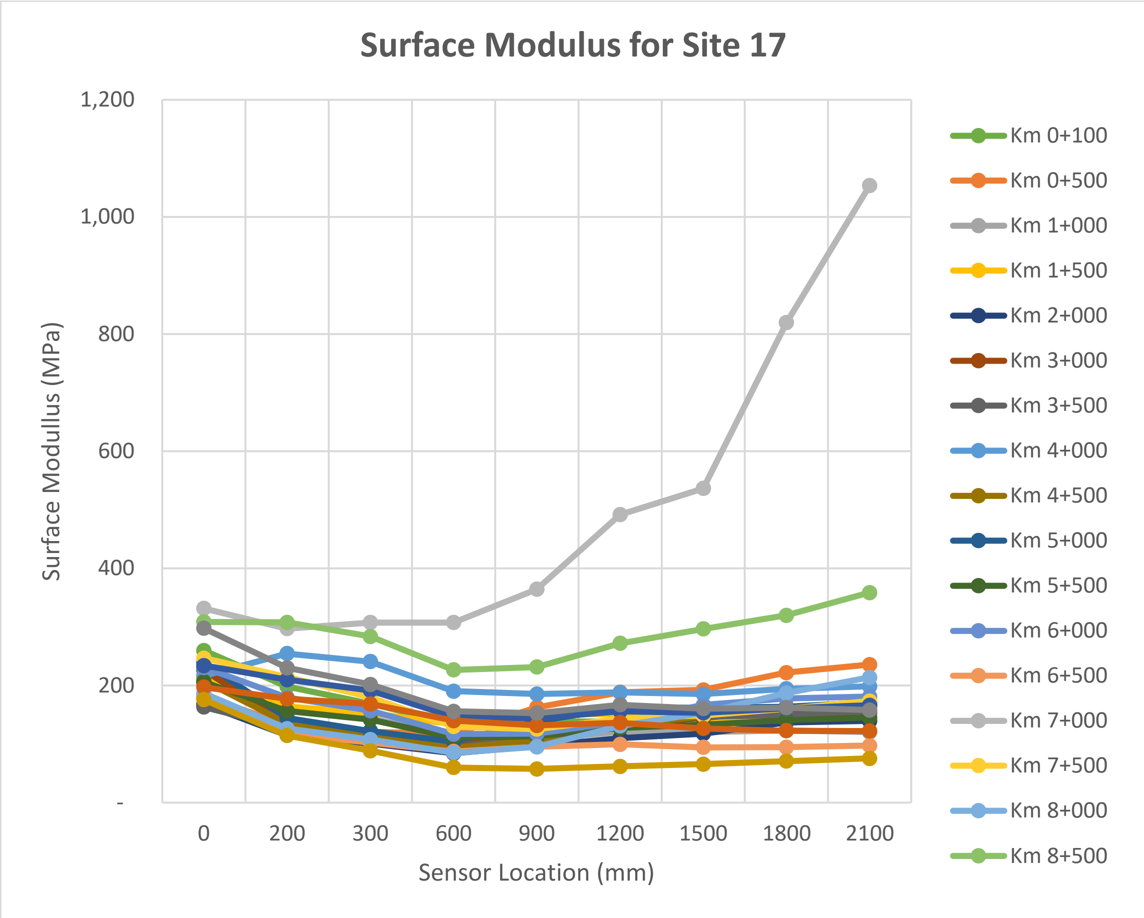
Surface Modulus for Site 17
Surface Modullus (MPa)
1,200
1,000
800
600
400
200
-
0
200
300
600
900
1200
1500
1800
2100
Sensor Location (mm)
Km 0+100
Km 0+500
Km 1+000
Km 1+500
Km 2+000
Km 3+000
Km 3+500
Km 4+000
Km 4+500
Km 5+000
Km 5+500
Km 6+000
Km 6+500
Km 7+000
Km 7+500
Km 8+000
Km 8+500

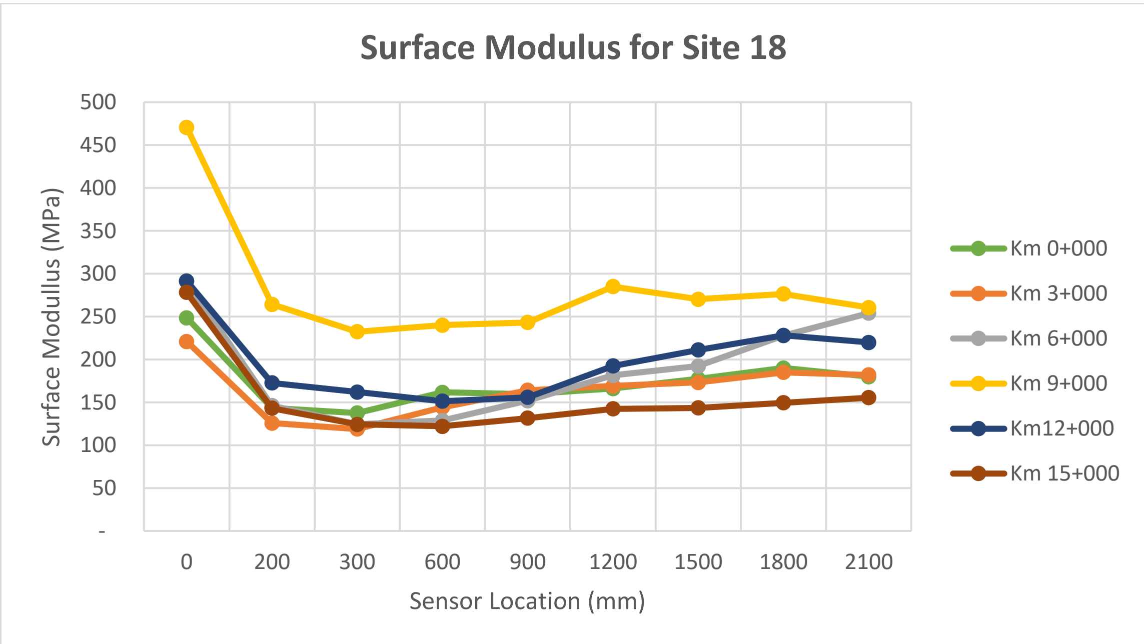
Surface Modulus for Site 18
Surface Modullus (MPa)
500
450
400
350
300
250
200
150
100
50
-
0
200
300
600
900
1200
1500
1800
2100
Sensor Location (mm)
Km 0+000
Km 3+000
Km 6+000
Km 9+000
Km12+000
Km 15+000

Appendix XI: Actual CBR Vs Predicted CBR using Models 1 to 11

Actual Lab CBR	Model 1 (RF)	Model 2 (LR)	Model 3 (ANN)	Model 4 (RF)	Model 5 (LR)	Model 6 (ANN)	Model 7 (RF)	Model 8 (LR)	Model 9 (ANN)	Model 10 (RF)	Model 11 (LR)
13	14	12	11	12	12	10	12	10	9	9	13
7	13	15	15	8	10	9	8	13	10	14	15
6	12	15	15	8	7	7	8	11	7	11	15
19	14	14	12	21	21	21	23	21	20	15	14
11	14	15	15	13	13	13	12	12	11	10	15
11	12	16	16	12	12	10	12	14	10	13	15
7	11	14	16	13	14	12	12	11	9	9	14
8	18	13	7	13	11	10	11	8	10	17	13
16	10	14	14	14	20	20	18	21	18	7	14
13	10	14	14	14	13	13	12	12	10	10	13
18	14	13	14	14	13	10	13	11	8	18	13
4	9	16	12	12	11	12	13	12	15	6	17
30	22	15	13	13	12	13	15	16	15	15	16
55	26	16	13	28	30	29	28	27	27	17	16
14	13	15	10	13	13	12	12	13	12	13	15
35	13	16	16	32	29	32	31	30	29	10	16
30	17	14	8	23	26	24	25	26	24	22	14
9	9	13	11	11	13	11	12	13	10	11	13
16	20	10	7	11	12	18	11	12	18	21	11
16	10	17	19	14	17	16	13	15	16	6	17
12	12	16	16	12	14	16	12	14	16	10	17
13	15	15	15	7	10	9	7	14	10	17	15
6	14	16	18	10	7	6	10	6	7	9	17
8	17	16	11	9	9	10	8	10	10	8	15
8	19	15	15	13	12	11	12	11	9	28	15